AD_____

Award Number:

W81XWH-08-2-0157

TITLE:

Glyburide – novel prophylaxis and effective treatment for traumatic brain injury

PRINCIPAL INVESTIGATOR:

J. Marc Simard, M.D., Ph.D.

CONTRACTING ORGANIZATION:

University of Maryland, Baltimore
Baltimore, MD 21201

REPORT DATE:

August 2010

TYPE OF REPORT:

Annual

PREPARED FOR: U.S. Army Medical Research and Materiel Command
Fort Detrick, Maryland 21702-5012

DISTRIBUTION STATEMENT:

[X] Approved for public release; distribution unlimited

REPORT DOCUMENTATION PAGE

Form Approved
OMB No. 0704-0188

1. REPORT DATE *(DD-MM-YYYY)*	**2. REPORT TYPE**	**3. DATES COVERED** *(From - To)*
01-08-2010	Annual	7 JUL 2009 - 6 JUL 2010

4. TITLE AND SUBTITLE
"Glyburide – novel prophylaxis and effective treatment for traumatic brain injury"

5a. CONTRACT NUMBER

5b. GRANT NUMBER
W81XWH-08-2-0157

5c. PROGRAM ELEMENT NUMBER

6. AUTHOR(S)
J. Marc Simard, M.D., Ph.D.

email: shave001@umaryland.edu

5d. PROJECT NUMBER

5e. TASK NUMBER

5f. WORK UNIT NUMBER

7. PERFORMING ORGANIZATION NAME(S) AND ADDRESS(ES)
University of Maryland, Baltimore

Baltimore, MD 21201

8. PERFORMING ORGANIZATION REPORT NUMBER

9. SPONSORING / MONITORING AGENCY NAME(S) AND ADDRESS(ES)
U.S. Army Medical Research
and Materiel Command
Fort Detrich, MD 21702-5012

10. SPONSOR/MONITOR'S ACRONYM(S)

11. SPONSOR/MONITOR'S REPORT NUMBER(S)

12. DISTRIBUTION / AVAILABILITY STATEMENT
Approved for public release; distribution unlimited

13. SUPPLEMENTARY NOTES

14. ABSTRACT
The overall subject of this project is blast-traumatic brain injury (blast-TBI) and the role of the SUR1-regulated $NC_{Ca\text{-}ATP}$ channel in blast-TBI. The specific objectives of this project include: (1) develop a standardized rat model of blast-TBI to study the direct transcranial effects of blast on the brain, independent of indirect transthoracic effects; (2) determine the role of the SUR1-regulated $NC_{Ca\text{-}ATP}$ channel in blast-TBI; (3) in normal human volunteers, determine the safety of the SUR1 blocker, glyburide, as it might be used as prophylaxis against blast-TBI. During the second year of this project, we completed a key objective – the development of a cranial-only blast injury apparatus (COBIA) for production of reliable, repeatable, "dose-dependent" blast-TBI, independent of transthoracic mechanisms of injury to the brain, along with the initial characterization of the pathophysiological consequences of direct cranial primary blast injury (dcPBI) produced by COBIA. Our results have been submitted for publication. The most important findings include: (i) many of the pathophysiological consequences of bTBI in humans are reproduced in our model, including subarachnoid hemorrhage, widespread microvascular and neuronal abnormalities, persistent vestibulomotor and learning difficulties; (ii) dcPBI does *not* result in malignant cerebral edema, suggesting that observations of malignant cerebral edema in humans with bTBI may be due to dcPBI complicated by some other injury, e.g., hemorrhagic shock.

15. SUBJECT TERMS
blast, traumatic brain injury, neurogenic pulmonary edema, mortality, caspase-3, beta-amylase precursor protein, sulfonylurea receptor

16. SECURITY CLASSIFICATION OF:			**17. LIMITATION OF ABSTRACT**	**18. NUMBER OF PAGES**	**19a. NAME OF RESPONSIBLE PERSON**
a. REPORT	**b. ABSTRACT**	**c. THIS PAGE**			USAMRMC
U	U	U	UU	98	**19b. TELEPHONE NUMBER** *(include area code)*

Table of Contents

INTRODUCTION: Narrative that briefly (one paragraph) describes the subject, purpose and scope of the research.

The overall subject of this research project is blast-traumatic brain injury (blast-TBI) and the role of the SUR1-regulated $NC_{Ca\text{-}ATP}$ channel in secondary injury following blast-TBI. The specific objectives of this research project may be summarized as follows: (1) develop a standardized rat model of blast-TBI, to permit study of direct transcranial effects of blast on the brain, independent of indirect transthoracic blast effects; (2) using this rat model, determine the specific role of the SUR1-regulated $NC_{Ca\text{-}ATP}$ channel in blast-TBI, including testing whether block of SUR1 using glyburide would show a beneficial effect in blast-TBI; (3) in normal human volunteers, determine the safety of oral glyburide as it might be used as prophylaxis against blast-TBI.

BODY: This section of the report shall describe the research accomplishments associated with each task outlined in the approved Statement of Work. Data presentation shall be comprehensive in providing a complete record of the research findings for the period of the report. Provide data explaining the relationship of the most recent findings with that of previously reported findings. Appended publications and/or presentations may be substituted for detailed descriptions of methodology but must be referenced in the body of the report. If applicable, for each task outlined in the Statement of Work, reference appended publications and/or presentations for details of result findings and tables and/or figures. The report shall include negative as well as positive findings. Include problems in accomplishing any of the tasks. Statistical tests of significance shall be applied to all data whenever possible. Figures and graphs referenced in the text may be embedded in the text or appended. Figures and graphs can also be referenced in the text and appended to a publication. Recommended changes or future work to better address the research topic may also be included, although changes to the original Statement of Work must be approved by the Army Contracting Officer Representative. This approval must be obtained prior to initiating any change to the original Statement of Work.

OBJECTIVE 1: develop a standardized rat model of blast-TBI, to permit study of direct transcranial effects of blast on the brain, independent of indirect transthoracic blast effects.

Background: In humans, TBI following an area-blast is a complex multi-faceted disease. Pathophysiologically, blast-TBI results in brain edema, swelling, hemorrhage, neuronal injury and neuronal death, leading to severe neurological and neuropsychological deficits and possibly death. Even omitting well-known mechanisms of secondary, tertiary and quaternary injury, the primary injury itself is complex, and is believed to occur by way of two distinct mechanisms: (i) direct transcranial propagation of the blast wave; (ii) indirect transmittal via the vasculature following blast to the thorax. Because the pathophysiological manifestations of TBI following area-blast in the human are so complex, dissecting out the various component mechanisms and their relative contribution to the overall pathophysiological response is of great importance for future design of treatment and prophylactic measures.

Essentially all of the existing work on blast-TBI exposes the subject's total body to an area-blast. Whereas this approach appropriately simulates the real-world combat experience, it does not permit assessment of direct blast injury to the brain in isolation of indirect injury to the brain due to blast injury to other organs, especially the lungs and major vessels within the thorax. Prior to the work we are reporting here and are actively pursuing, no animal model existed to examine the direct transcranial mechanism of blast-TBI, independent of the indirect transthoracic mechanism.

As a result of these considerations, the committee reviewing our original proposal requested that we specifically focus on further developing, perfecting and assessing the direct blast-TBI model that we had utilized to obtain some of our preliminary data.

Introduction. Successful development of a usable, standardized model system for direct blast-TBI entails several sub-objectives:

(**a**) the design and fabrication of an apparatus for reproducible, graded blast directed to the cranium that would minimize exposure of the thorax;

(**b**) establishing the range of blast intensity that would be used for later biological study, including the determination of the threshold intensity for lethality; (empirically determining the "intensity-response relationship" for a given biological outcome variable is needed to allow later assessment of a given pharmacological treatment or prophylaxis in "shifting" the apparent intensity-response relationship to the right);

(**c**) characterize the basic pathophysiological, systemic response to direct sublethal blast, to ascertain the effect of brain injury on systemic variables.

Objective 1a: Cranium-only blast injury apparatus (COBIA)

The device and its validation are described in detail in the accompanying manuscript.

Objectibe 1b – determining the threshold for lethality

This is described in detail in the accompanying manuscript.

It should be noted that an unexpected finding of our studies is that virtually all deaths due direct cranial primary blast injury (dcPBI) occur rapidly, within 1 min. Our studies indicate that only 6% of deaths are delayed (see accompanying manuscript). A similar observation has been reported in other rodent models of blast-TBI which utilize shock tubes to generate blast waves. We speculate that this observation may indicate that delayed deaths due to malignant cerebral edema as observed in humans may not be due simply to dcPBI, but may be due to dcPBI complicated by other injuries, specifically hemorrhagic shock. Although we did not propose to examine this in our original application, we are planning to pursue this line of investigation because of its absolutely critical importance for translation to warfighters at risk for bTBI.

Objectibe 1c – pathophysiological responses to sublethal blast

We have carried out experiments to characterize the effects of dcPBI on standard physiological variables, including oxygen saturation, blood pressure, heart rate, blood gases etc. These experiments are described in detail in the accompanying manuscript.

We have carried out experiments to characterize the neurofunctional consequences of dcPBI:

1. Experiments showing alteration in performance on the accelerating RotaRod that persist for the one week of testing after dcPBI are described in detail in the accompanying manuscript.

2. Additional experiments showing alteration in performance on rapid spatial learning (Morris water maze) that persist for the 3 weeks of testing are briefly described here (these experiments are still ongoing). Rats exposed to dcPBI (517 kPa) were

tested for incremental lear ning and for rapid lear ning. Incremental learning was significantly abnormal on days 14–18, as were the memory probe and the rapid learning probe (see figure below). To our knowledge, these are the first data in a rodent model of bTBI to show persistent neuroc ognitive deficits this lo ng after inj ury. We are presently collecting data from other animals similarly injur ed and we plan to write up these important findings soon for publication.

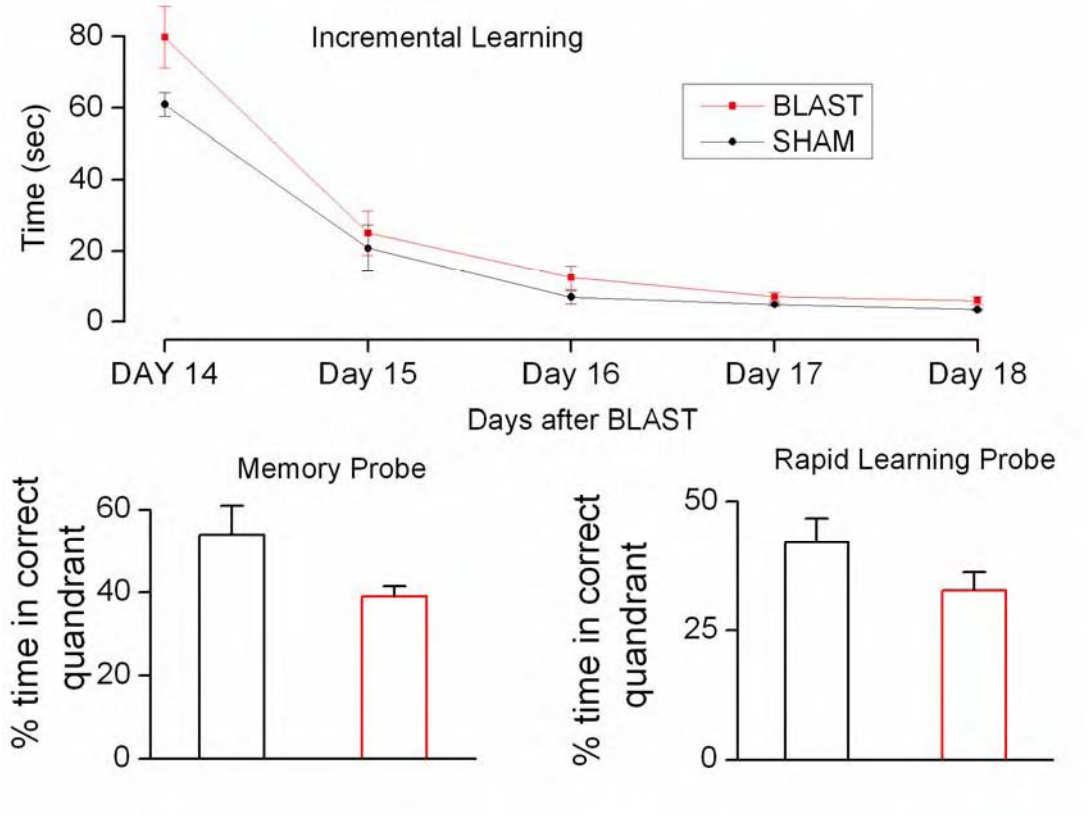

OBJECTIVE 2: using this rat model, determine t he specific role of the SUR1-regulated NC $_{Ca\text{-}ATP}$ c hannel in blast-TBI, includ ing testing whether block of SUR1 using glibenclamide would show a beneficial effect in blast-TBI.

Background. Several reports from this lab have es tablished that the SUR1-regulated NC$_{Ca\text{-}ATP}$ channel plays a critical role in va rious forms or CNS injury, including brain ischemia,(Simard et al., 2006; Simard et al., 2009c) subarachnoid hemorrhage,(Simard et al., 2009a) and brain(Sim ard et al., 2009b) and spinal cord(Simard et al., 2007) contusive injur y.(Simard et al., 2008) In these diseas e processes, the SUR1-regulated NC $_{a\text{-}ATP}$ channel plays a critical role in cellu lar (cytotoxic) edema, in formation of ioni c and vasogenic edema, and in hemorrhagic transformation. Preliminary data presented with the original proposal demonstrated that

the regulatory subunit of the channel was upregulated following blast-TBI produced by our original apparatus.

Introduction. Determining the specific role of the SUR1-regulated $NC_{Ca\text{-}ATP}$ channel in direct blast-TBI entails several sub-objectives:

(**a**) assessing the time course and cellular localization for *de novo* upregulation of SUR1, the regulatory subunit of the channel;

(**b**) assessing the time course and cellular localization for *de novo* upregulation of TRPM4, the pore-forming subunit of the channel;

(**c**) assessing the effect of the SUR1 blocker, glyburide, on direct blast-TBI, by determining whether it shifts the apparent intensity-response relationship to the right

SUR1 in neurons, white matter and capillaries following blast-TBI. We have begun experiments to assess *de novo* upregulation of the regulatory subunit of the channel, SUR1, following direct blast-TBI induced by COBIA.

Some of these findings were reviewed in last year's report. Additional figures showing SUR1 upregulation are shown in the appended powerpoint presentation. These experiments on SUR1 are still ongoing.

TRPM4 in neurons, white matter and capillaries following blast-TBI. This activity has not yet been started.

Effect of the SUR1 blocker, glyburide, on outcome following blast-TBI. This activity has not yet been started.

OBJECTIVE 3: in normal human volunteers, determine the safety of oral glibenclamide as it might be used as prophylaxis against blast-TBI.

The SUR1 blocker, glyburide, in normal human volunteers. This activity is scheduled to begin this year. University of Maryland IRB approval was recently obtained. The protocol and consent have had an initial Army HRPO review, and are in the queue for Senior reviewer feedback.

KEY RESEARCH ACCOMPLISHMENTS: Bulleted list of key research accomplishments emanating from this research.

- Completion of development, construction and implementation of COBIA for production of reliable, repeatable, "dose-dependent" blast-TBI, independent of transthoracic mechanisms of blast injury to the brain.
- Using COBIA, demonstration of significant effects of blast-TBI on neurobehavioral function and on pathophysiological manifestations (IgG, caspase-3 and β-APP immunolabeling), independent of transthoracic mechanisms of blast injury to the brain.
- Using COBIA, demonstration of significant effects of blast-TBI on upregulation of SUR1, the regulatory subunit of the SUR1-regulated $NC_{Ca\text{-}ATP}$ channel that has been

widely implicated in is chemic and traumatic injury to th e CNS, further strengthening the rationale for prophylaxis and treatment using the SUR1 inhibitor, glyburide.

- Preparation of a det ailed manuscript describing our experiments to date with dcPBI (appended).
- Oral presentation of our progress to date to Dr. Kenneth Curley (appended).

REPORTABLE OUTCOMES: Provide a list of reportable outcomes that have resulted from this research to include: manuscripts, abstracts, presentations; patents and licenses applied for and/or issued; degrees obtained that are supported by this award; development of cell lines, tissue or serum repositories; infomatics such as databases and animal models, etc.; funding applied for based on work supported by this award; employment or research opportunities applied for and/or received based on experience/training supported by this award.

- Abstract submission to the upcoming Military Health Research Forum (MHRF) conference, to be held in Kansas City, Missouri August 31–September 3, 2009.
- Submission of manuscript to the Journal of Neurotrauma

CONCLUSION: Summarize the results to include the importance and/or implications of the completed research and when necessary, recommend changes on future work to better address the problem. A "so what section" which evaluates the knowledge as a scientific or medical product shall also be included in the conclusion of the report.

Overall, the project is on track as planned in our original propos al. There are two ver y important results to date:

(i) completion of the dev elopment phase of COBIA, and validat ing its utility for production of dcPBI

(ii) using COBIA, demonstrating that dcPBI reproduces numerous aspects of the pathophysiology of blast-TBI in humans, including widespread microvascular and neuronal injury, and prolonged vestibulomotor and neurocognitive deficits

(iii) early stage demonstration of invo lvement of SUR1 in s econdary injury novel discovery that primary blast injury to the brain does not result in malignant cerebral edema, brain sw elling or any apprec iable delayed death, s uggesting that delayed death in hum ans f ollowing bTBI may be due to p rimary blas t injury complicated by some other mechanism, possibly hemorrhagic shock . We believe that this observation is high ly important, and that it merits further investigation.

REFERENCES: List all references pertinent to the report using a standard journal format (i.e. format used in *Science, Military Medicine*, etc.).

None

APPENDICES: Attach all appendices that contain information that supplements, clarifies or supports the text. Examples include original copies of journal articles, reprints of manuscripts and abstracts, a curriculum vitae, patent applications, study questionnaires, and surveys, etc.

1. Manuscript submitted to J. Neurotrauma
2. Powerpoint presentation presented to Dr. Kenneth Curley on July 16, 2010.

SUPPORTING DATA: All figures and/or tables shall include legends and be clearly marked with figure/table numbers.

none

Rodent Model of Direct Cranial Primary Blast Injury

Reed Kuehn,[1] Philippe F. Simard,[2] Ian Driscoll,[1]

Kaspar Keledjian,[2] Alicia Williams,[1] Grant Bochicchio,[3,6]

Volodymyr Gerzanich,[2] J. Marc Simard[2,4,5]

[1]Department of Surgery, Walter Reed Army Medical Center, Washington, DC

Departments of [2]Neurosurgery, [3]Surgery, [4]Physiology and [5]Pathology

University of Maryland School of Medicine, Baltimore, MD

[6]R. Adams Cowley Shock Trauma Center, Baltimore, MD

Correspondence: Dr. J. Marc Simard

Department of Neurosurgery

22 S. Greene St., Suite S12D

Baltimore, MD 21201-1595

telephone: 410-328-0850

facsimile: 410-328-0124

email: msimard@smail.umaryland.edu

Keywords: traumatic brain injury, primary blast injury, β-amyloid precursor protein

Running Title: direct cranial primary blast injury

ABSTRACT

Traumatic brain injury resulting from an explosive blast is one of the most serious wounds suffered by warfighters. Here, we describe a novel rodent model of direct cranial primary blast injury (dcPBI) in which a blast overpressure is delivered exclusively to the head, with no exposure of the remainder of the body. We constructed and validated a Cranium Only Blast Injury Apparatus (COBIA) to deliver blast overpressures to the cranium, based on detonation of .22 caliber cartridges of smokeless powder. Lethal dcPBI (LD_{50} ~515 kPa) was associated with apparent brainstem failure, characterized by immediate apnea leading to cardiac arrest that could not be overcome by cardiopulmonary resuscitation and ventilatory support. Pathological examination showed widespread subarachnoid hemorrhages without intraventricular or intracerebral hemorrhages or parenchymal contusions, and no pulmonary abnormalities. Sub-lethal dcPBI was associated with apnea lasting up to 15 sec, with the duration depending on the magnitude of the peak overpressure. Delayed death was rare in animals that survived the initial apneic event. Physiological and pathological assessments revealed transient abnormalities in oxygen saturation and milder subarachnoid hemorrhages. Immunolabeling for IgG, β-amyloid precursor protein (β-APP), and activated caspase-3 revealed widespread injuries in cortex, cerebellum, thalamus and brainstem, including extravasated IgG, microvascular stasis and neuronal and axonal abnormalities. Neurological assessment showed significant abnormalities in performance on the accelerating RotaRod that persisted unchanged for the one week of observation. We conclude that severe blast may be

survivable with protection of the torso, but without protection of the face and head, may predispose to persistent neurological dysfunction.

INTRODUCTION

Explosive munitions cause more than half of all injuries sustained in military combat, and are responsible for an increasing number of civilian casualties (Aboutanos et al., 1997; Belanger et al., 2009; Bochicchio et al., 2008; Coupland et al., 1999a; Coupland et al., 1999b; Frykberg et al., 1988). Traumatic brain injury due to an explosive blast (blast-TBI or bTBI) is one of the most serious wounds suffered by warfighters in modern conflicts. bTBI can range from overt injuries marked by soft tissue damage to the face and scalp complicated by open brain injury, to more insidious injuries with no external physical damage that manifest as persistent neurocognitive or psychological abnormalities (Belanger et al., 2009; Cernak et al., 1996; Cernak et al., 1999a; Cernak et al., 1999b; Clemedson, 1956; Denny-Brown, 1945; Elder et al., 2009).

Tremendous progress has been made in understanding the pathophysiology of primary blast injury (PBI) to the brain that is caused by the intense transient overpressure of the blast wave generated by an explosion. Most importantly, the so-called “thoracic mechanism” has come to be recognized, whereby the brain is believed to be injured indirectly by a blast wave that impacts the gas-filled thoracic cavity and is transmitted to the brain by way of major blood vessels in the neck (Cernak et al., 1996; Cernak et al., 2001; Courtney et al., 2009; Long et al., 2009). This concept has been pivotal in driving the implementation of body armor to protect the torso including the chest, and thereby protect the brain from indirect injury. Preclinical work has confirmed the importance of this approach in protecting against the thoracic mechanism of PBI to the brain. (Long et al., 2009; Svetlov et al., 2010).

As the use of torso protection gains ascendancy, offensive countermeasures naturally include the use of greater blast forces to overcome this protection. Such countermeasures result in exposing unprotected parts of the body, especially the face and other parts of the head, to blast forces that might not have been survivable before the introduction of body armor. The transmission of a blast wave through the skull to the brain has long been postulated (Clemedson, 1956), but this “direct” mechanism of injury has garnered less attention than the “indirect” thoracic mechanism, owing perhaps to the impression that the brain is protected from direct injury by the relatively rigid skull. However, it has been shown that a blast wave can traverse the cranium of the rat almost unchanged (Chavko et al., 2007). Numerical simulations that take into account the physical properties of the skull and other tissues of the head exposed to an explosive blast indicate that a nonlethal blast can interact with CNS tissues to cause brain injury (Moore et al., 2009; Moss et al., 2009). A blast wave may induce sufficient flexure of the skull to generate damaging loads within the brain, or it may deposit kinetic energy at boundaries between tissues of different density.

To our knowledge, no experimental work has investigated the effects of a blast overpressure delivered exclusively to the head, with the goal of assessing the effect of direct cranial PBI (dcPBI) that is uncomplicated by indirect PBI to the brain mediated by the thoracic mechanism. Here, we describe a novel rodent model of dcPBI in which a blast overpressure is delivered locally to the head, with no exposure of the remainder of the body to the overpressure, and with support of the head designed to preclude impact-acceleration injury to the brain. In this

model, pulmonary injury was absent. Many, but not all, of the neuropathological and neurobehavioral abnormalities reportedly associated with bTBI in humans were present in this model of dcPBI, including subarachnoid hemorrhage and persistent vestibulomotor abnormalities. Notably absent were the brain swelling and delayed death from malignant cerebral edema that have been frequently reported in humans.

METHODS

COBIA

The Cranium Only Blast Injury Apparatus (COBIA) is constructed of several elements (Fig. 1). The central component of COBIA is a .22 caliber, single shot, powder-actuated tool (Ramset RS22, ITW RAMSET, Glendale Heights, IL). The tool was modified by removing the piston that normally drives the fastener, making the tool function like a firearm and allowing the blast wave to propagate undamped through the barrel. The tool is held vertically using a custom fabricated stand, which also serves to neutralize the "safety" of the tool. The blast is directed downwards into a "blast dissipation chamber" (BDC), which interfaces snugly with the muzzle of the tool. BDCs of different sizes are used to adjust the magnitude of the blast overpressure that is delivered to the head. BDCs are fabricated of various lengths of polyvinyl chloride (PVC) pipe, with the shortest chamber delivering the largest blast overpressure to the head (Table 1). The BDC terminates at the "blast dissipation chamber-cranium interface" (BDCCI). The BDCCI is a circular section of PVC pipe (cut from a Tee connector) that holds the rat's head in place. The interface with the scalp is lined with an O-ring made of

synthetic foam rubber. The blast wave is generated by firing a .22 caliber crimped brass cartridge (power hammer loads, “power level” 2 or 4, brown and yellow color coding; 128±4 and 179±5 mg of smokeless powder, respectively).

Measurements of blast waveforms

Pressure measuring system. The overpressures generated by blasts from COBIA and from the pressure-step generator used for validation (see below) were recorded using a precision dynamic piezoelectric pressure transducer (150 pC/psi; 0.002–12 kHz; Model 100-P, Columbia Research Laboratories, Inc., Woodlyn PA) and charge amplifier (Model 4601, Columbia Research Laboratories, Inc.). The transducer was connected to the charge amplifier using a 2 m long cable with a 100 pF capacitor in parallel with the input. The output of the charge amplifier was digitized (DigiData 1200, Axon Instruments, Foster City, CA; sampling frequency, 333 kHz) and waveforms were stored for offline analysis using pClamp software (version 7; Axon Instruments). The output of the charge amplifier is very sensitive to the setting of the “transducer sensitivity control”, which adjusts for the total input capacitance, including that for the specific piezoelectric transducer (nominally, 150 pF), the input cable (~100 pF/m) and the input capacitor (100 pF).

Pressure-step generator. Although the charge amplifier was factory-calibrated, we sought to independently verify the calibration for the range of pressures that we would be studying. We constructed a device to generate pressure-steps of known magnitude that could be recorded by the pressure measuring system. The pressure-step generator consisted of two chambers, a source chamber and a test chamber, separated by a solenoid-operated valve

(Asco, Florham Park, NJ, #8262G202 120/60; normally closed) (Fig. 2A). The source chamber (22,712 ml) was pressurized using an air compressor (Porter-Cable, 6 gallon, Model #C2002-WK), with the exact pressure adjusted to the desired value using a bleed valve, and measured using a precision static pressure gauge (Precision Instrument Co., Kennesaw, GA; 4001 heavy duty 4 inch; 0.5% accuracy full scale). The test chamber (15 ml) included a valve to allow decompressing the test chamber after each test cycle, and an end-cap to interface with the piezoelectric pressure transducer being tested. The apparatus was capable of generating pressure-steps from 0 to 600 kPa with a rise-time (from 10% to 90%) of ~9 ms. Generating a pressure-step did not result in any measureable drop in pressure in the source chamber, due to the large difference in volume between the chambers.

Validating the pressure measuring system. Pressure-steps from 0 to 137.9–551.6 kPa, in increments of 68.9 kPa, were generated using the pressure-step generator, and were recorded using the pressure measuring system. All measurements were repeated in triplicate. Because the pressure measuring system acts like a second-order band-pass filter, measurements of steady-state pressures were not possible and some “ringing” of the peak was observed (Fig. 2B). Therefore the decay phases of the recorded waveforms (from the peak out to 1000 msec) were fit with a second order exponential equation ($\tau 1$, 230–300 msec; $\tau 2$, 50–90 msec) to estimate the peak pressure. Values from the fits were plotted against the steady-state input pressure, showing excellent agreement; a least-squares fit of the data yielded a slope of 1.025 and an intercept

of -7.1 kPa (Fig. 2C), confirming proper calibration of the pressure measuring system.

Blast injury procedure

All procedures were approved by the Institutional Animal Care and Use Committee of the University of Maryland School of Medicine. This research was conducted in compliance with the Animal Welfare Act Regulations and other Federal statutes relating to animals and experiments involving animals and adheres to the principles set forth in the Guide for Care and Use of Laboratory Animals, National Research Council, 1996. Male Long-Evans rats (250-300 gm; Harlan, Indianapolis, IN) were anesthetized (60 mg/kg ketamine plus 7.5 mg/kg xylazine, intraperitoneally), intubated with an endotracheal tube (Tomcat Kendall, Mansfield, MA) and were allowed to breathe air spontaneously. Core temperature was maintained at 37° C using an isothermal pad (Deltaphase, Braintree Scientific, Braintree, MA). Hair was clipped from the dorsum of the head. The rat was positioned prone with the vertex carefully placed against the O-ring of the BDCCI. Just prior to detonation, a small balloon under the rat's snout was inflated to 10 kPa to promote contact between the scalp and the O-ring, and to cushion the head from downward acceleration during the blast. After the blast, the rat was removed from the apparatus and was observed for apnea. If spontaneous respiration did not resume within 10 sec, the endotracheal tube was connected to a ventilator (MicroVent, Hallowell, Pittsfield, MA; gas, compressed air) and ventilatory support as well as chest massage were instituted and maintained until either spontaneous cardiopulmonary function resumed or until

cardiac arrest was deemed to be irreversible. Survivors were nursed on a heating pad until they recovered spontaneous movements. For sham injury, all of the above was performed except for detonating the cartridge.

Overall, we studied 160 rats in 2 series of experiments, series 1 (79 rats) with BDCs having an internal diameter of 2.05 cm, and series 2 (81 rats) with BDCs having an internal diameter of 2.54 cm. The experiments in series 1 were conducted using BDCs of various lengths and cartridges of "power level" 2 and 4, and were designed to determine the best combination of BDC size and cartridge power to obtain the desired biological response. Experiments in series 2 were all conducted using cartridges of "power level" 4 and BDCs of various lengths (all internal diameter, 2.54 cm). The 79 rats in series 1 included 62 with dcPBI that provided usable data, 4 intended for dcPBI that were excluded for various technical reasons (abnormal baseline variables, anesthesia-related death before injury, improper positioning in the BDCCI), and 13 with sham injuries; of the 62 with usable dcPBI, 9 died following injury, 11 were euthanized at 24 hr, 32 were euthanized at 7 days, and 10 were euthanized at later times. The 81 rats in series 2 included 65 with dcPBI that provided usable data, 8 intended for dcPBI that were excluded for various technical reasons (as above), and 8 with sham injuries; of the 65 with usable dcPBI, 25 died following injury, 2 were euthanized at 24 hr, and 38 were euthanized at 10 days or beyond.

Physiological measurements

All rats underwent continuous pulse-oximetry and heart rate recordings with the sensor placed on the hindlimb (Mouse Ox™; STARR Life Sciences Corp., Oakmont, PA). Readings were taken at baseline, immediately after intubation,

and then continuously for 30 min after the injury or sham procedure. A group of 33 rats (7 that died shortly after dcPBI plus 26 rats that survived), underwent cannulation of the tail artery, which was performed after induction of anesthesia and prior to injury; arterial access was used to monitor arterial blood pressure (CyQ; CyberSense Inc., Nicholasville, KY) and, in some rats, arterial blood gases (iSTAT; Heska Inc., Loveland, CO).

Neurofunctional testing

The accelerating RotaRod test was used to assess coerced locomotor activity (Hamm, 2001). Rats were placed on the drum of the accelerating RotaRod (starting at 4 rpm, accelerating at rate of 2 rpm every 5 sec up to a maximum of 45 rpm; IITC, Life Science, Woodland Hills, CA), with 3 trials separated by 20 min administered on each day of testing. We report the average latency to falling off of the drum.

Pathology

Necropsies (gross examination of brains and lungs) were performed on all rats that died of dcPBI; microscopic examination (H&E sections) of brain and lungs was performed on 10 rats that died of dcPBI and on 13 rats with sub-lethal dcPBI that were euthanized at 24 hr. Rats that died shortly after injury were rapidly perfused with saline to remove intravascular contents and were perfusion-fixed using 4% paraformaldehyde. Rats that survived were euthanized using a lethal dose of pentobarbital intraperitoneally, after which they were perfused with saline followed by paraformaldehyde fixative, as above. The brains and lungs were harvested and photographed to document subarachnoid hemorrhages and other abnormalities. The fixed brains were cut sagitally and

scanned at high resolution to assess for intraventricular or intraparenchymal hemorrhages or contusions. The tissues were then processed for paraffin embedding, sectioned and stained with hematoxylin and eosin (H&E) for microscopic examination.

Immunohistochemistry

For immunolabeling, perfusion-fixed brains were cryoprotected with 30% sucrose. Cryosections (10 μm) were mounted on slides, blocked in 5% goat serum with 0.2% Triton X-100 in PBS for 1 hr, then incubated overnight with primary antibody directed against rat IgG (1:200; catalogue #SC-2011; Santa Cruz Biotechnology, Santa Cruz, CA), β-APP (1:200; catalogue #51-2700; Invitrogen, Camarillo, CA), or activated (cleaved) caspase-3 (1:200; catalogue #9661, Cell Signaling Technology, Danvers, MA) at 4° C. Sections were washed 3 times in phosphate buffered saline, then incubated in the dark with fluorescent-labeled secondary antibody (1:500; goat anti-rabbit AlexaFlour555, Invitrogen). After 1 hr, the slides were washed and cover-slipped with Prolong Antifade reagent with DAPI (P36931, Invitrogen). Control experiments included the omission of primary antibody. Low and high power photomicrographs were taken using a CoolSNAP camera (Nikon), and images were adjusted for brightness and contrast using IPLab Software.

Statistical analysis

Unless otherwise noted, values are given as mean±S.E. Data were analyzed using a repeated measures one-way ANOVA with Bonferroni comparisons. Effects were judged to be statistically significant if $P < 0.05$.

RESULTS

Blast Overpressures generated by COBIA

Blast waves generated by COBIA were measured using a dynamic pressure sensor imbedded in a model of the rat head and positioned where the rat's cranium would be in the BDCCI. Recordings of the blast waves showed a large brief transient overpressure, followed by smaller slower transient under- and overpressures that were fully damped within 2 sec (Fig. 3A). At high temporal resolution, the initial overpressure was found to be complex, and included an initial transient lasting 50–100 μsec, followed by a "quasi-static" pressure component. Notably, the initial complex overpressures generated by COBIA resembled published recordings of blast waveforms obtained in an armored vehicle penetrated by shaped charge munitions (Fig. 3B).

COBIA was designed so that BDCs of different lengths would generate blast overpressures of different magnitude. The average peak overpressures recorded using a variety of BDCs and two different power level cartridges ranged from 250 to >1,000 kPa (Table 1). As a first approximation, the magnitudes of the peak overpressures generated using BDCs of different lengths followed the inverse square law (Fig. 3C).

The velocities of the blast waves generated by COBIA were not measured, but could be estimated from fluid dynamic considerations. The relationship between peak overpressure and velocity in air is given by (Harvey et al., 1984; Zel'dovich et al., 1966):

$$P + P_0 = P_0\left[1 + \frac{2\gamma}{(\gamma+1)}\left(\frac{U_s^2}{C^2} - 1\right)\right],$$

where P is the shock overpressure (kPa); P_o is the atmospheric pressure (101.3 kPa); γ is the specific heat ratio (for air, γ=1.4); U_S is the shock velocity (m/sec); C is the velocity of sound in air (343 m/sec). Thus, an overpressure of 500 kPa is estimated to have a supersonic velocity of 784 m/sec.

Lethal primary blast injury to the cranium

At the time of dcPBI, rats were intubated endotracheally and breathed room air spontaneously. Immediately after lethal dcPBI, rats exhibited opisthotonus, i.e., an extreme, dorsally hyperextended posture of the spine with strong extension of the tail. All rats subjected to dcPBI experienced apnea, but with lethal dcPBI, apnea was persistent and was followed within 30–45 sec by cardiac arrest. In 7 rats, continuous monitoring of blood pressure and heart rate using an intra-arterial catheter failed to show any rise in pressure or fall in heart rate during the first 15-30 sec, suggesting the absence of a surge in circulating catecholamines or in vagal tone; systolic blood pressure fell only after cardiac arrest. Mortality was related to the magnitude of the blast overpressure to which the head was exposed. Exposures below 450 kPa were never fatal, whereas exposures to 650 kPa and higher were associated with >85% mortality; the LD50 was ~515 kPa (Fig. 4A). Fatality was invariably associated with apnea that could not be reversed – mechanical ventilation and cardiac massage never succeeded in resuscitating rats with prolonged apnea (>15 sec). The rapid onset and profound nature of cardiopulmonary arrest following dcPBI was consistent with a central mechanism involving the brainstem, i.e., apparent brainstem failure.

Necropsies were performed on all rats with lethal dcPBI, to further investigate the cause of death. The scalp at the site of maximum blast exposure was always slightly discolored, but showed no evidence of hemorrhage, contusion or laceration (Fig. 4B). Subgaleal hemorrhages and skull fractures were not observed. All brains excised following lethal dcPBI invariably showed extensive subarachnoid hemorrhages on the dorsal surfaces of the cerebrum and cerebellum, as well as on ventral surfaces including the entorhinal cortex and brainstem (Fig. 4C). In 10 rats, unprocessed sagittal sections of perfused brains confirmed the presence of subarachnoid hemorrhages but revealed no apparent intraventricular or intraparenchymal hemorrhages or contusions, and no overt damage to the brainstem (Fig. 4D). Paraffin sections stained with H&E generally confirmed these findings, although in five rats, one or two microscopic hemorrhages <200 μm were identified in the brainstem (Fig. 4E). H&E sections of the lungs from 10 rats showed no evidence of overt damage or hemorrhage (Fig. 4F). Thus, death was best attributed to brainstem failure due to neural dysfunction in the absence of appreciable tissue damage.

Notably, rats that survived the initial apneic event almost invariably recovered and survived; delayed deaths were rare. Of the 34 rats that died as a result of dcPBI (9 in series 1 and 25 in series 2), all but one in each series died within 1 min of dcPBI. The other 2 rats died at ~30 min and 12 hr, with the specific reason for the delayed death not determined.

Sub-lethal primary blast injury to the cranium

As noted above, all rats with dcPBI became apneic. For survivors, the duration of apnea was generally related to the magnitude of the peak overpressure and was typically less than 12–15 sec (Fig. 5A).

We monitored standard physiological parameters during the 30 min following sub-lethal blast injury. Sub-lethal dcPBI resulted in a significant but brief decline in oxygen saturation attributable to apnea, but no significant change in blood pressure, heart rate, blood gases, serum electrolytes or serum glucose (Fig. 5B,C,D). The absence of any appreciable changes in these variables suggested minimal if any pulmonary effects of the direct cranial blast.

Necropsies were performed at 24 hr on 13 rats that survived dcPBI (414–655 kPa). As with lethal dcPBI, subarachnoid hemorrhages were an invariant finding, but the amount of blood and the extent of the hemorrhages was less than with lethal dcPBI (Fig. 6A). Unprocessed sagittal sections and paraffin sections stained with H&E revealed no abnormalities, similar to findings with lethal dcPBI.

We used IgG immunolabeling as an indicator of microvascular dysfunction. In perfused brains, IgG immunolabeling is normally absent (Fig. 6D). However, IgG immunolabeling may be found under pathological conditions, including: (i) microvascular stasis or thrombosis that prevents intravascular clearance by perfusion; (ii) endothelial injury that results in abnormal cellular uptake; (iii) extravasation associated with formation of vasogenic edema due to breakdown of the blood-brain-barrier (Simard et al., 2009a; Simard et al., 2009b). In 8 rats examined at 1–7 days after sub-lethal dcPBI (427 and 517 kPa), IgG immunolabeling was typically observed in the cerebellum (Fig. 6B,C) in the

thalamus (Fig. 6E–G) as well as in the cerebral cortex (Fig. 7B). In some areas, diffuse labeling suggested regions of vasogenic edema (Fig. 6C,E), but in numerous instances, distinct microvascular labeling appeared to be attributable to microvascular stasis or thrombosis (Fig. 6B,F,G).

We used β-APP immunolabeling as an indicator of neuronal dysfunction. After injury, persistent axonal transport leads to bulbous accumulations of β-APP in damaged axons (Blumbergs et al., 1995; Bramlett et al., 1997; Pierce et al., 1996; Stone et al., 2000). In addition, injured neurons often exhibit an increase in cytoplasmic β-APP in their perikarya (Itoh et al., 2009; Kilbourne et al., 2009). In 8 rats examined at 1–7 days after sub-lethal dcPBI (427 and 517 kPA), β-APP labeling that is characteristic of axonal injury was identified in parietal (Fig. 7A) and entorhinal (Fig. 7C) cortex. In addition, cerebellar Purkinje cells typically showed increased levels of cytoplasmic β-APP that coincided with labeling for activated caspase-3 (Fig. 7D,E).

We used the accelerating RotaRod test to gauge neurological function. Following sub-lethal dcPBI (427 and 517 kPA), performance was significantly degraded compared to controls, with the abnormality persisting for the entire week of observation (Fig. 7F).

DISCUSSION

Blast injury is classified into four phases, each of which can result in brain injury (http://www.bt.cdc.gov/masscasualties/explosions.asp). Primary blast injury (PBI) is caused by the blast wave itself. Secondary blast injury results from

ballistic fragments penetrating into the head or body. Tertiary blast injury is caused by the ‘‘blast wind’’, a forceful air flow that accelerates the head and body and causes impact injuries. Quaternary blast injury incorporates other mechanisms including hemorrhagic shock and chemical or thermal injuries (Chen et al., 2009). Of the four mechanisms, only the first, PBI, is unique to an explosive blast; the last three yield TBI and other bodily injuries that are indistinguishable from those encountered in settings unrelated to blast. PBI involving the brain appears to be further divisible, based on two distinguishable mechanisms, direct PBI due to the blast wave striking the cranium proper, and indirect PBI due to the thoracic mechanism (see Introduction). Within this complex compilation of multiple mechanisms of bTBI, arguably the least well understood is direct PBI to the brain. The model that we developed and validated here using COBIA was designed specifically to focus on direct PBI to the brain. Previous studies on rodent models of bTBI, including those utilizing shock tubes to generate blast waves (Long et al., 2009; Svetlov et al., 2010), have provided invaluable advances in understanding bTBI, but the brain injuries in those studies may have resulted from some mixture of direct PBI to the brain, indirect PBI to brain mediated via the thoracic mechanism, and by tertiary injury to the brain due to the gas venting jet of the shock tube. Further advances in understanding the cellular and molecular events underlying bTBI will likely come from detailed comparisons of injuries produced by single vs. multiple mechanisms with instruments like COBIA vs. shock tubes.

Blast waves generated by COBIA

We generated blast waves by detonating smokeless powder inside of crimped brass .22 caliber cartridges. The .22 caliber cartridges were detonated inside of a commercial .22 caliber powder-actuated tool, with the tool modified by removing its piston. This modification made the tool resemble a firearm, and allowed undamped propagation of the blast wave within the barrel of the tool and into the BDC. The blast waves generated by COBIA bore features that are relevant to real-world explosions. At low temporal resolution, the blast waveforms from COBIA resembled simple Friendlander waves. However, at higher temporal resolution, reflections from the barrel of the tool and from the BDC resulted in complex waveforms with post-peak overpressures that resembled those recorded in simulated combat situations (Fig. 3B). The peak overpressures generated by COBIA ranged from 250 to >1,000 kPa (Table 1), with specific values determined using BDCs of different sizes and cartridges of different power levels. The peak overpressures generated by COBIA may be compared with those generated in shock tube experiments, which typically utilize peak overpressures of 40–350 kPa for whole-body exposures (Bauman et al., 1997; Cernak et al., 2001; Chavko et al., 2007; Long et al., 2009; Petras et al., 1997; Saljo et al., 2000). Calculations based on liquid dynamic theory indicated that the velocities of the blast waves generated by COBIA were on the order of 750 m/sec, comparing favorably to velocities calculated in simulations of humans experiencing sublethal air-blasts, wherein the blast wave is propagating at a velocity of 450 m/sec when it reaches the body (Moss et al., 2009).

COBIA and pulmonary effects

In our experiments with sub-lethal dcPBI, we observed only a small reversible effect on oxygen saturation, with all other indicators of pulmonary and other vital physiological functions remaining unaffected. In addition, histopathological examination of the lungs was unremarkable. Together, these findings indicate that COBIA had minimal if any pulmonary effects. By contrast, whole body as well as thorax-alone exposure of rats to lesser blast insults leads to unmistakable abnormalities involving the lungs. With whole body exposure, one study (129 kPa) found diffuse, moderate-to-marked hemorrhage, congestion and edema in the lungs (Bauman et al., 1997); another study (339 kPa) reported petechiae, ecchymoses, blebs, and isolated or confluent hemorrhages in the trachea and lungs (Cernak et al., 2001). With thorax-alone exposure, one study (69 kPa) found widespread areas of hemorrhage that could be confluent and involve up to 30% of the lungs; another study (304 kPa) reported a fall in mean arterial pressure, a decrease of systolic and diastolic pressures, bradycardia, and tachypnea and a significant decrease of pH in both arterial and venous blood (Cernak et al., 1996). Given the well-documented sensitivity of the lungs to PBI, our data clearly establish that in our model, spillover of the primary insult to the lungs was minimal and if it occurred, did not have any important physiological consequence.

COBIA and CNS effects

Lethal blast. We found that exposures of the cranium to peak overpressures below 450 kPa were never fatal, whereas exposures to 650 kPa and higher were associated with high mortality; the LD50 was ~515 kPa. Animals with lethal dcPBI died rapidly of cardiopulmonary arrest following prolonged

apnea. By comparison, whole-body exposure of rats to blast is associated with an LD50 that is ~2 times smaller, 250 kPa (Richmond et al., 1961; Richmond et al., 1962). The reason for the apparent 2-fold difference in sensitivity associated with cranium-only exposure compared to whole-body exposure is not known, but numerous factors could potentially contribute. First, it must be borne in mind that pressure measurements may not be standardized between laboratories. Although the Richmond data cited above indicated an LD50 of 250 kPa, data from another laboratory indicate that whole-body exposure to 240 kPa peak overpressure is non-lethal, causes no visible damage to the brain, and shows no evidence of damage on routine histological evaluation (Saljo et al., 2000). Additional reasons include the possibility that: (i) a certain degree of protection is afforded by the scalp and skull; (ii) amplification of the blast wave occurs after it enters the torso as it propagate to the head; (iii) there is added injury due to systemic effects of blast that are absent with cranium-only exposure; and (iv) the cause of death with whole body exposure does not involve the CNS exclusively. Determining the cause(s) for the apparent differences in sensitivity will require additional investigations, including repeating our experiments on rats after craniectomy.

Death following dcPBI almost invariably occurred very rapidly (<1 min) and appeared to be due to primary brainstem failure without overt contusive or similar tissue-damaging injury. The rats exhibited opisthotonic posturing and apnea, both of which reflect brainstem dysfunction. We did not attempt any pharmacological intervention, but intubation, mechanical ventilation and cardiac massage failed to prevent cardiac arrest. Apnea is also reported with shock tube

experiments (Long et al., 2009). When examined at necropsy, the lungs and other organs except the brain appeared to be normal. Gross examination of the brain showed extensive diffuse subarachnoid hemorrhages, but no internal brain injury. Almost invariably, animals that survived the first several minutes after blast injury did not die later; only 2 of 35 deaths were delayed.

Our findings regarding rapidity of death and pathology from fatal blast injury may be compared to reports on rats following whole-body exposure to blast. With whole body exposure, animals that die are found to have multifocal hemorrhages in the meninges, cerebrum and cerebellum, although whether these hemorrhages were intraparenchymal or not was unclear (Bauman et al., 1997). Also, 50% of deaths occur with 2 min, and all occur within 30 min of the insult (Richmond et al., 1962). It is not clear from available reports what the specific cause of death is following whole body exposure to blast, but the rapid times to death (2 min) argue against entities such as malignant cerebral edema and neurogenic pulmonary edema, and favor instead primary brainstem failure involving cardiac and respiratory centers.

In humans, severe blast injury often results in delayed death that is commonly attributed to cerebral edema and brain swelling (Bauman et al., 2009; Ling et al., 2009). To our knowledge, delayed death has not been reported following blast exposure of rats, suggesting that cerebral edema and brain swelling may not be prominent effects of blast, at least in this species. Transient edema and a modest rise in intracranial pressure have been reported in rats exposed to repeated whole-body blast, but the effects observed were small and non-lethal (Saljo et al., 2009). It appears that the threshold for blast-induced

fatal brainstem injury is lower than that for microvascular dysfunction, at least in the rat. If this is also true in humans, it would suggest that cases of brain edema and swelling may actually not be attributable to dcPBI alone, but may represent dcPBI complicated by some other insult such as hemorrhage or hypotension (DeWitt et al., 2009). Understanding this complex relationship is of paramount importance because of the critical therapeutic implications.

Sublethal effects–neuropathology. Rats with exposure of the head alone to peak overpressures of 500 kPa or less were likely to survive. Animals that survived blast awoke from anesthesia without undue delay and typically could right themselves and sit; spontaneous activity was blunted but they never lapsed into coma or unresponsiveness.

When examined 24 hr after injury, these animals exhibited subarachnoid hemorrhages over the cerebrum, cerebellum and brainstem, although not as prominently as in animals with mortal blast injury. Subarachnoid hemorrhages were observed in rats that survived exposures of 414–655 kPa. The literature suggests a rather steep pressure-response relationship for neuropathological injury in rats with whole-body exposure: whereas 147 kPa overpresssure results in subarachnoid hemorrhage, necrosis, cortical cell loss, gliosis, and infiltration, exposure to 22% smaller overpressures (114 kPa) results in no detectable neuropathological changes (Long et al., 2009).

Sub-lethal dcPBI was associated with abnormal immunolabeling of perfused brains for IgG, consistent with microvascular injury. The abnormalities included scattered regions of microvascular stasis and patches suggestive of vasogenic edema. In some cases, these abnormalities were located in regions near

a subarachnoid hemorrhage, suggesting a possible relationship. However, widespread or generalized extravasation of IgG was not observed, consistent with the absence of malignant cerebral edema, the absence of brain swelling, and the near absence of delayed death. A modest transient increase in intracranial pressure to 16 mm Hg was reported after 3 successive blasts (60 kPa) over 20 min that was attributed to edema formation (Saljo et al., 2009), but overall, brain swelling and malignant edema are not prominent features in any of the rat models reported.

Arguably the most telling abnormalities found with sub-lethal dcPBI involved immunolabeling for β-APP. Both axonal and neuronal abnormities were frequently identified that were broadly similar to findings reported in other forms of TBI (Blumbergs et al., 1995; Bramlett et al., 1997; Itoh et al., 2009; Kilbourne et al., 2009; Pierce et al., 1996; Stone et al., 2000). Abnormalities in β-APP were widespread, involving dorsal and ventral cortex, cerebellum and deep brain regions. The abnormalities in axonal β-APP that we observed likely reflect an injury similar to that identified in other studies of bTBI using silver stains (Long et al., 2009; Svetlov et al., 2010). Pronounced changes in the neuronal cytoskeleton have been reported after blast exposure, with a redistribution of neurofilament proteins in neuronal perikarya that is believed to predispose to delayed nerve cell loss (Saljo et al., 2000). In addition, the perikaryal abnormalities in β-APP that we observed correlated with the abnormal presence of activated caspase-3, which is associated with apoptotic cell death. Neurons in the rat brain may be injured by exposure to overpressures as low as 20 kPa

(Moochhala et al. 2004), with exposure to higher levels (100-300 kPa) causing significant injury to both neuronal and glial cells (Cernak et al., 2001; Kaur et al., 1995; Saljo et al., 2010).

More detailed characterizations of the cellular and axonal abnormalities produced by dcPBI are required, but the findings reported here suggest that the abnormalities identified to date by immunolabeling for β-APP and activated caspase-3 may account for the persistent vestibulomotor abnormalities that we observed in the accelerated RotaRod test. Previous studies with whole-body exposure to blast in rodents found that vestibulomotor abnormalities normalized within one week of injury (Long et al., 2009), although in other studies, abnormalities in wheel running (Bauman et al., 1997) and in an active avoidance task (Cernak et al., 2001) persisted for 5 days. Models in which functional deficits endure is particularly important because bTBI in humans is well known to be associated with long-lasting neurofunctional abnormalities (Finkel, 2006; Ling et al., 2009).

In summary, we developed and validated a novel model of bTBI that is unique in allowing study of the direct effects of blast on the brain, uncomplicated by indirect effects mediated via the thoracic mechanism or other mechanisms of injury. There is no doubt that in combat and other real-life situations, both direct and indirect mechanisms of PBI, as well as secondary, tertiary and quarternary mechanisms, all play crucial roles in determining the overall outcome from bTBI. However, we postulate that understanding the specific contribution of each of these seperate mechanisms will lead to important insights that will improve the

eventual protection and treatment of the unfortunate warfighters and civilians who are victims of bTBI.

Acknowledgements

This work was supported by a grant to JMS from the Department of the Army (PT074766; the U.S. Army Medical Research Acquisition Activity, 820 Chandler Street, Fort Detrick MD 21702-5014 is the awarding and administering acquisition office). The information in this article does not necessarily reflect the position or the policy of the United States Government, and no official endorsement should be inferred.

Table 1. Peak Overpressures with various BDCs

BDC	Length BDC (with BDCCI) (cm)	Diameter BDC (cm)	Peak Overpressure[1] Power Level 2 (kPa)	Peak Overpressure Power Level 4 (kPa)
1	9.5	2.05	579	1372
2	10.5	2.05	545	1054
3	14.5	2.05	483	869
4	19	2.05	414	655
5	30	2.05	303	483
6	17	2.54	421	669
7	19.5	2.54	365	655
8	22	2.54	317	545
9	23.25	2.54	303	531
10	24.5	2.54	290	517
11	27	2.54	262	462
12	28.25	2.54	276	448
13	29.5	2.54	269	427

[1]The values shown are the means of 5-10 test firings.

Literature Cited

ABOUTANOS,M.B. and BAKER,S.P. (1997). Wartime civilian injuries: epidemiology and intervention strategies. J. Trauma **43,** 719-726.

BAUMAN,R.A., ELSAYED,N., PETRAS,J.M., and WIDHOLM,J. (1997). Exposure to sublethal blast overpressure reduces the food intake and exercise performance of rats. Toxicology **121,** 65-79.

BAUMAN,R.A., LING,G., TONG,L., et al. (2009). An introductory characterization of a combat-casualty-care relevant swine model of closed head injury resulting from exposure to explosive blast. J. Neurotrauma **26,** 841-860.

BELANGER,H.G., KRETZMER,T., YOASH-GANTZ,R., PICKETT,T., and TUPLER,L.A. (2009). Cognitive sequelae of blast-related versus other mechanisms of brain trauma. J. Int. Neuropsychol. Soc. **15,** 1-8.

BLUMBERGS,P.C., SCOTT,G., MANAVIS,J., WAINWRIGHT,H., SIMPSON,D.A., and MCLEAN,A.J. (1995). Topography of axonal injury as defined by amyloid precursor protein and the sector scoring method in mild and severe closed head injury. J. Neurotrauma **12,** 565-572.

BOCHICCHIO,G.V., LUMPKINS,K., O'CONNOR,J., et al. (2008). Blast injury in a civilian trauma setting is associated with a delay in diagnosis of traumatic brain injury. Am. Surg. **74,** 267-270.

BRAMLETT,H.M., KRAYDIEH,S., GREEN,E.J., and DIETRICH,W.D. (1997). Temporal and regional patterns of axonal damage following traumatic brain injury: a beta-amyloid precursor protein immunocytochemical study in rats. J. Neuropathol. Exp. Neurol. **56,** 1132-1141.

CERNAK,I., SAVIC,J., IGNJATOVIC,D., and JEVTIC,M. (1999a). Blast injury from explosive munitions. J. Trauma **47,** 96-103.

CERNAK,I., SAVIC,J., MALICEVIC,Z., et al. (1996). Involvement of the central nervous system in the general response to pulmonary blast injury. J. Trauma **40,** S100-S104.

CERNAK,I., SAVIC,J., ZUNIC,G., PEJNOVIC,N., JOVANIKIC,O., and STEPIC,V. (1999b). Recognizing, scoring, and predicting blast injuries. World J. Surg. **23,** 44-53.

CERNAK,I., WANG,Z., JIANG,J., BIAN,X., and SAVIC,J. (2001). Ultrastructural and functional characteristics of blast injury-induced neurotrauma. J. Trauma **50,** 695-706.

CHAVKO,M., KOLLER,W.A., PRUSACZYK,W.K., and MCCARRON,R.M. (2007). Measurement of blast wave by a miniature fiber optic pressure transducer in the rat brain. J. Neurosci. Methods **159,** 277-281.

CHEN,Y.C., SMITH,D.H., and MEANEY,D.F. (2009). In-vitro approaches for studying blast-induced traumatic brain injury. J. Neurotrauma **26,** 861-876.

CLEMEDSON,J.C. (1956). Blast injury. Physiol Rev. **36,** 336-354.

COUPLAND,R.M. and MEDDINGS,D.R. (1999a). Mortality associated with use of weapons in armed conflicts, wartime atrocities, and civilian mass shootings: literature review. BMJ **319,** 407-410.

COUPLAND,R.M. and SAMNEGAARD,H.O. (1999b). Effect of type and transfer of conventional weapons on civilian injuries: retrospective analysis of prospective data from Red Cross hospitals. BMJ **319,** 410-412.

COURTNEY,A.C. and COURTNEY,M.W. (2009). A thoracic mechanism of mild traumatic brain injury due to blast pressure waves. Med. Hypotheses **72,** 76-83.

DENNY-BROWN,D. (1945). Cerebral concussion. Physiol Rev. **25,** 296-325.

DEWITT,D.S. and PROUGH,D.S. (2009). Blast-induced brain injury and posttraumatic hypotension and hypoxemia. J. Neurotrauma **26,** 877-887.

ELDER,G.A. and CRISTIAN,A. (2009). Blast-related mild traumatic brain injury: mechanisms of injury and impact on clinical care. Mt. Sinai J. Med. **76,** 111-118.

FINKEL,M.F. (2006). The neurological consequences of explosives. J. Neurol. Sci. **249,** 63-67.

FRYKBERG,E.R. and TEPAS,J.J., III (1988). Terrorist bombings. Lessons learned from Belfast to Beirut. Ann. Surg. **208,** 569-576.

HAMM,R.J. (2001). Neurobehavioral assessment of outcome following traumatic brain injury in rats: an evaluation of selected measures. J. Neurotrauma **18,** 1207-1216.

HARVEY,J., NANDAKUMAR,J., and KRISHNAN,L.V. (1984). Dynamic calibration of shock overpressure transducers . Pramana **22,** 447-451.

ITOH,T., SATOU,T., NISHIDA,S., TSUBAKI,M., HASHIMOTO,S., and ITO,H. (2009). Expression of amyloid precursor protein after rat traumatic brain injury. Neurol. Res. **31,** 103-109.

KAUR,C., SINGH,J., LIM,M.K., NG,B.L., YAP,E.P., and LING,E.A. (1995). The response of neurons and microglia to blast injury in the rat brain. Neuropathol. Appl. Neurobiol. **21,** 369-377.

KILBOURNE,M., KUEHN,R., TOSUN,C., et al. (2009). Novel model of frontal impact closed head injury in the rat. J. Neurotrauma **26,** 2233-2243.

LING,G., BANDAK,F., ARMONDA,R., GRANT,G., and ECKLUND,J. (2009). Explosive blast neurotrauma. J. Neurotrauma **26,** 815-825.

LONG,J.B., BENTLEY,T.L., WESSNER,K.A., CERONE,C., SWEENEY,S., and BAUMAN,R.A. (2009). Blast overpressure in rats: recreating a battlefield injury in the laboratory. J. Neurotrauma **26,** 827-840.

MOORE,D.F., JERUSALEM,A., NYEIN,M., NOELS,L., JAFFEE,M.S., and RADOVITZKY,R.A. (2009). Computational biology - modeling of primary blast effects on the central nervous system. Neuroimage. **47 Suppl 2,** T10-T20.

MOSS,W.C., KING,M.J., and BLACKMAN,E.G. (2009). Skull flexure from blast waves: a mechanism for brain injury with implications for helmet design. Phys. Rev. Lett. **103,** 108702.

PETRAS,J.M., BAUMAN,R.A., and ELSAYED,N.M. (1997). Visual system degeneration induced by blast overpressure. Toxicology **121,** 41-49.

PIERCE,J.E., TROJANOWSKI,J.Q., GRAHAM,D.I., SMITH,D.H., and MCINTOSH,T.K. (1996). Immunohistochemical characterization of alterations in the distribution of amyloid precursor proteins and beta-amyloid peptide after experimental brain injury in the rat. J. Neurosci. **16,** 1083-1090.

RICHMOND,R., CLARE,V.R., GOLDIZEN,V.C., PRATT,D.E., SANCHEZ,R.T., and WHITE,C.S. (1961). Biological effects of overpressures of 400 milliseconds duration and its employment in biomedical experiments. Aerosp. Med. **32,** 997-1008.

RICHMOND,R., GOLDIZEN,V.C., CLARE,V.R., et al. (1962). The biologic response to overpressure. III. Mortality in small animals exposed in a shock tube to sharprising overpressures of 3 to 4 msec duration. Aerosp. Med. **33,** 1-27.

SALJO,A., BAO,F., HAGLID,K.G., and HANSSON,H.A. (2000). Blast exposure causes redistribution of phosphorylated neurofilament subunits in neurons of the adult rat brain. J. Neurotrauma **17,** 719-726.

SALJO,A., BOLOURI,H., MAYORGA,M., SVENSSON,B., and HAMBERGER,A. (2010). Low-level blast raises intracranial pressure and impairs cognitive function in rats: prophylaxis with processed cereal feed. J. Neurotrauma **27,** 383-389.

SALJO,A., SVENSSON,B., MAYORGA,M., HAMBERGER,A., and BOLOURI,H. (2009). Low-level blasts raise intracranial pressure and impair cognitive function in rats. J. Neurotrauma **26,** 1345-1352.

SIMARD,J.M., GENG,Z., WOO,S.K., et al. (2009a). Glibenclamide reduces inflammation, vasogenic edema, and caspase-3 activation after subarachnoid hemorrhage. J. Cereb. Blood Flow Metab **29,** 317-330.

SIMARD,J.M., YUROVSKY,V., TSYMBALYUK,N., MELNICHENKO,L., IVANOVA,S., and GERZANICH,V. (2009b). Protective effect of delayed treatment with low-dose glibenclamide in three models of ischemic stroke. Stroke **40,** 604-609.

STONE,J.R., SINGLETON,R.H., and POVLISHOCK,J.T. (2000). Antibodies to the C-terminus of the beta-amyloid precursor protein (APP): a site specific marker for the detection of traumatic axonal injury. Brain Res. **871,** 288-302.

STUHMILLER,J., PHILLIPS,Y., and RICHMOND,R. (1991). The physics and mechanisms of primary blast injury., in: *Textbook of Military Medicine. Conventional Warfare: Ballistic, Blast, and Burn Injuries*. R.Bellamy and R.Zajtchuk (eds), Department of the Army, Office of the Surgeon General, Borden Institute: Washington, D.C., pps. 241-270.
Ref Type: Book Chapter

SVETLOV,S.I., PRIMA,V., KIRK,D.R., et al. (2010). Morphologic and Biochemical Characterization of Brain Injury in a Model of Controlled Blast Overpressure Exposure. J. Trauma .

ZEL'DOVICH,Y.B. and RAIZER,Y.P. *Physics of Shock Waves and High-Temperature Hydrodynamic Phenomena*. Academic Press: New York.

Ref Type: Book, Whole

Fig. 1. Cranium Only Blast Injury Apparatus (COBIA). A: Image of COBIA, showing the vertically oriented gun interfacing with the blast dissipation chamber (BDC), which connects in turn to the BDC-cranium interface (BDCCI). **B–D:** Views of the BDCCI before (**B**) and after (**C,D**) positioning the intubated, anesthetized rat; note the uninflated balloon in **B** which when inflated to 10 kPa, promotes contact between the scalp and the O-ring of the BDCCI, and cushions the head from downward acceleration during the blast. **E:** Image of several of the BDCs used, identified by the numbers referred to in Table 1; to the left are shown the brass coupler that interfaces between the barrel of the gun and the BDC, and the BDCCI.

Fig. 2. Validation of the pressure measuring system. A: The pressure step generator used to validate the pressure measuring system (see Methods for description). **B:** The input pressure step and the output waveform recorded during a validation test run; the inset shows the peak of the recorded waveform to illustrate ringing, and the double exponential fit used to estimate the peak value. **C:** Plot of the steady-state input pressures vs. the measured peak pressures estimated from double exponential fits; a least squares fit of the data indicated a slope of 1.025 and an intercept of -7.1 kPa, confirming proper calibration of the pressure measuring system.

Fig. 3. Pressure waveforms generated by COBIA. A: Pressure waveforms generated by COBIA shown at 3 temporal resolutions, with the lowest resolution showing the typical appearance of a Friedlander wave. **B:** Comparison of a

pressure waveform generated by COBIA (**left**) and a published waveform of a blast recorded in an armored vehicle penetrated by a shaped charge munition (**right**); adapted from (Stuhmiller et al., 1991). **C:** Plot the inverse of the square root of the peak overpressures (right-sided ordinate) generated using BDCs of different lengths and cartridges of different power levels vs. the length of the blast dissipation chamber (BDC), demonstrating the linear relationship expected for the inverse square law; the values of the peak overpressures are given on the left-sided ordinate; data from Table 1; BDC internal diameter, 2.05 cm (■, ▲) and 2.54 cm (●, ▼).

Fig. 4. Lethal direct cranial primary blast injury (dcPBI). A: Plot of the percent mortality vs. peak overpressure, showing an LD_{50} ~515 kPa; data from 51 rats, all obtained with BDC's of 2.54 cm internal diameter (series 2). **B:** Image of the scalp at the site of maximum blast exposure following lethal dcPBI, showing discoloration but otherwise minimal signs of injury. **C:** Images of dorsal and ventral brain surfaces showing extensive subarachnoid hemorrhages following lethal dcPBI. **D:** Images of unprocessed parasagittal sections showing the absence of internal hemorrhages following lethal dcPBI. **E:** H&E-stained sections of the brainstem following lethal dcPBI mostly confirming the absence of internal brain hemorrhages (**left**), but occasionally showing one or two microhemorrhages <200 μm (**right**). **F:** H&E-stained sections of the lungs following lethal dcPBI showing normal appearing parenchyma.

Fig. 5. Sub-lethal direct cranial primary blast injury (dcPBI). A: Plot of the duration (mean ± S.E.) of apnea vs. peak overpressure; data from 3–12 rats at each point; 30 rats total. **B:** Plot of the oxygen saturation during 30 min following sub-lethal dcPBI (517 kPa) in 6 sham and 19 injured rats; *, $P<0.05$. **C:** Plot of systolic blood pressure during 30 min following sub-lethal dcPBI (427–517 kPa; 26 rats). **D:** Bar graphs comparing blood gases, serum electrolytes and serum glucose before and 30 min after dcPBI (427–517 kPa; 17 rats).

Fig. 6. Sub-lethal direct cranial primary blast injury (dcPBI) – microvascular abnormalities. A: Image of the dorsal surface of the brain 24 hr after sublethal dcTBI (427 kPa), showing the presence of subarachnoid hemorrhage. **B–G:** Cryosections of cerebellum (**B–D**) and thalamus (**E–G**) immunolabeled for rat IgG 24 hr after sub-lethal dcPBI (517 kPa) (**B,C,E,F,G**) or following sham injury (**D**), showing no labeling in uninjured control (**D**), diffuse pattern of labeling suggestive of vasogenic edema (**C,E**), or distinct microvascular labeling consistent with stasis or thrombosis (**B,F,G**).

Fig. 7. Sub-lethal direct cranial primary blast injury (dcPBI) – neuronal abnormalities. A: Cryosection of the parietal cortex immunolabeled for β-amyloid precursor protein (β-APP) and co-labeled for neuron-specific NeuN, showing bulbous accumulations of β-APP in damaged axons 24 hr after sub-lethal dcPBI (517 kPa). **B,C:** Cryosection of the entorhinal cortex immunolabeled for IgG and co-labeled for β-APP, showing tissue injury near the

tip with surrounding penumbral vasogenic edema and β-APP upregulation 24 hr after sub-lethal dcPBI (517 kPa). **C:** Cryosection of the cerebellar cortex immunolabeled for β-APP and co-labeled for activated caspase-3, showing prominent upregulation of both in Purkinje cells 24 hr after sub-lethal dcPBI (517 kPa). **D:** Performance on the accelerating RotaRod in sham-injured rats (n=16) and in rats with sublethal dcPBI (427 kPa, n=14; 517 kPa, n=5), showing significant abnormalities that persisted for the entire week of testing; *, $P<0.05$; **, $P<0.01$.

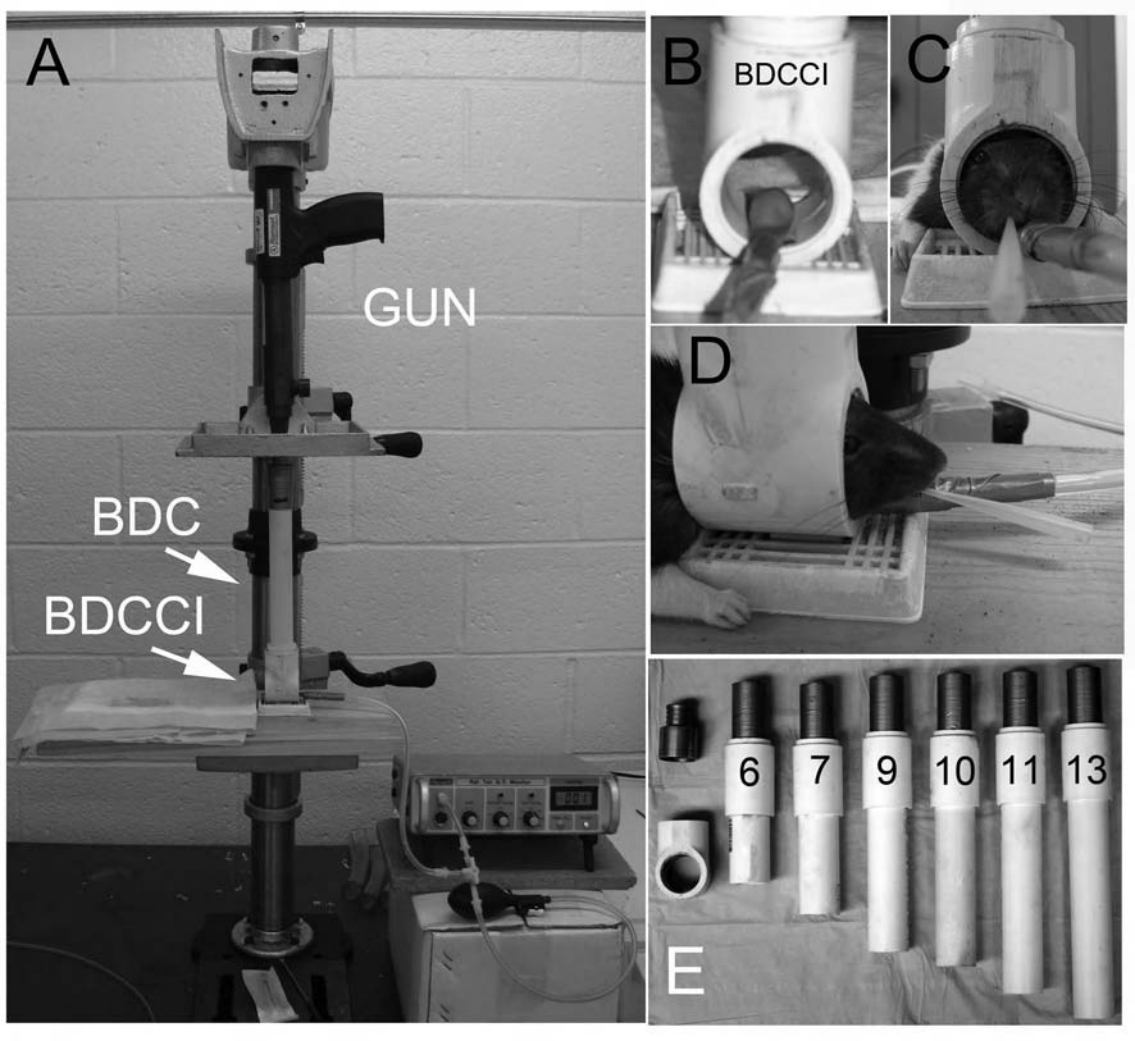
A
GUN
BDC
BDCCI
B
BDCCI
C
D
6
7
9
10
11
13
E

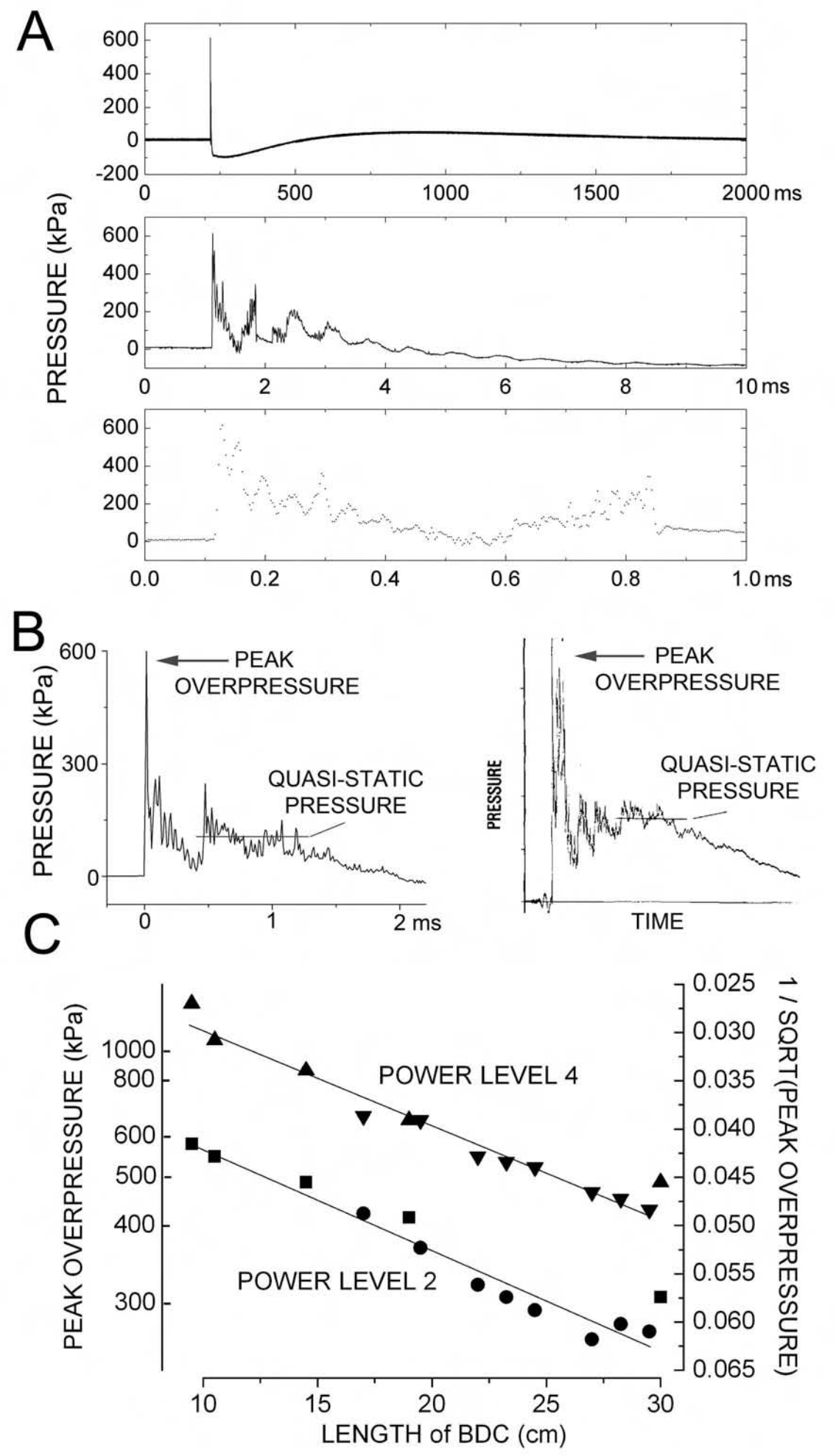
A
PRESSURE (kPa)
600
400
200
0
-200
0
500
1000
1500
2000 ms
600
400
200
0
0
2
4
6
8
10 ms
600
400
200
0
0.0
0.2
0.4
0.6
0.8
1.0 ms
B
PRESSURE (kPa)
600
300
0
PEAK
OVERPRESSURE
QUASI-STATIC
PRESSURE
0
1
2 ms
PRESSURE
PEAK
OVERPRESSURE
QUASI-STATIC
PRESSURE
TIME
C
PEAK OVERPRESSURE (kPa)
1000
800
600
500
400
300
POWER LEVEL 4
POWER LEVEL 2
1 / SQRT(PEAK OVERPRESSURE)
0.025
0.030
0.035
0.040
0.045
0.050
0.055
0.060
0.065
10
15
20
25
30
LENGTH of BDC (cm)

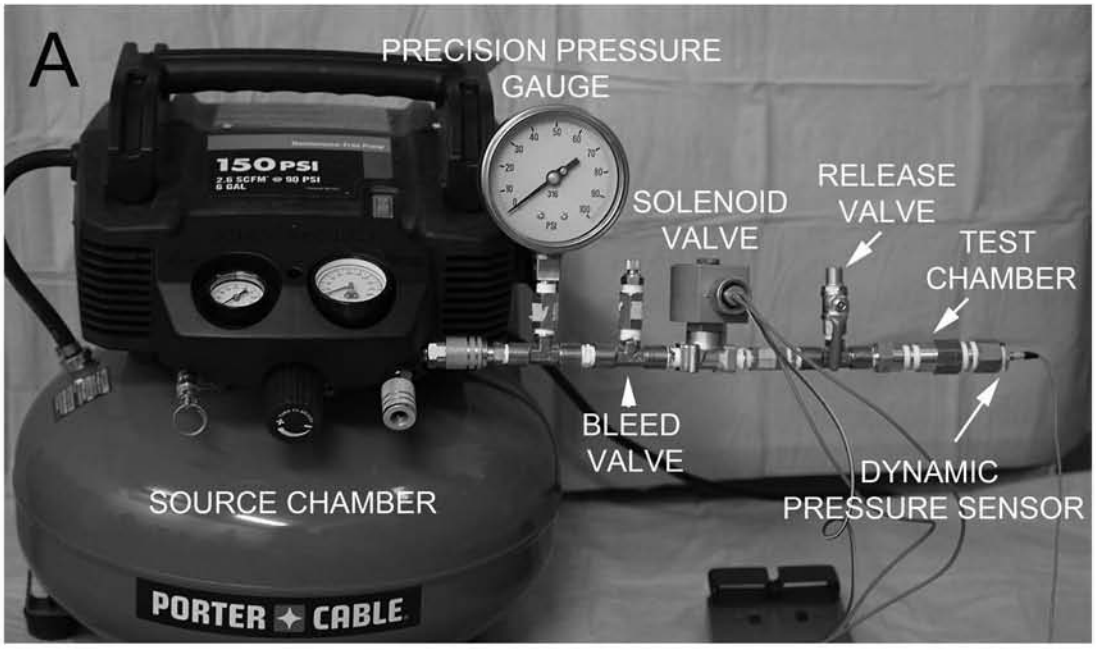
A
PRECISION PRESSURE GAUGE
SOLENOID VALVE
RELEASE VALVE
TEST CHAMBER
BLEED VALVE
DYNAMIC PRESSURE SENSOR
SOURCE CHAMBER
150 PSI
PORTER CABLE

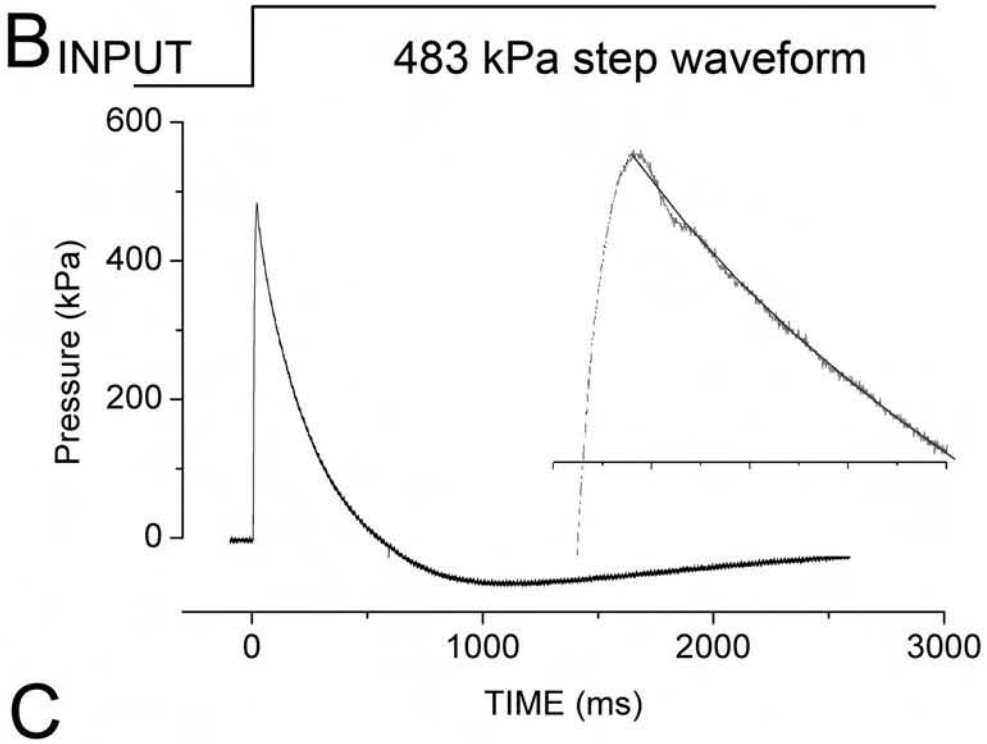
B
INPUT
483 kPa step waveform
600
400
200
0
Pressure (kPa)
0
1000
2000
3000
TIME (ms)

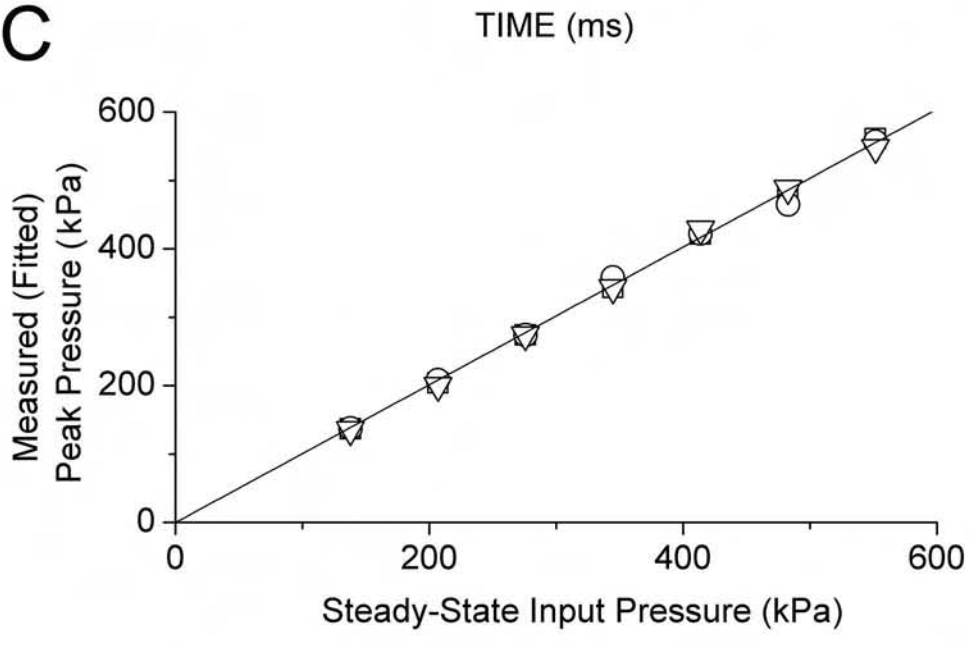
C
600
400
200
0
Measured (Fitted) Peak Pressure (kPa)
0
200
400
600
Steady-State Input Pressure (kPa)

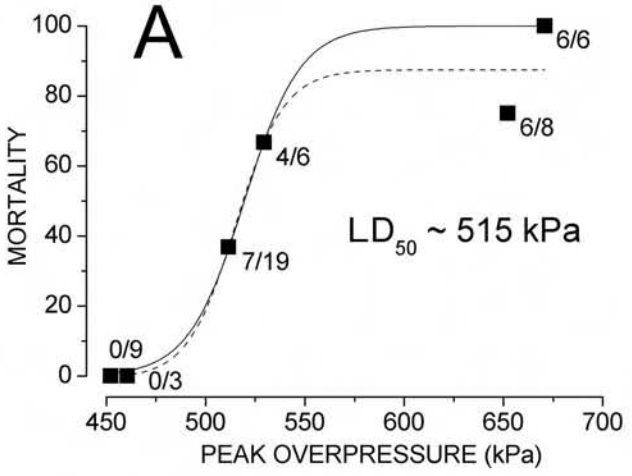
A
100
80
60
40
20
0
MORTALITY
6/6
6/8
4/6
7/19
0/9
0/3
LD50 ~ 515 kPa
450
500
550
600
650
700
PEAK OVERPRESSURE (kPa)

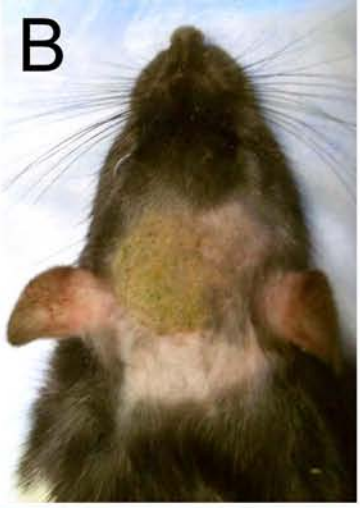
B

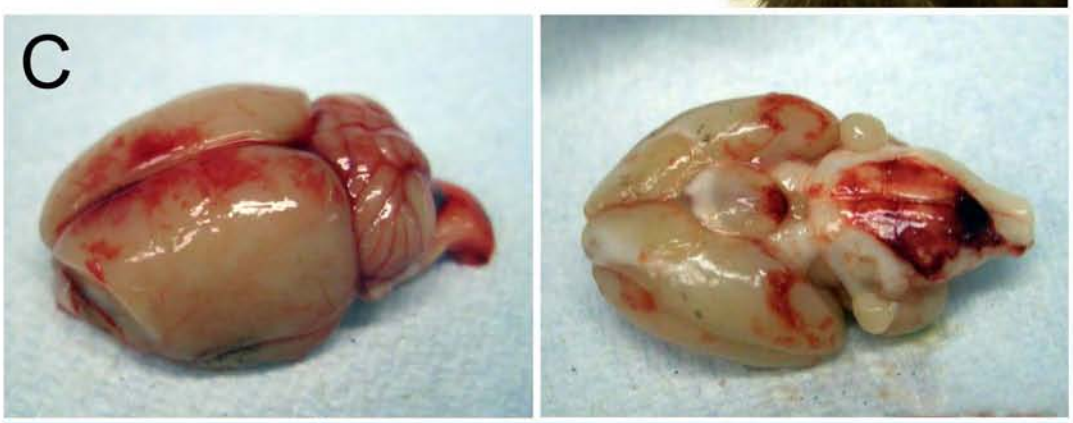
C


D

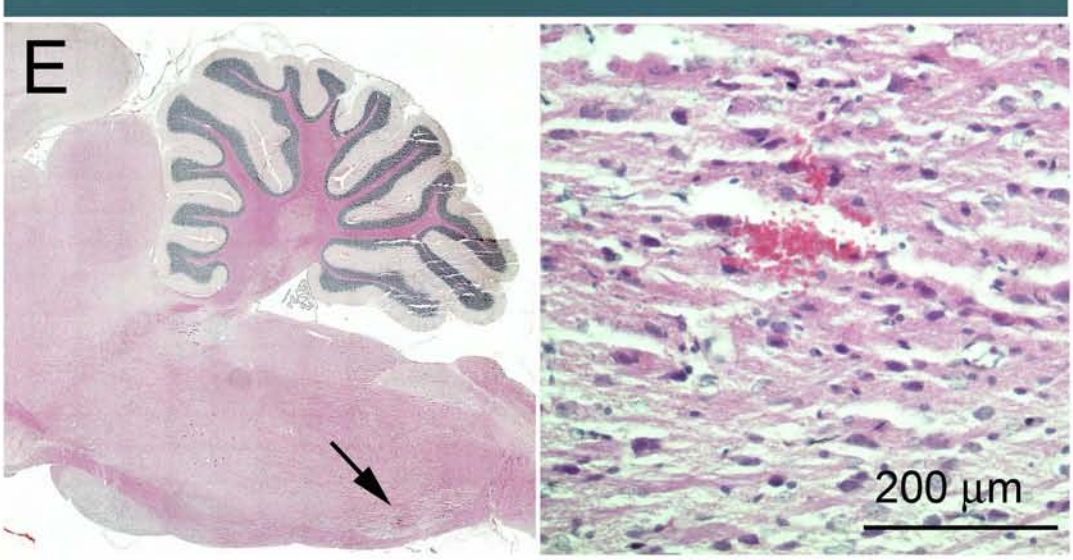
E
200 µm


F

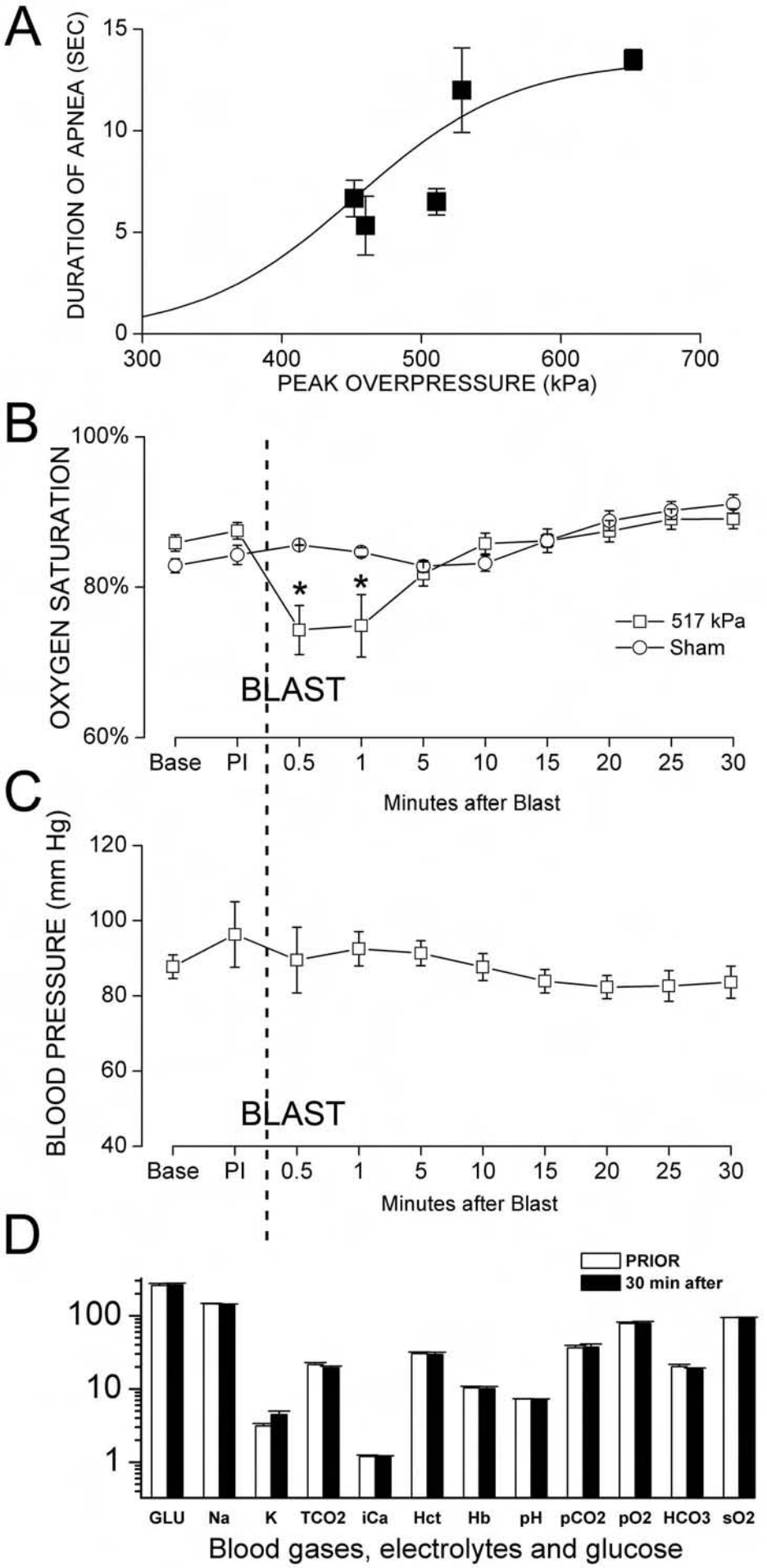
A
DURATION OF APNEA (SEC)
15
10
5
0
300
400
500
600
700
PEAK OVERPRESSURE (kPa)
B
OXYGEN SATURATION
100%
80%
60%
*
*
517 kPa
Sham
BLAST
Base
PI
0.5
1
5
10
15
20
25
30
Minutes after Blast
C
BLOOD PRESSURE (mm Hg)
120
100
80
60
40
BLAST
Base
PI
0.5
1
5
10
15
20
25
30
Minutes after Blast
D
PRIOR
30 min after
100
10
1
GLU
Na
K
TCO2
iCa
Hct
Hb
pH
pCO2
pO2
HCO3
sO2
Blood gases, electrolytes and glucose

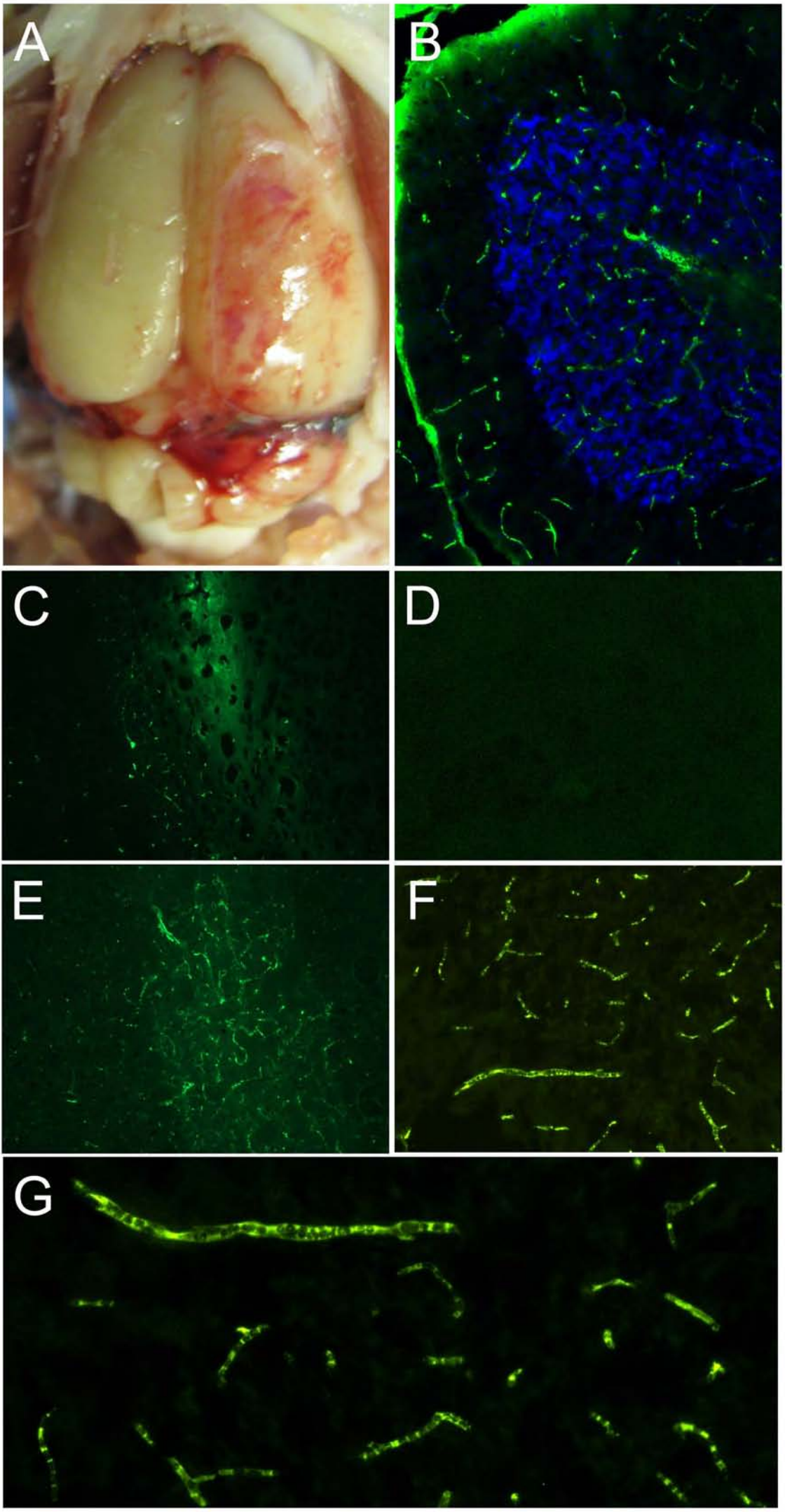
A
B
C
D
E
F
G

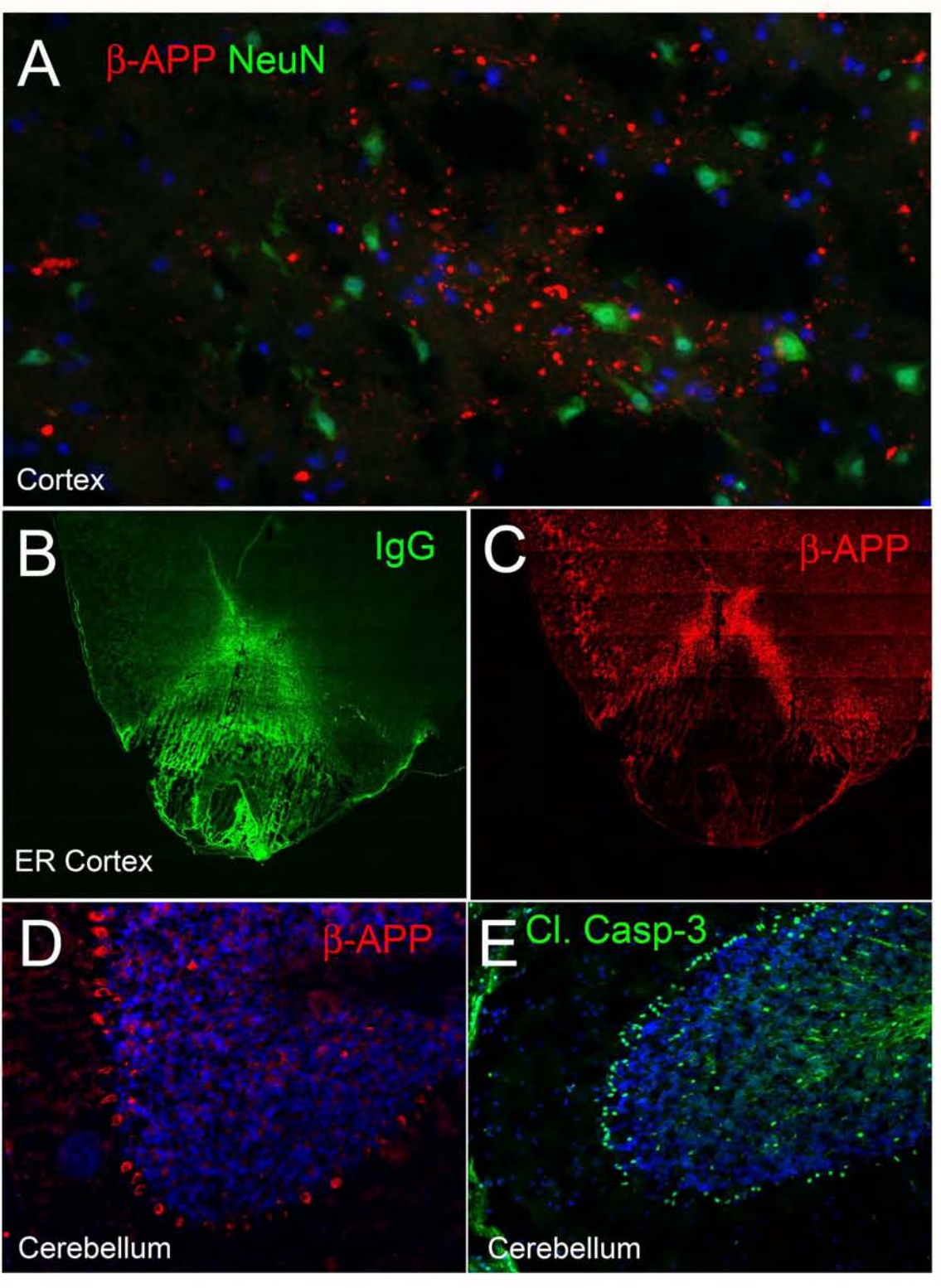
A
β-APP NeuN
Cortex
B
IgG
ER Cortex
C
β-APP
D
β-APP
Cerebellum
E
Cl. Casp-3
Cerebellum

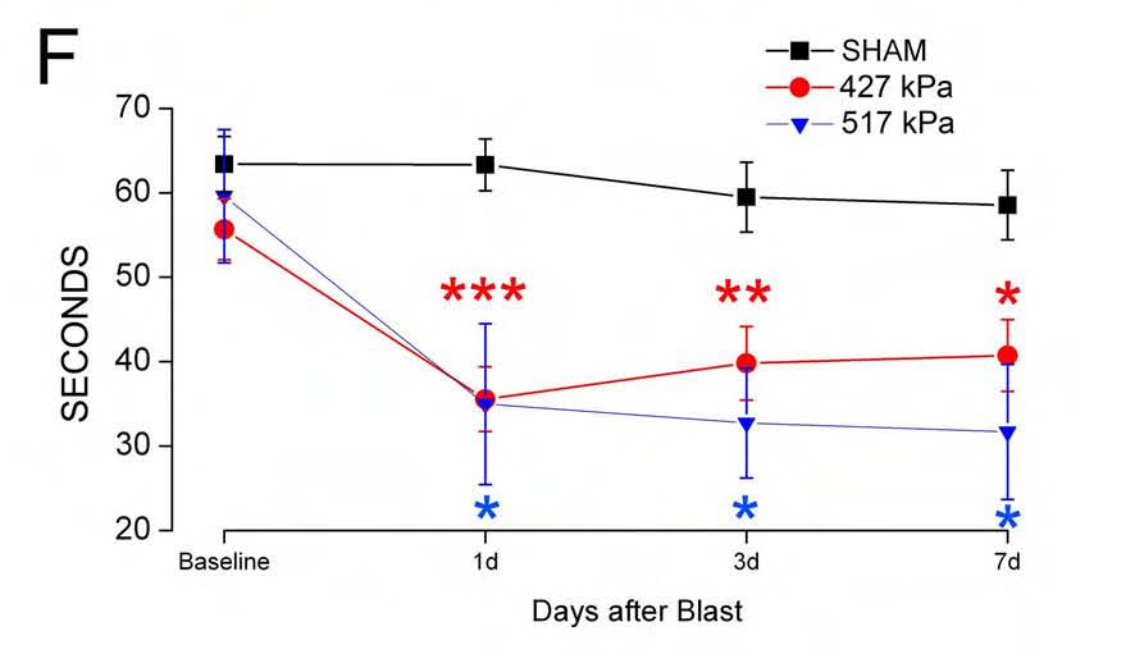
F
SHAM
427 kPa
517 kPa
SECONDS
70
60
50
40
30
20
***
**
*
*
*
*
Baseline
1d
3d
7d
Days after Blast

Direct Cranial Blast Rodent Model of Blast Traumatic Brain Injury

University of Maryland School of Medicine

Walter Reed Army Medical Center

J. Marc Simard, Philippe F. Simard, Reed Kuehn,
Ian Driscoll, Kaspar Keledjian, Svetlana Ivanova,
Turhan Coksaygan, Grant Bocchicchio,
Volodymyr Gerzanich

Blast-TBI – Background

- Multiple mechanisms of primary, secondary, tertiary and quaternary blast injury
- Primary injury to the brain is complex:
  - direct transcranial propagation of the blast wave;
  - indirect transmittal via the vasculature following blast to the thorax (Cernak et al., 2001; Long et al., 2009)

Blast-TBI
Urgent Research Needs

- Rat model of direct blast-TBI that yields:
  - reproducible, graded blast directed to the cranium
  - minimizes head movement (2^{nd} injury)
  - minimizes exposure of the thorax and airway / lungs
- Standardized model
  - Blast generator (shock tube vs. detonation)
  - Attention to “route” of injury (transcranial vs. via thorax)

Cranium-Only Blast Injury Apparatus COBIA

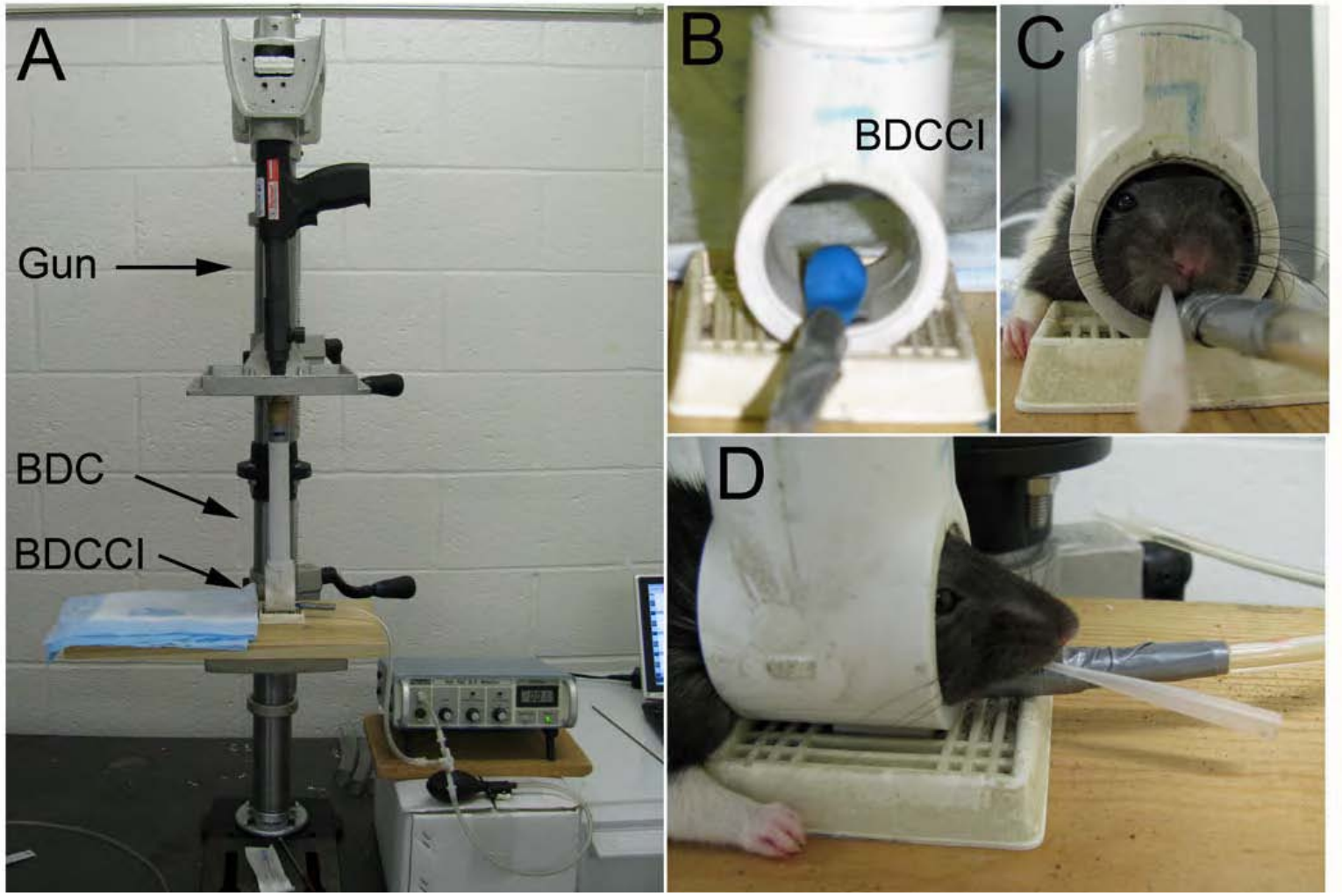

Blast Dissipation Chambers

Blast waveforms from COBIA

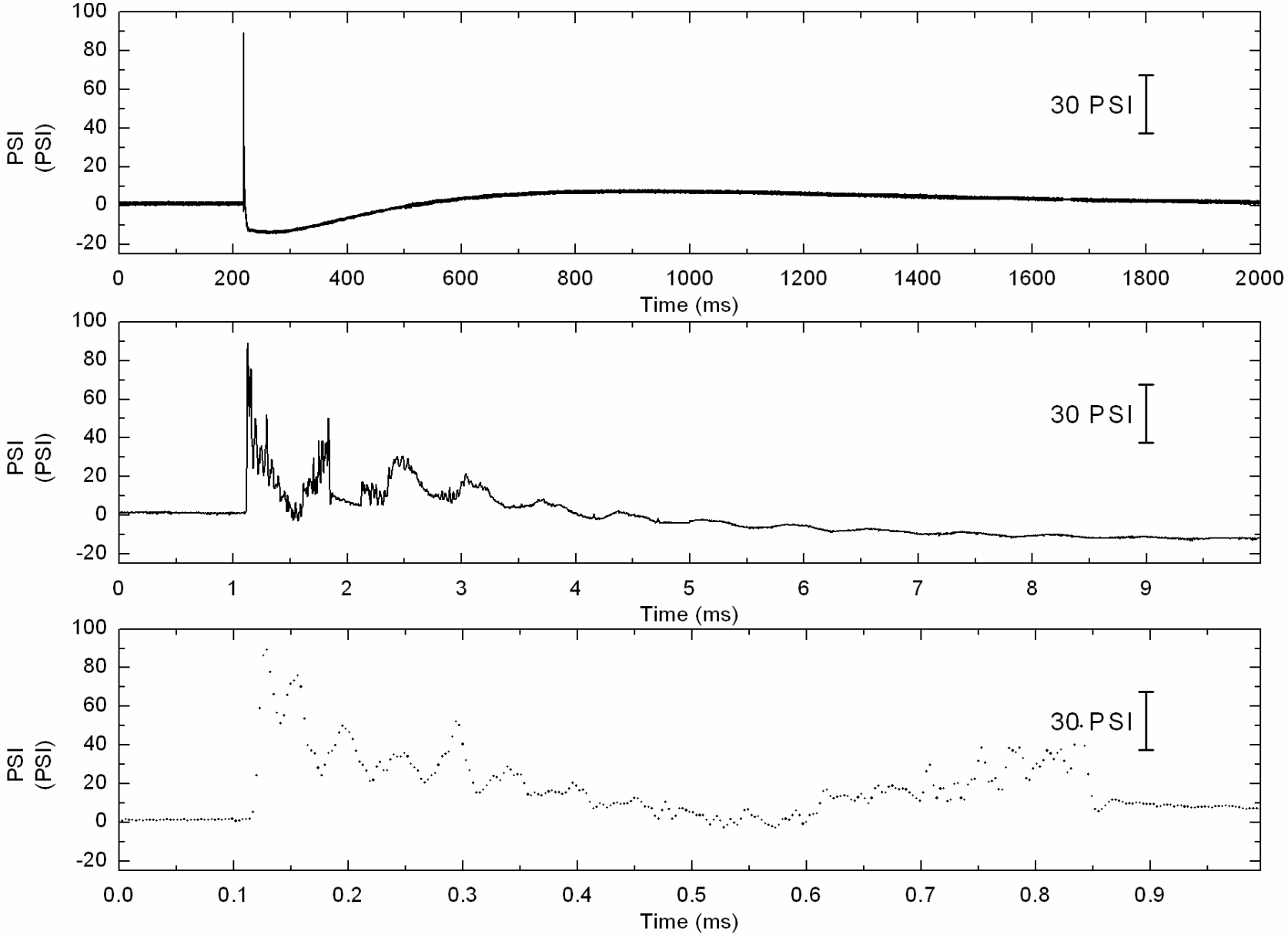

Blast waveforms
COBIA vs. real-world

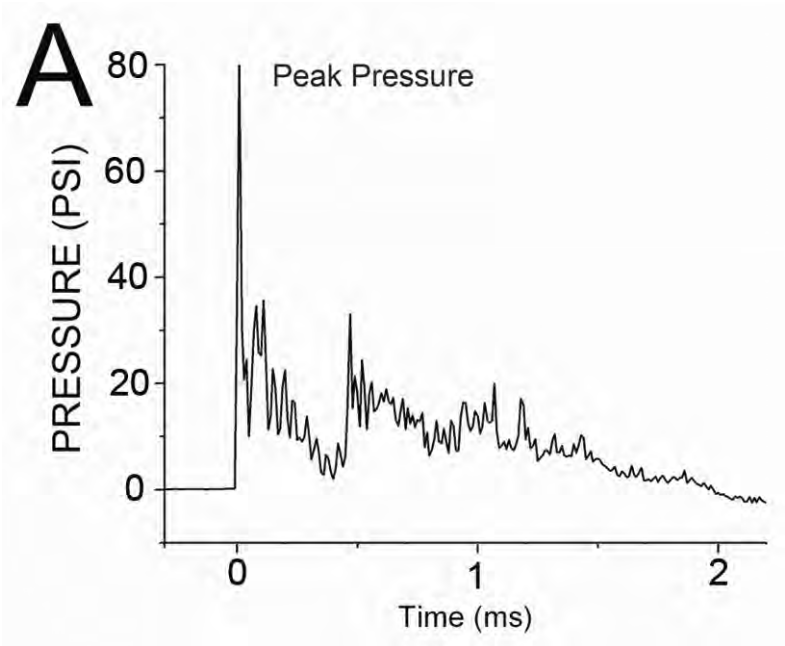

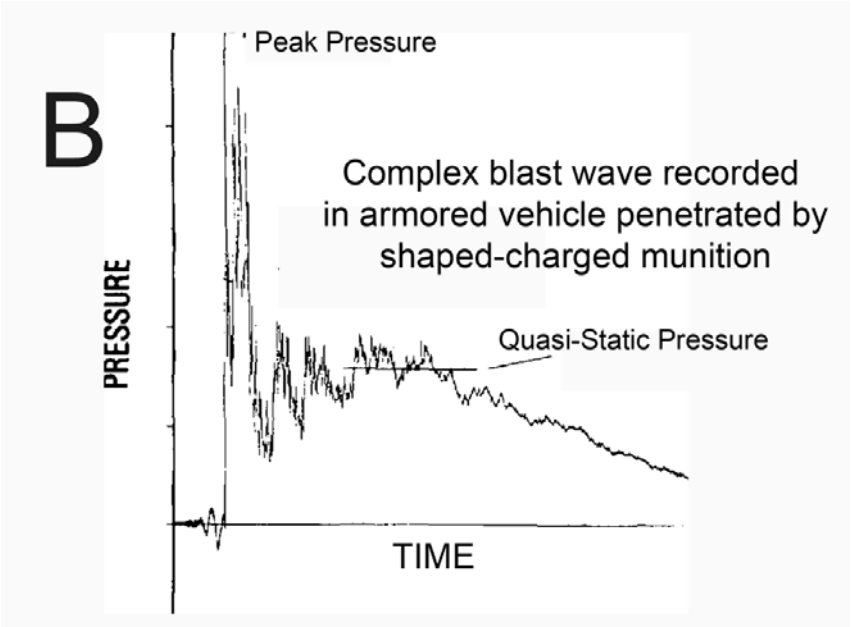

FEATURES OF COBIA

- Gradable peak overpressure
- Blast is directed from above
  - ventral surface of the head is supported and protected by an inflated balloon
  - minimizes impact/translation-induced trauma
- Blast is confined to a narrow corridor (2.54 cm)
  - Airway is outside of the corridor
  - Thorax is outside of the corridor
- Blast is generated by detonating smokeless powder
  - shock wave
  - no gas venting jet to impact head (as with shock tube)

Pressure Measuring System

Columbia Research Laboratories, Inc.

Model 4601
Charge Amplifier

Model 100-P

Charge Amplifier

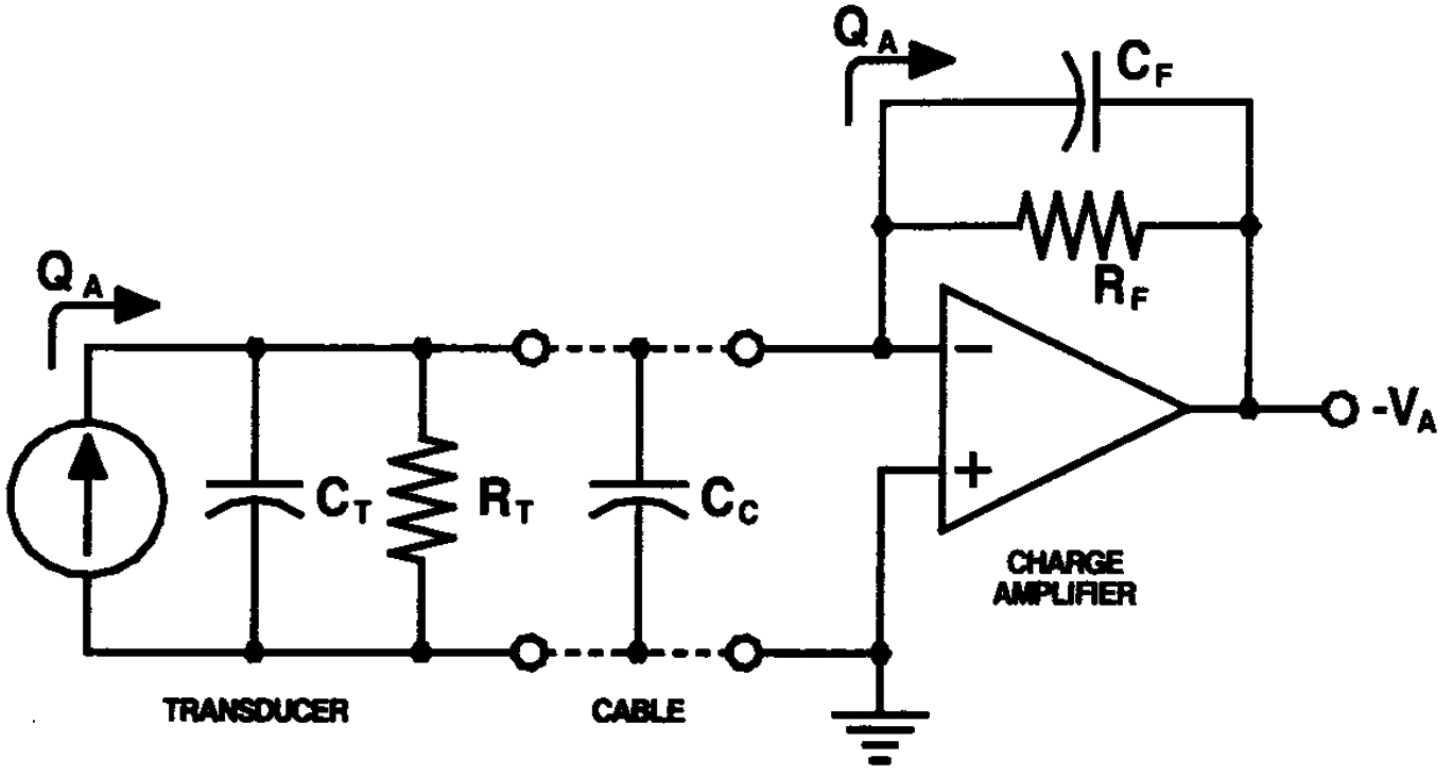

Validation of Measuring System

Source vs. test chambers: 22,712 vs. 15 ml

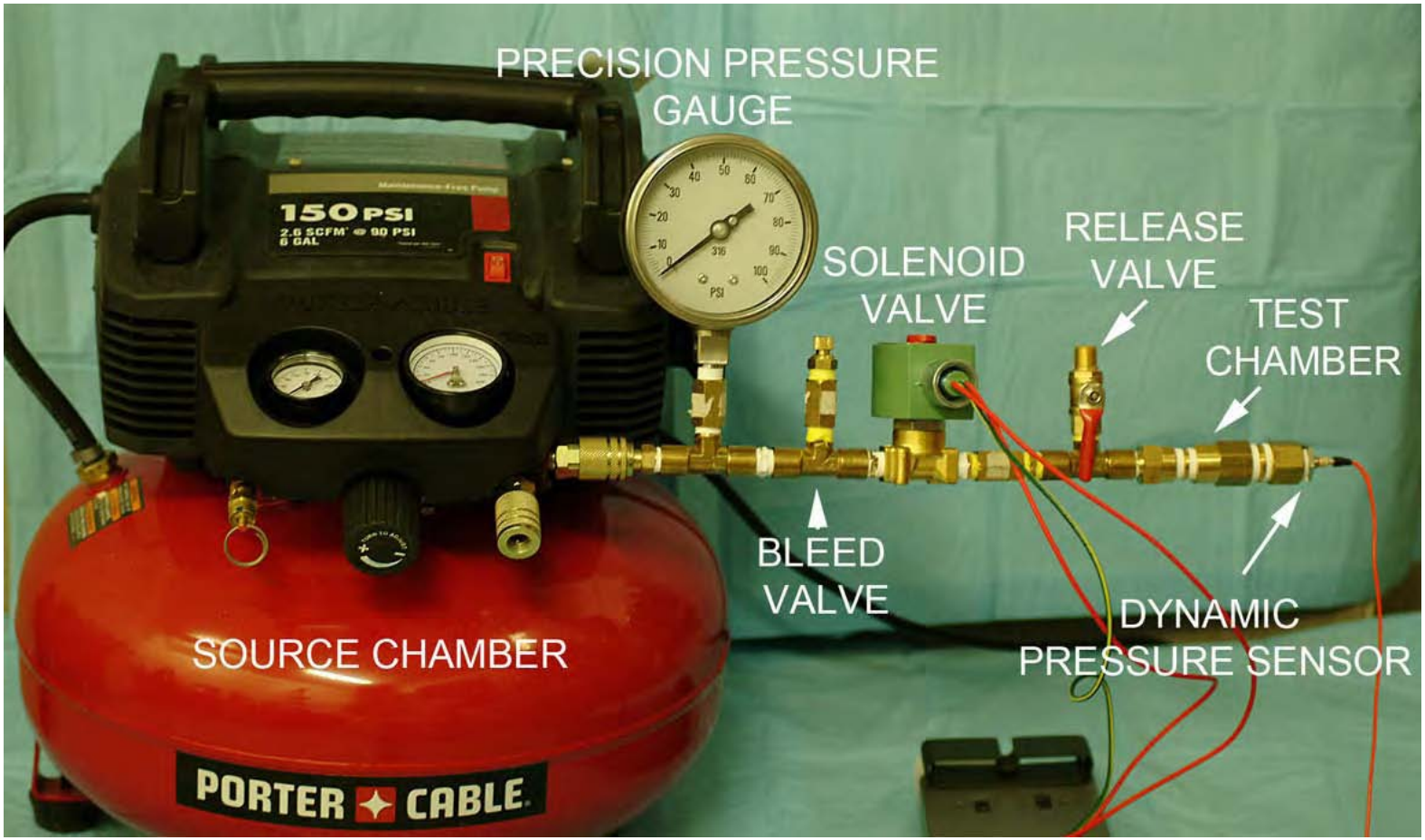

Validation of Measuring System

INPUT	70 psi step waveform

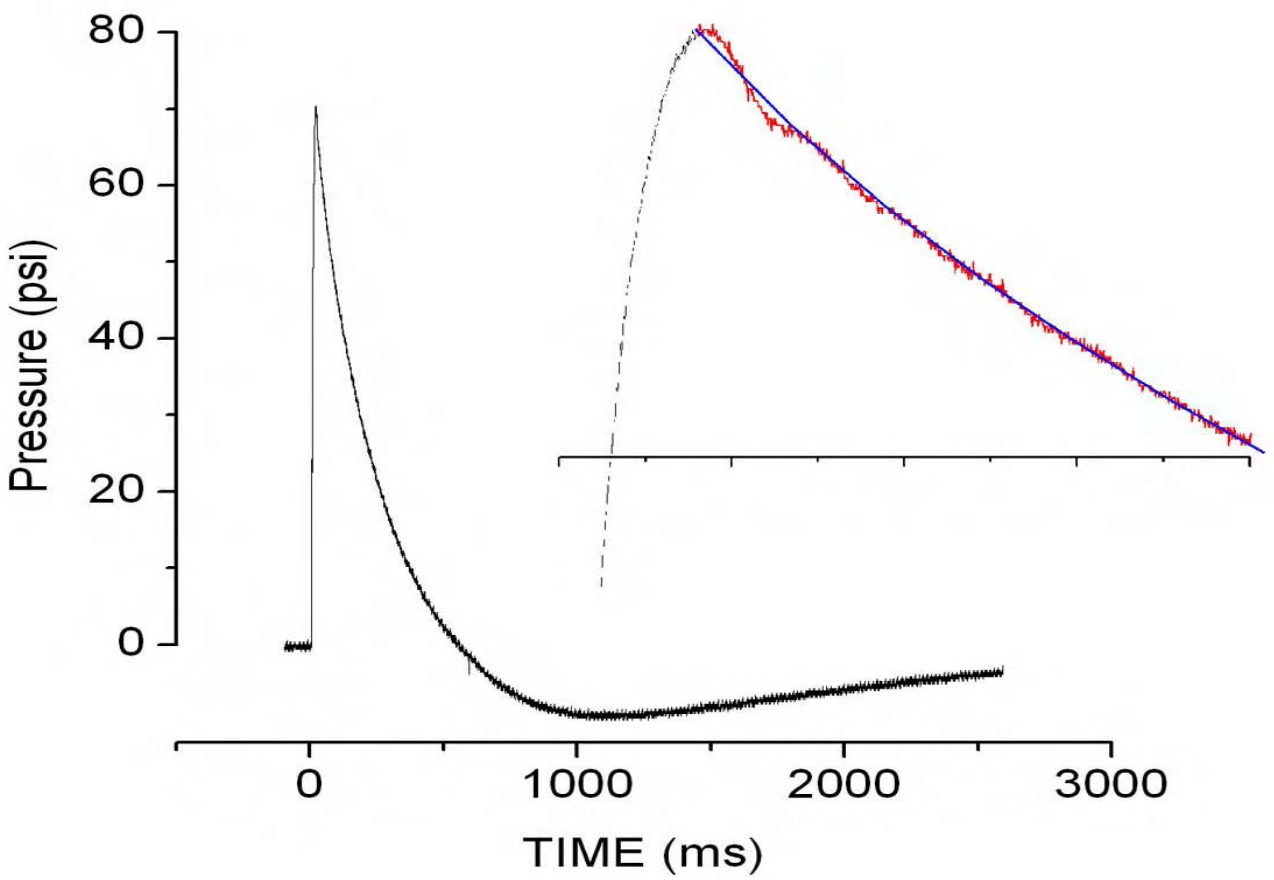

Validation of Measuring System

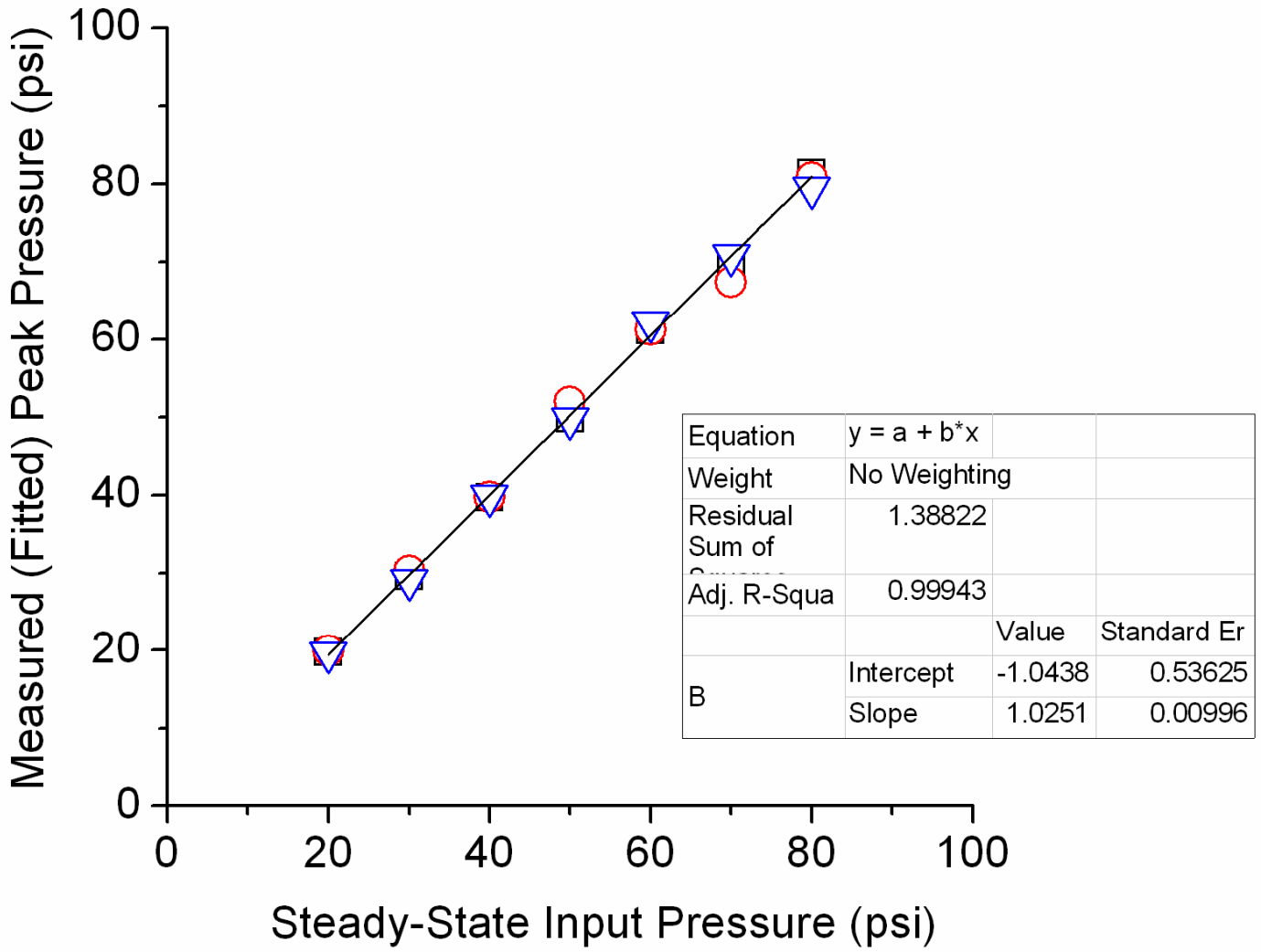

Blast Dissipation Chambers

Peak Overpressures

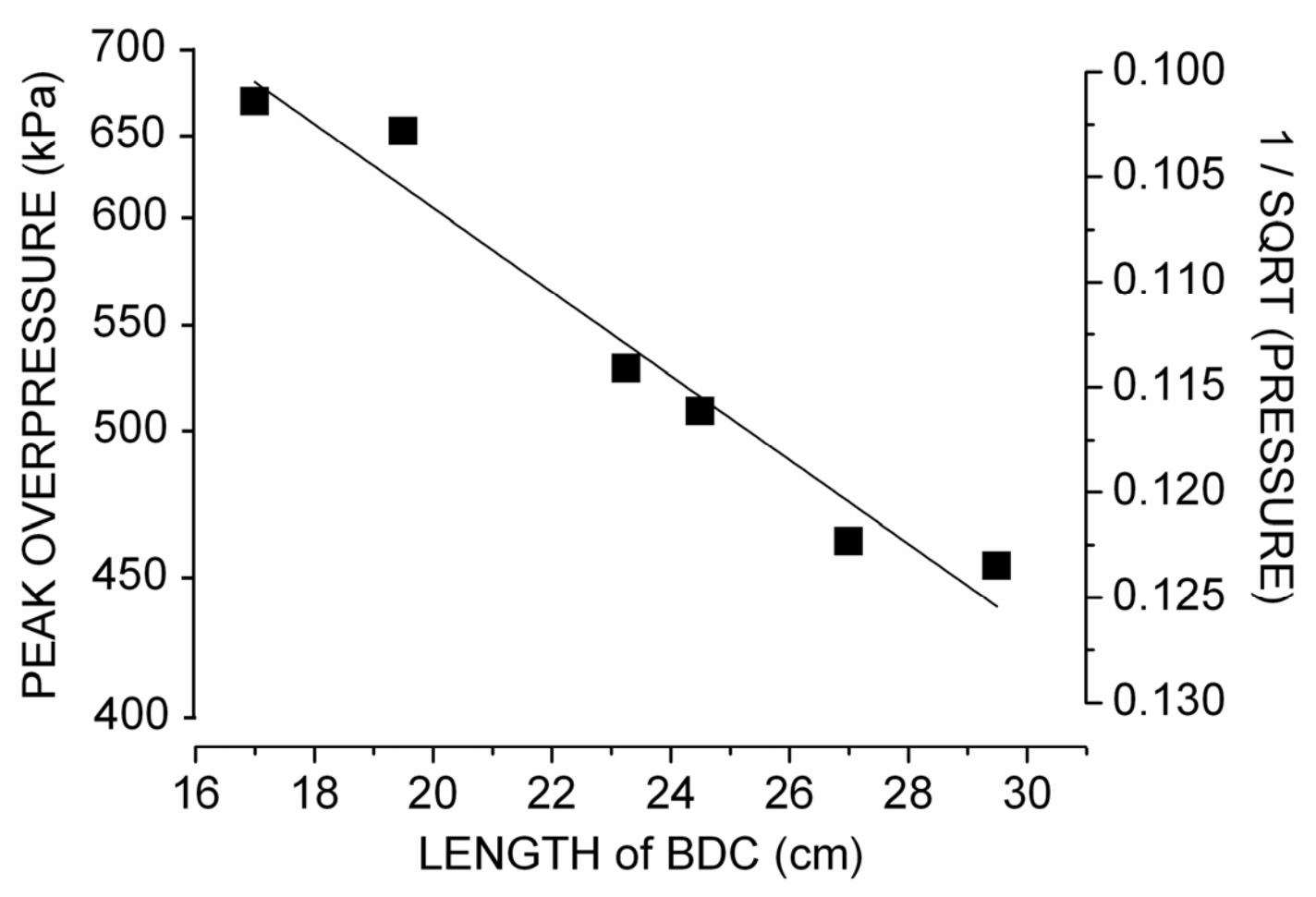

Site of Primary Blast Injury
→ only skin discoloration

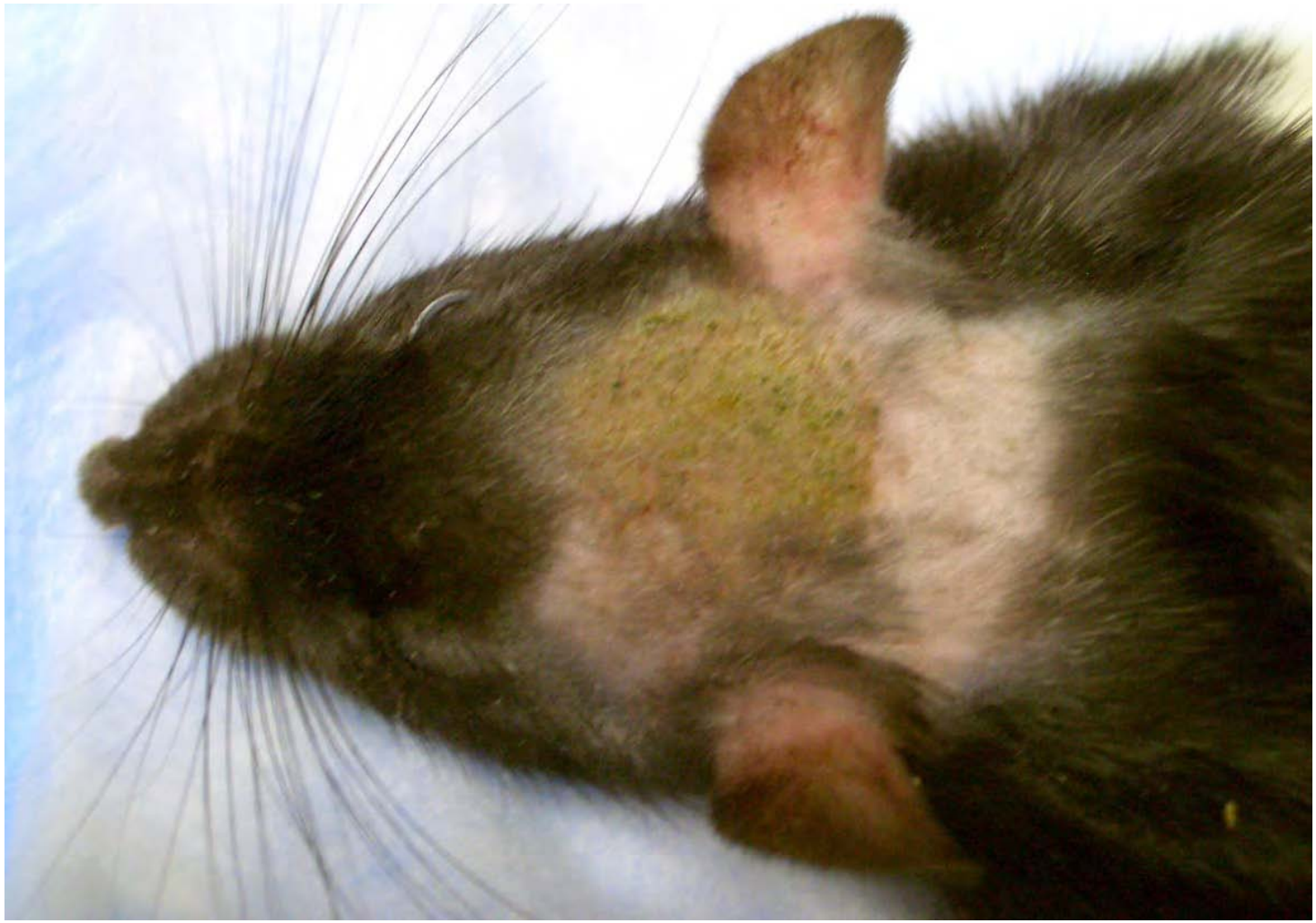

Lethal blast-TBI

→ immediate subarachnoid hemorrhages

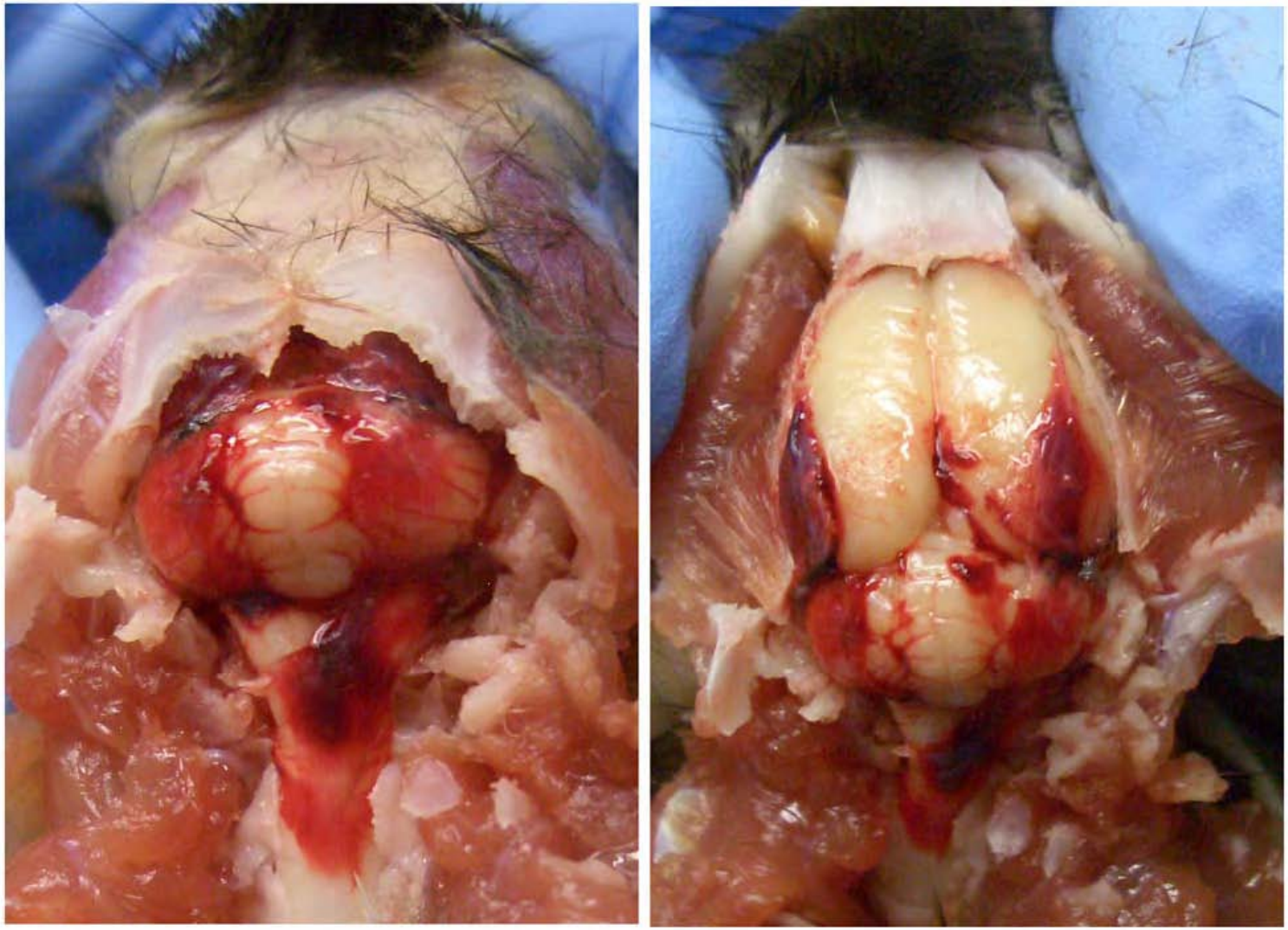

Lethal blast-TBI

→ immediate subarachnoid hemorrhages dorsal and ventral surfaces of the brain

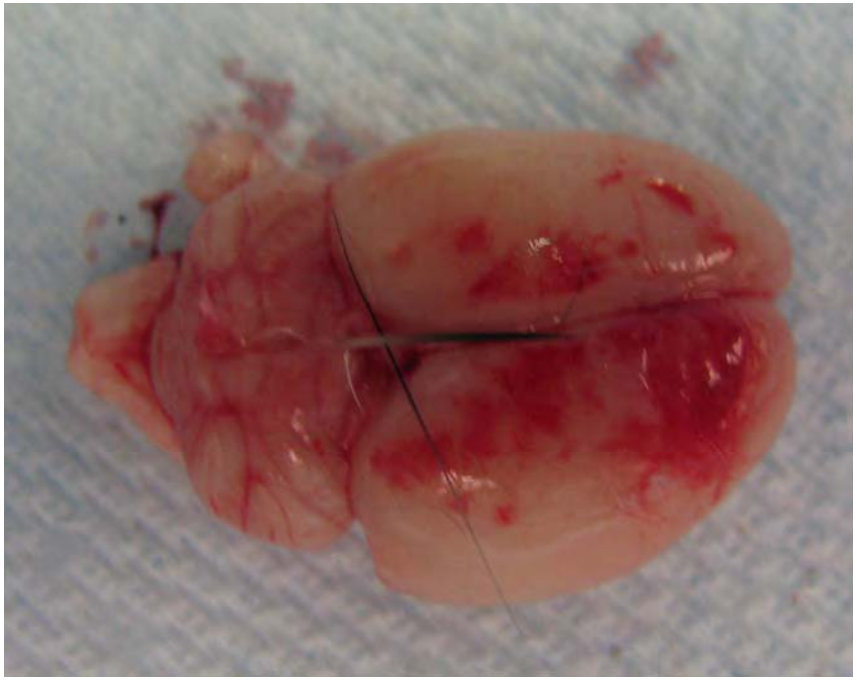

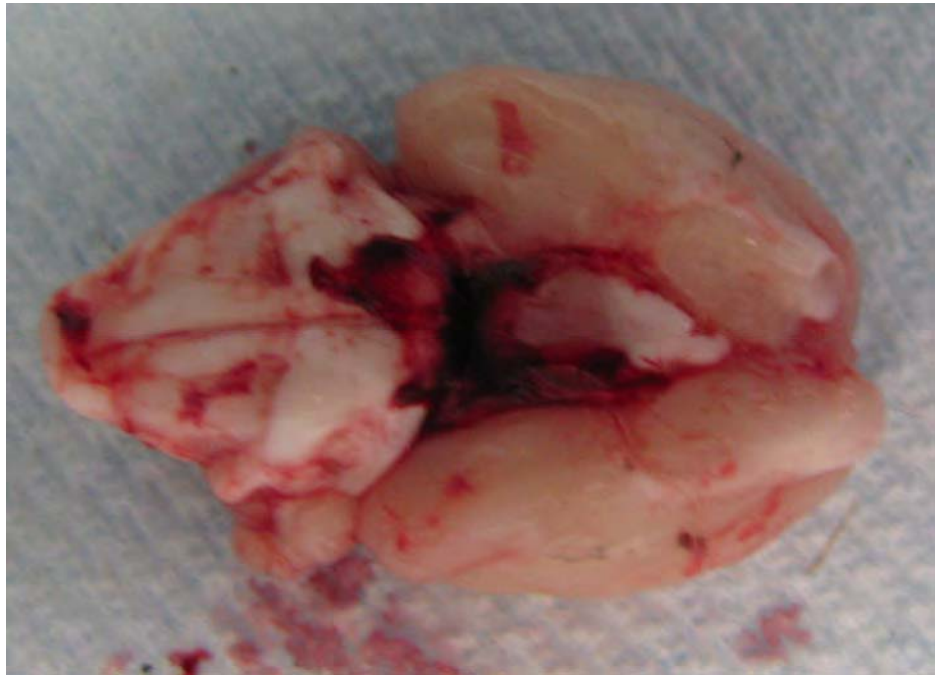

Lethal blast-TBI

→ no intracerebral hemorrhages

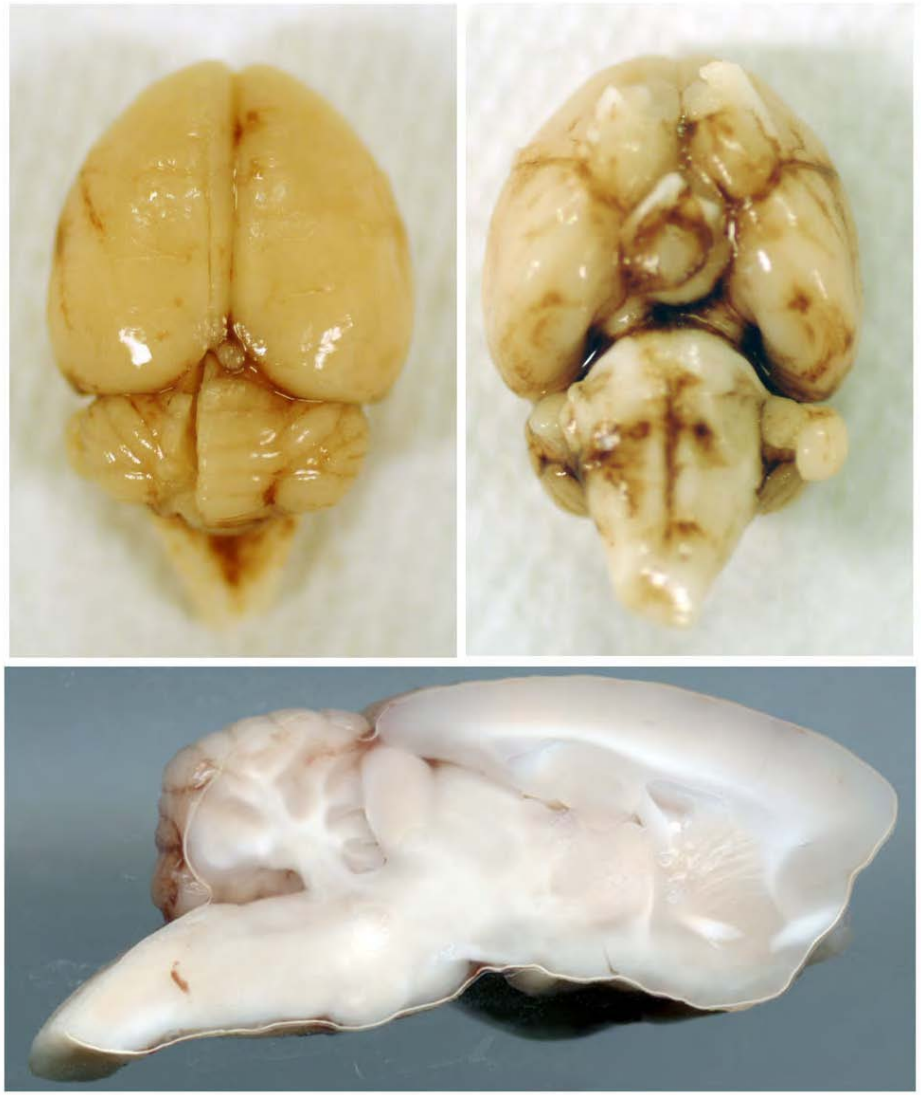

Lethal blast-TBI

→ subarachnoid hemorrhage

→ no intracerebral hemorrhage

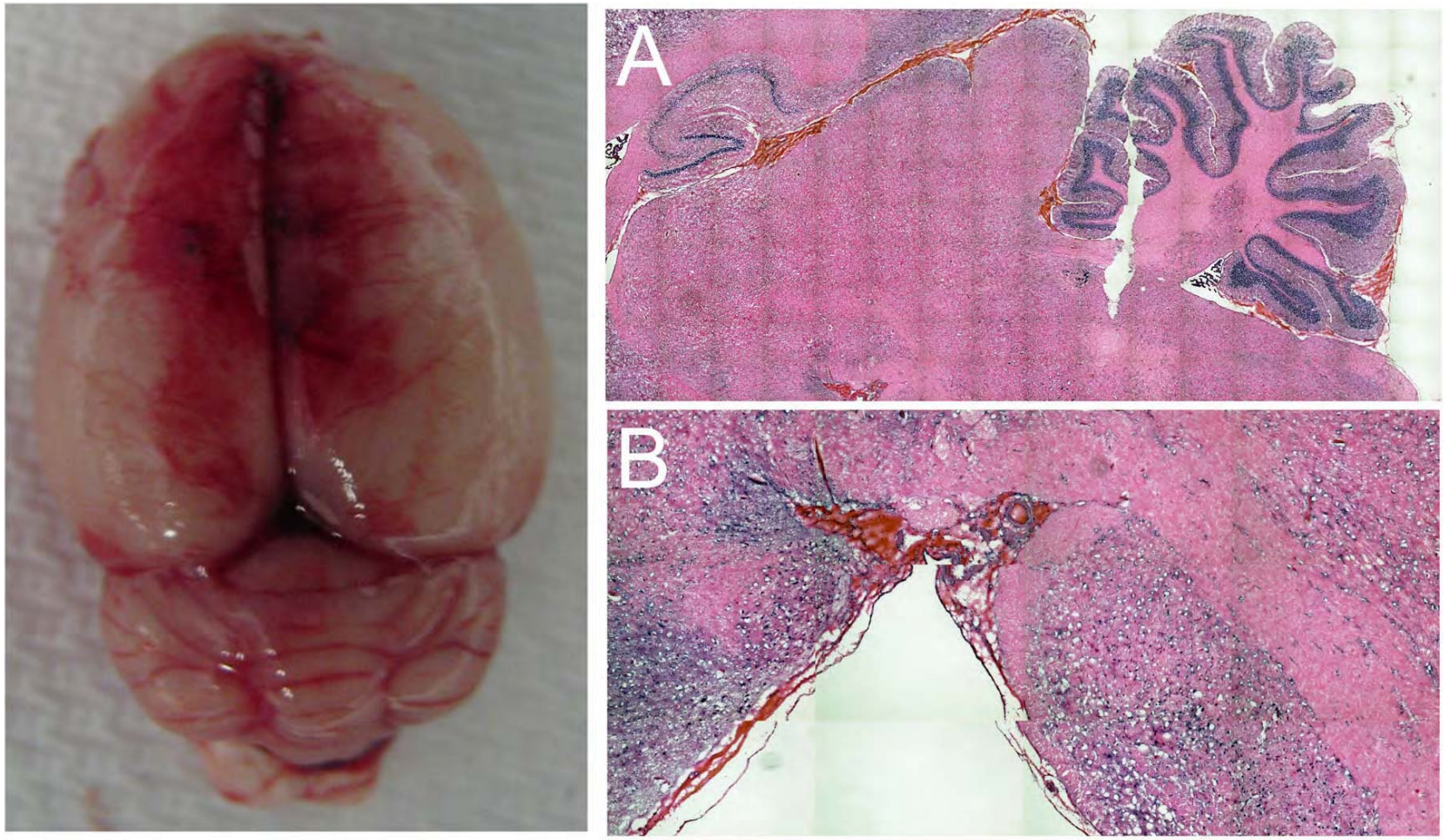

Sub-lethal blast-TBI

→ immediate subarachnoid hemorrhage

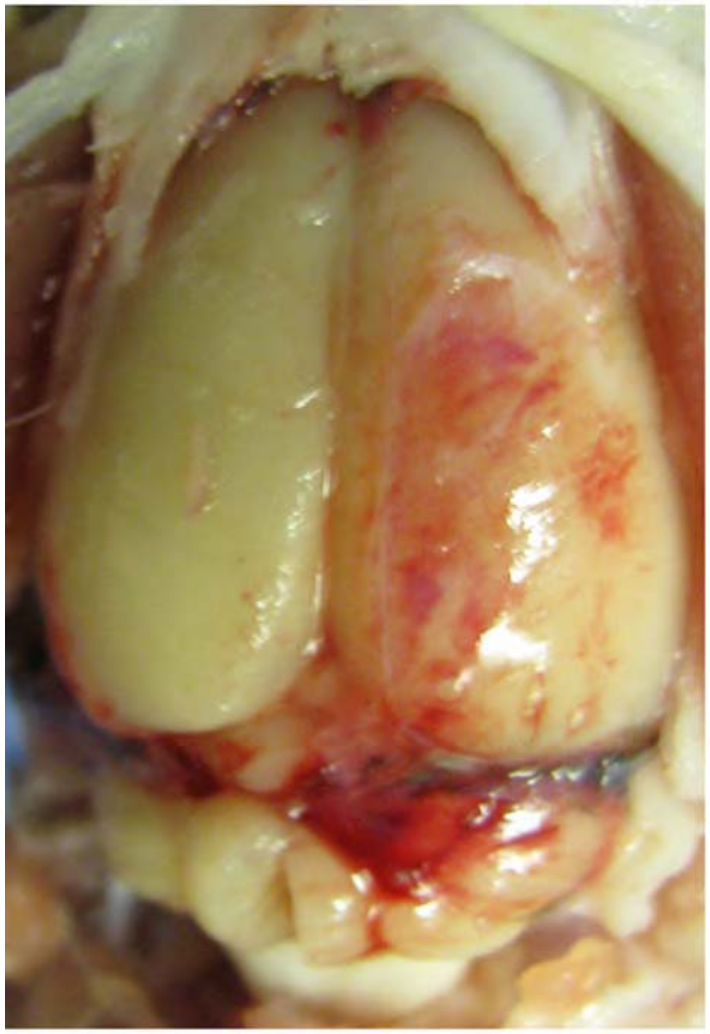

MORTALITY

→ all deaths are immediate

→ no delayed deaths

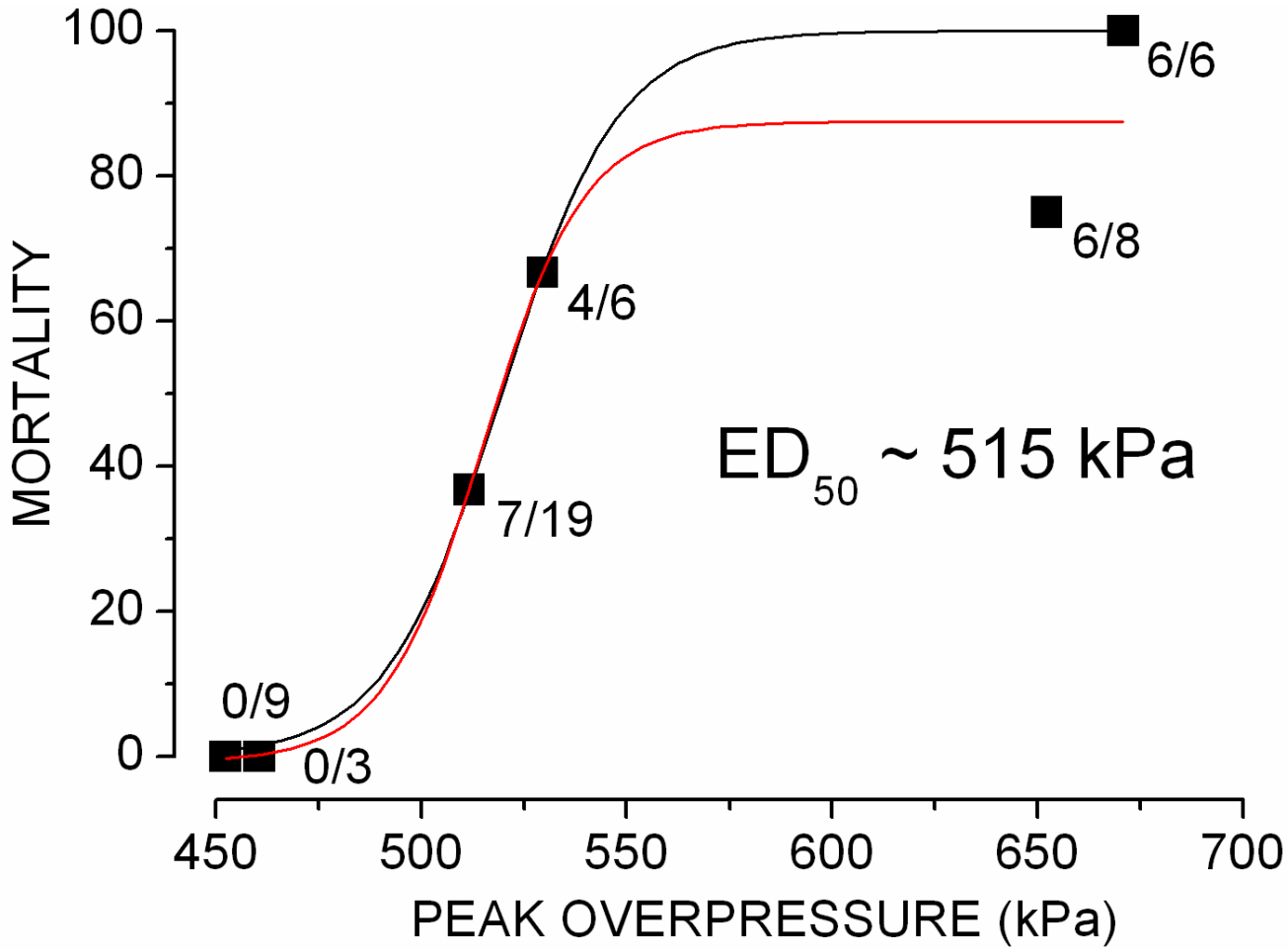

APNEA

- Duration of apnea – dose dependent
- Prolonged apnea (up to 15 sec)
  - Cardiopulmonary arrest
  - Intubation, ventilation, resuscitation completely ineffective
  - No accompanying rise in BP
  - As if the brainstem simply shut down

Apnea in Sub-Lethal Blast-TBI

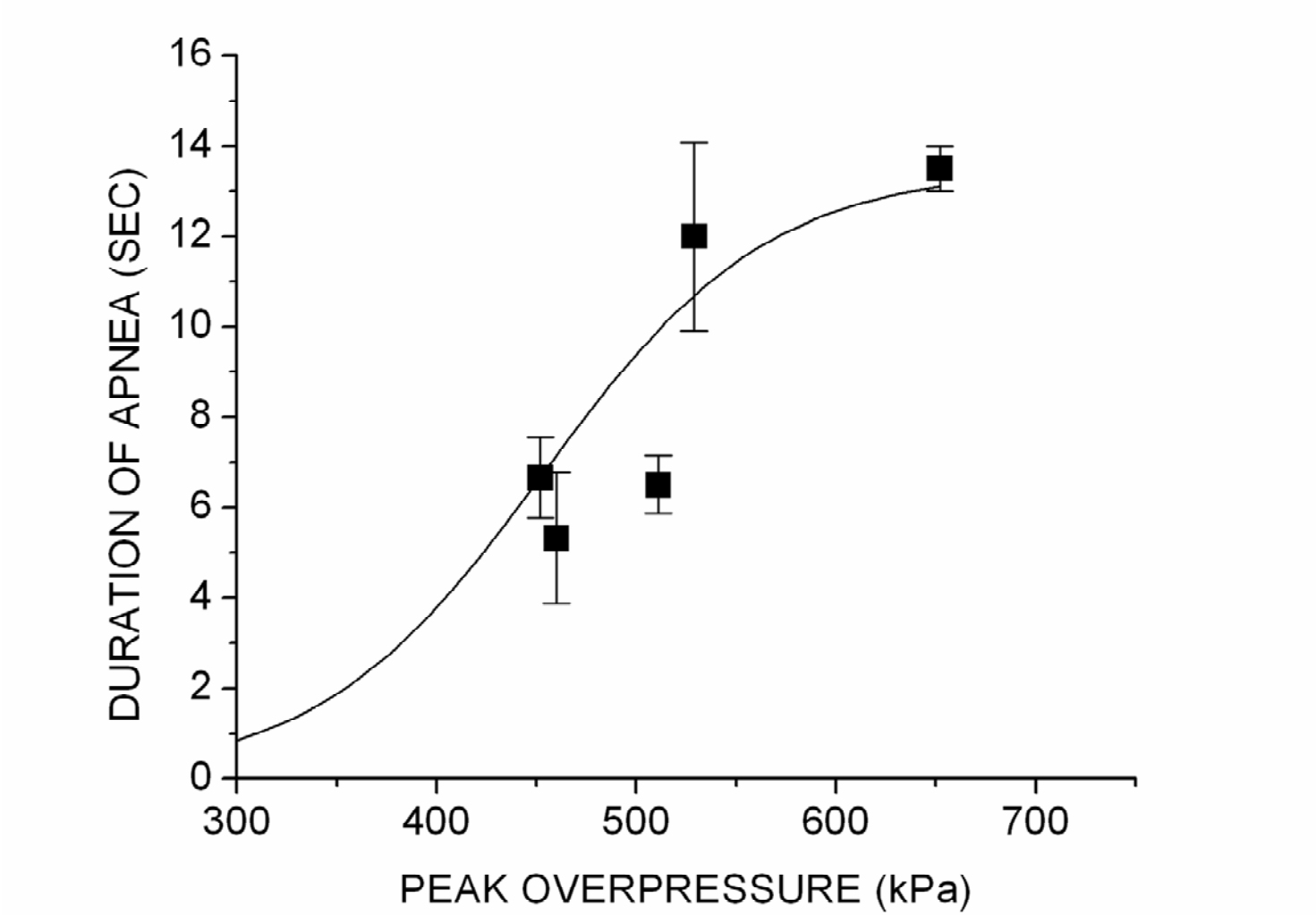

Lethal blast-TBI

→ no lung parenchymal injury

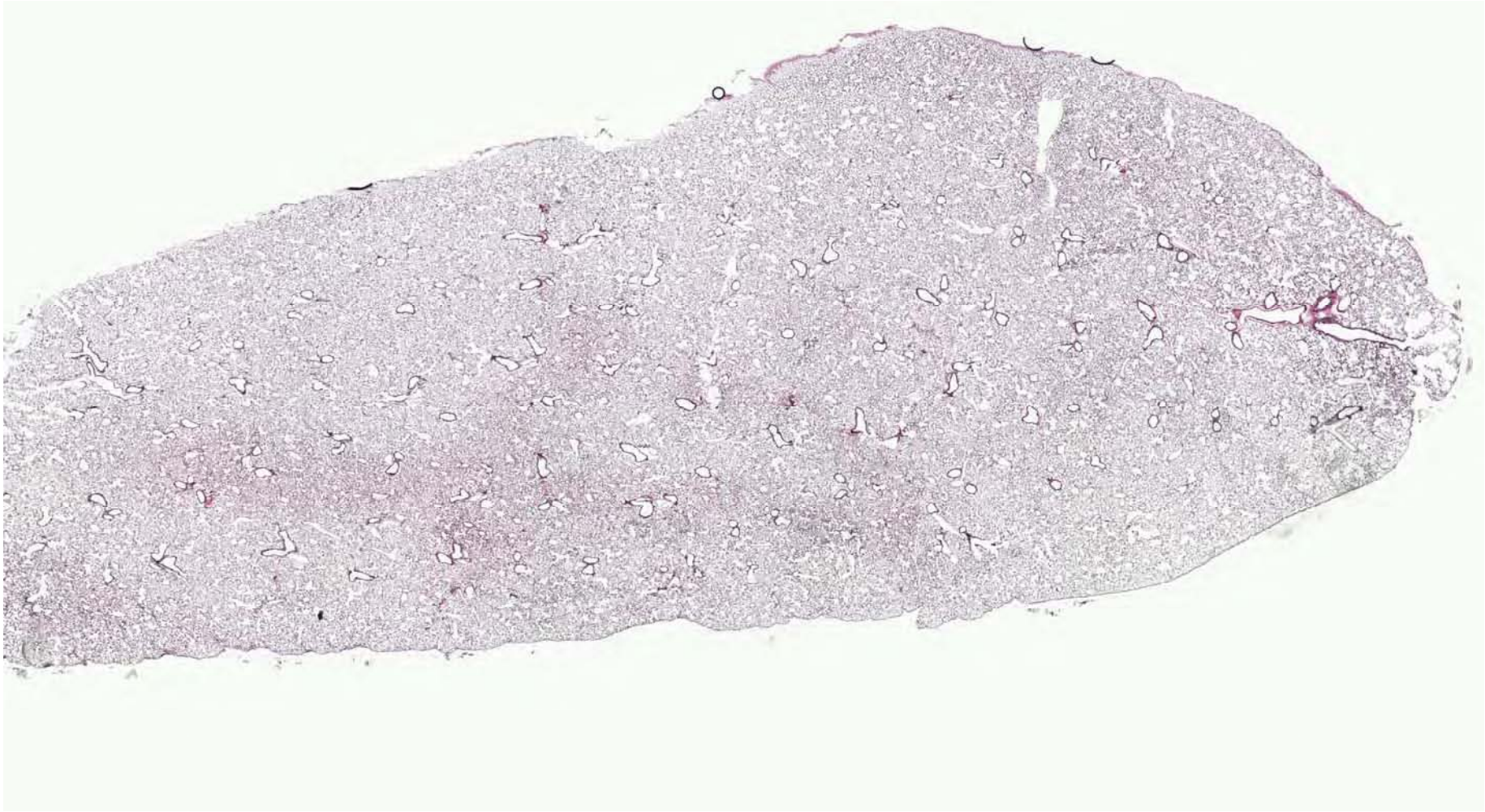

Sublethal Blast-TBI

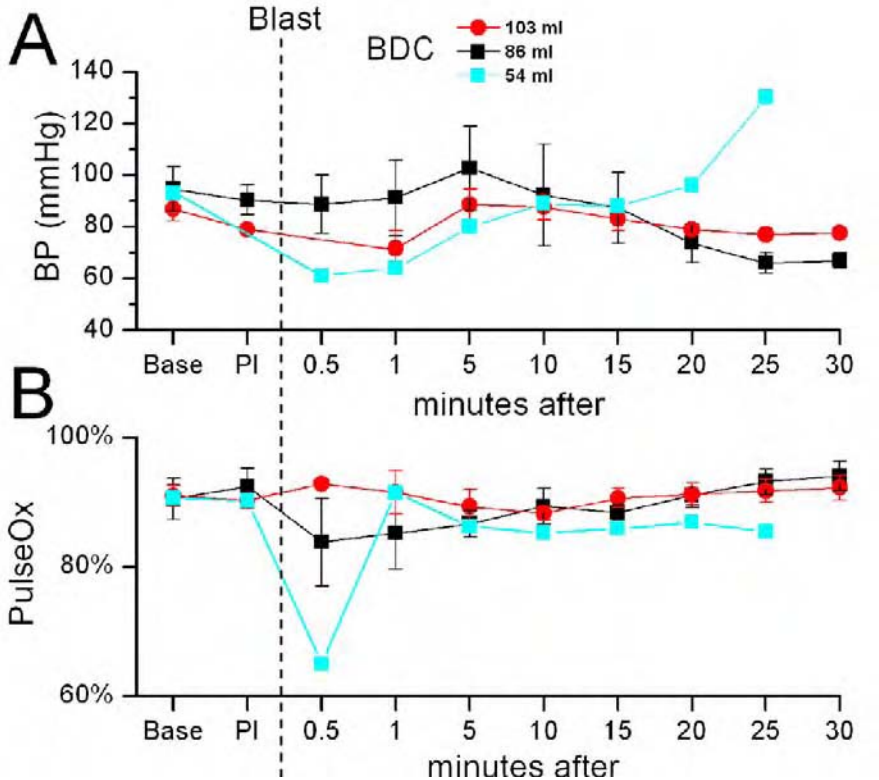

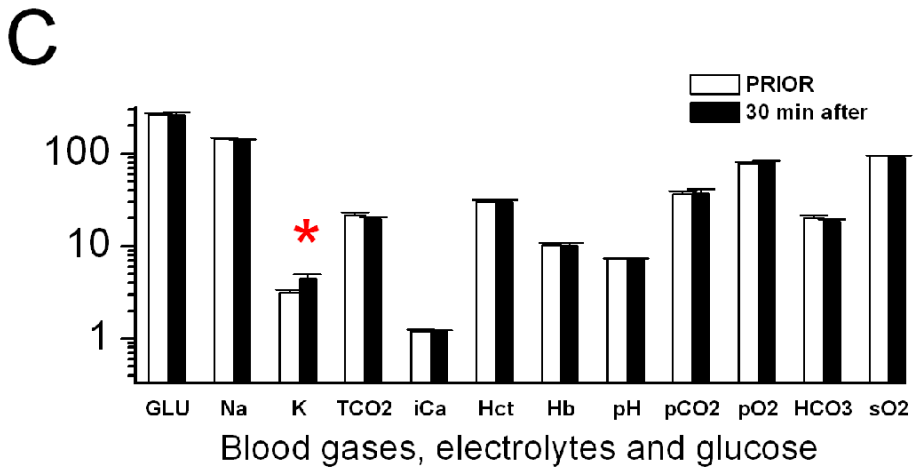

Axonal β-APP and NEUN in cortex 24 hr after blast-TBI

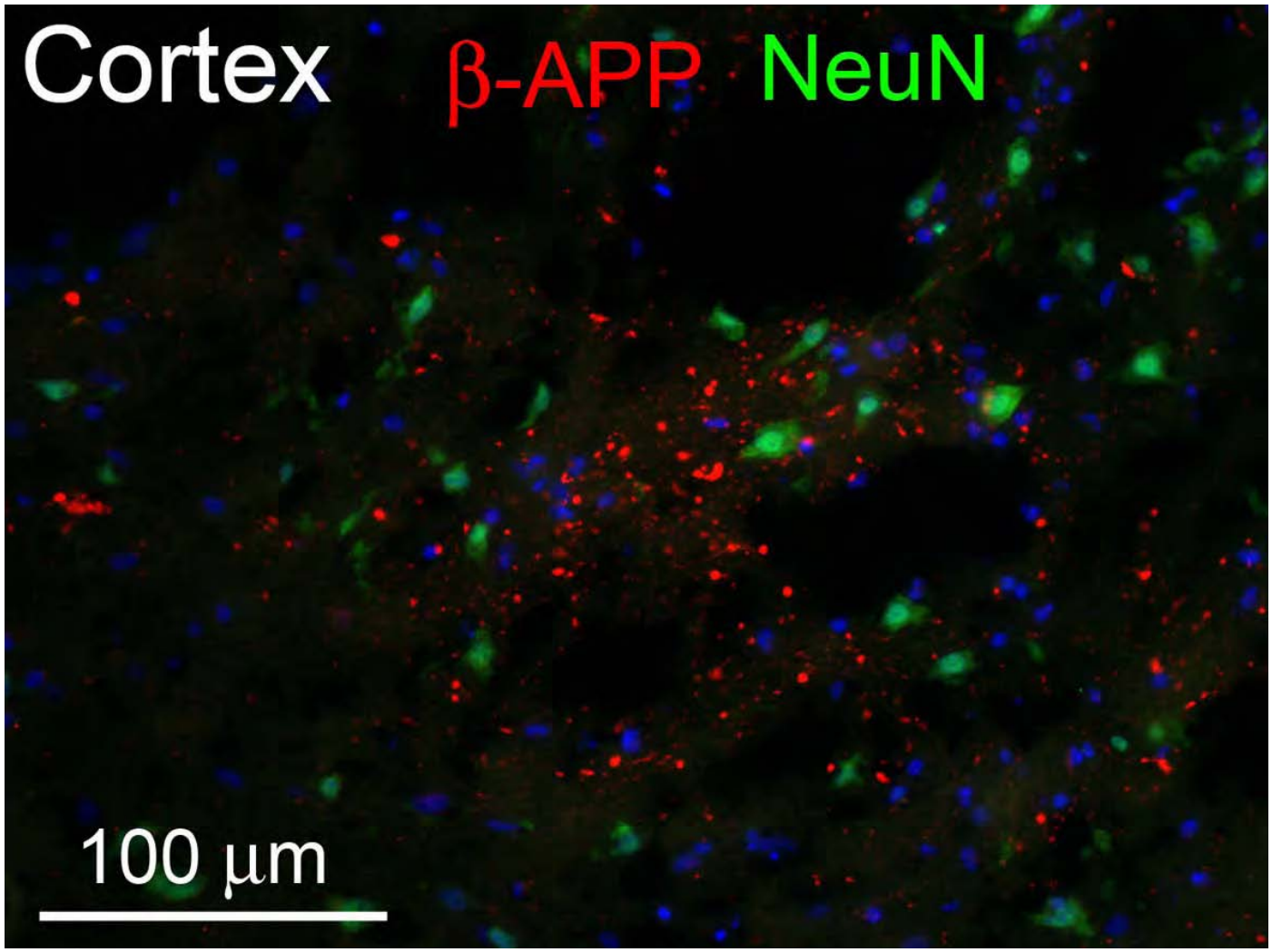

Contre-coup Injury to the Entorhinal Cortex 48 hr after blast-TBI

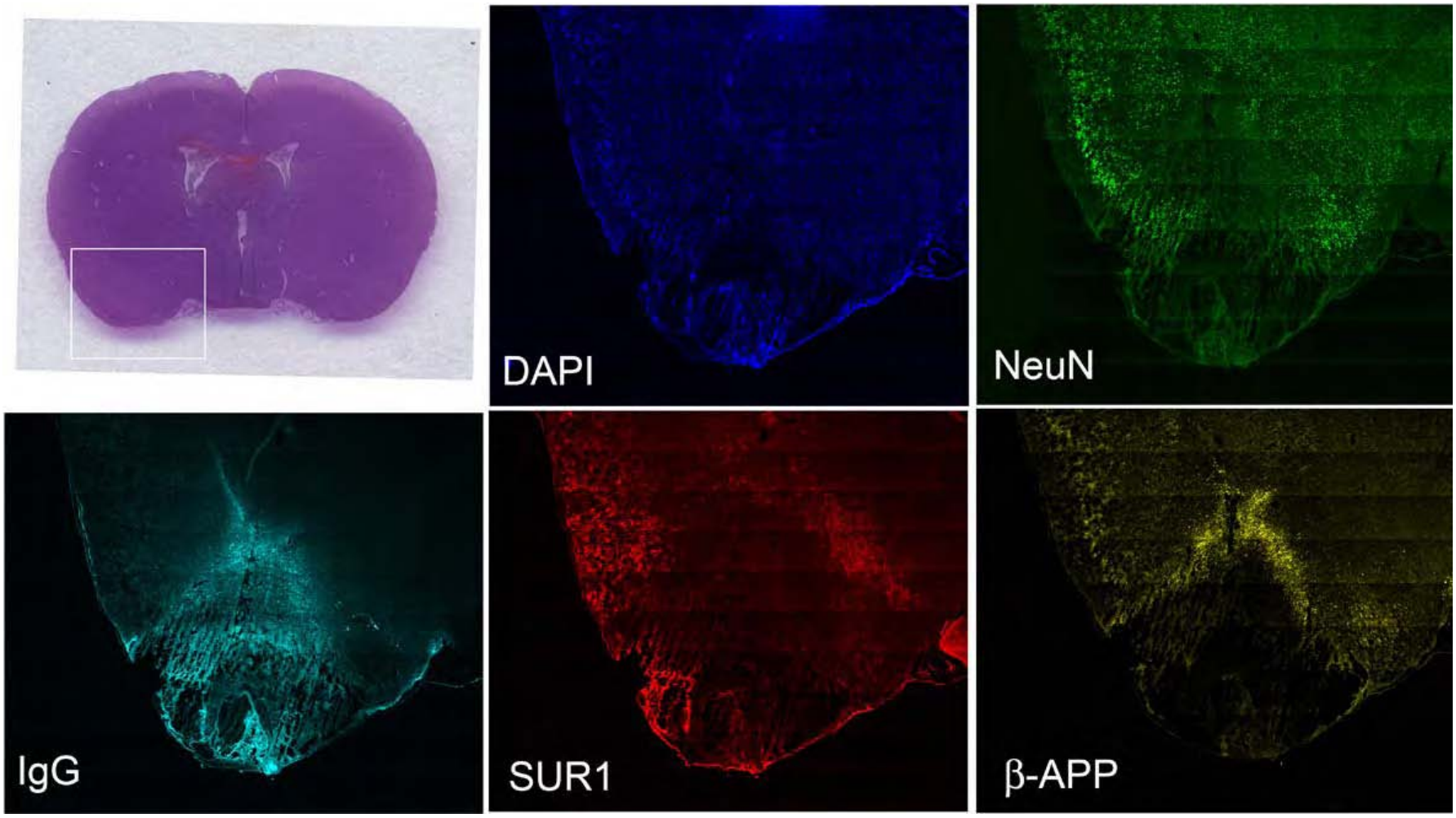

IgG extravasation in Thalamus and Cerebellum 48 hr after blast-TBI → minimal vasogenic edema

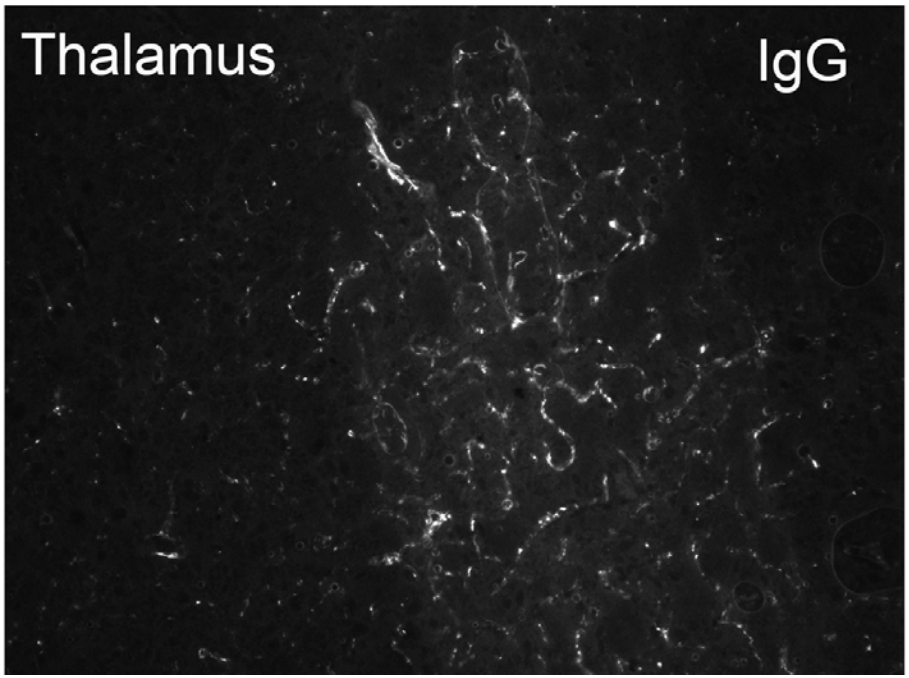

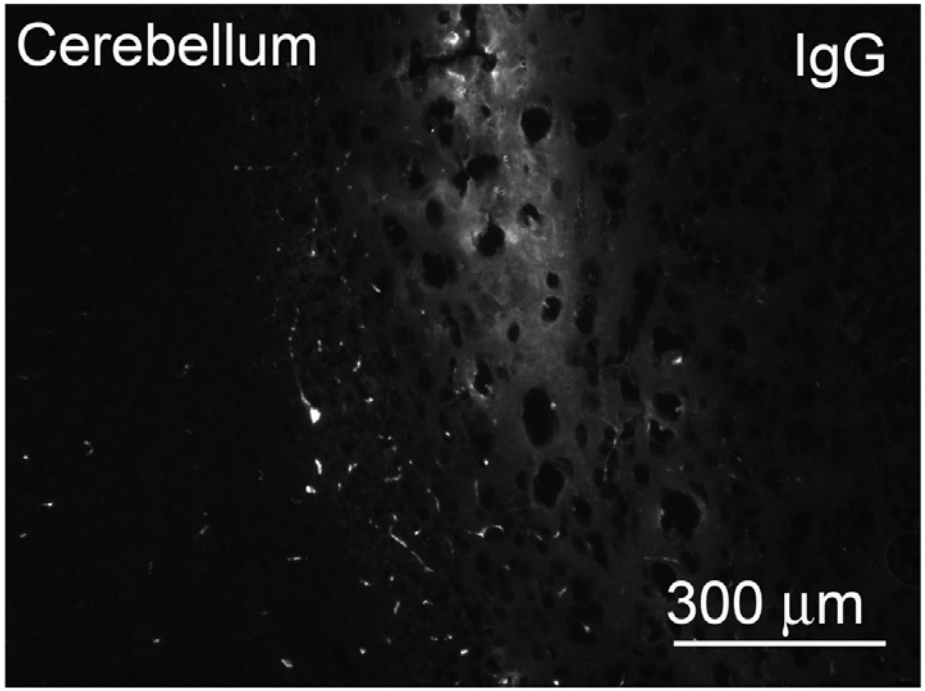

β-APP in Cerebellum
48 hr after blast-TBI

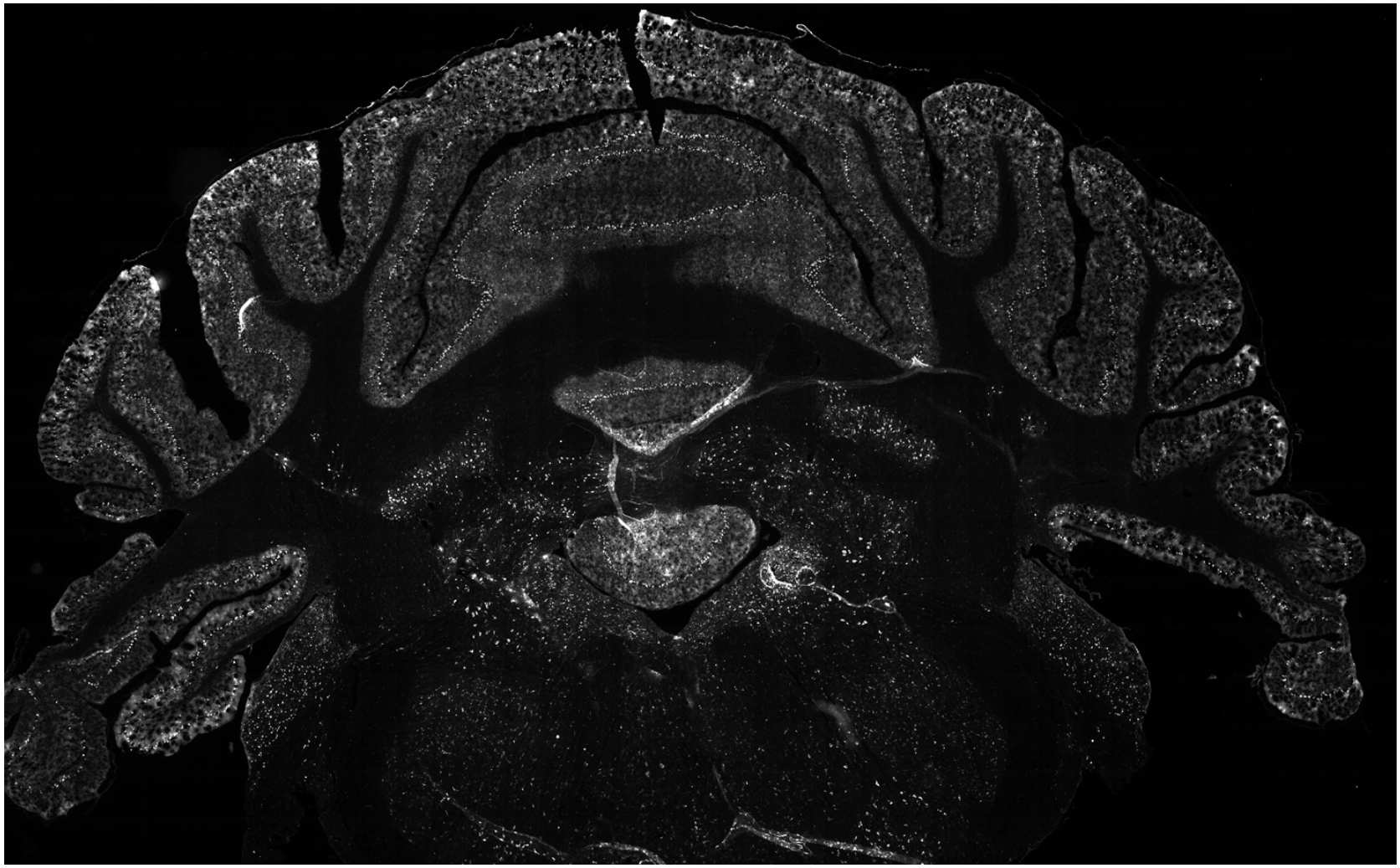

SUR1 upregulation in the path of the blast 48 hr after blast-TBI

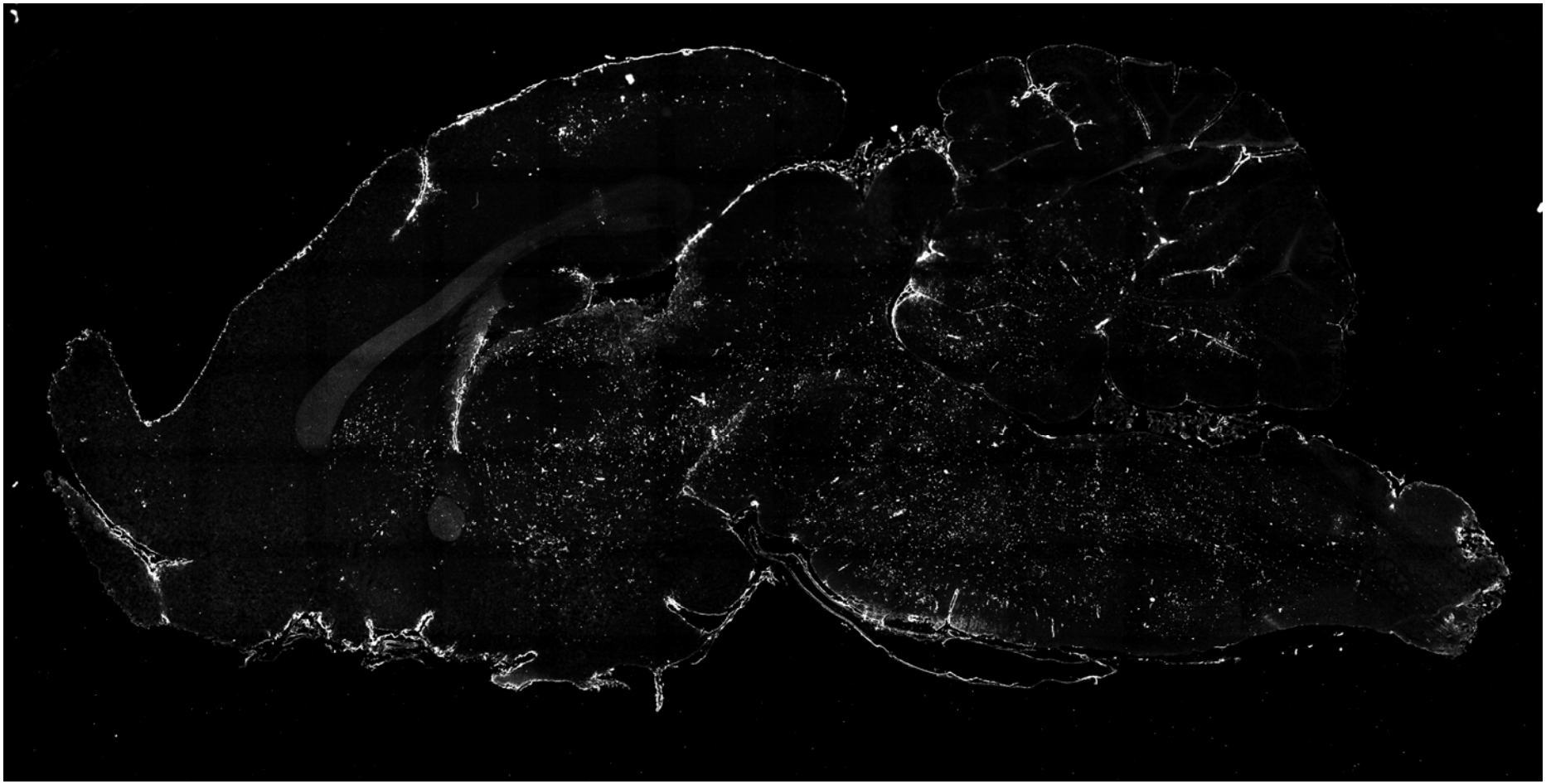

SUR1 upregulation in cortex, caudate and thalamus 48 hr after blast-TBI

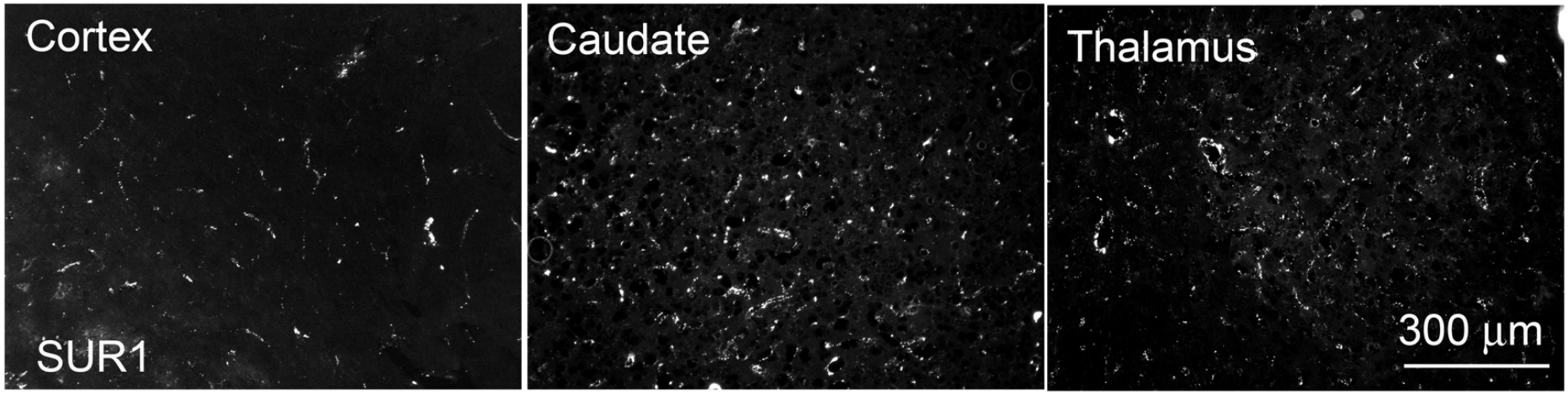

Neuronal β-APP and SUR1 co-localize in cerebellar Purkinje cells 48 hr after blast-TBI

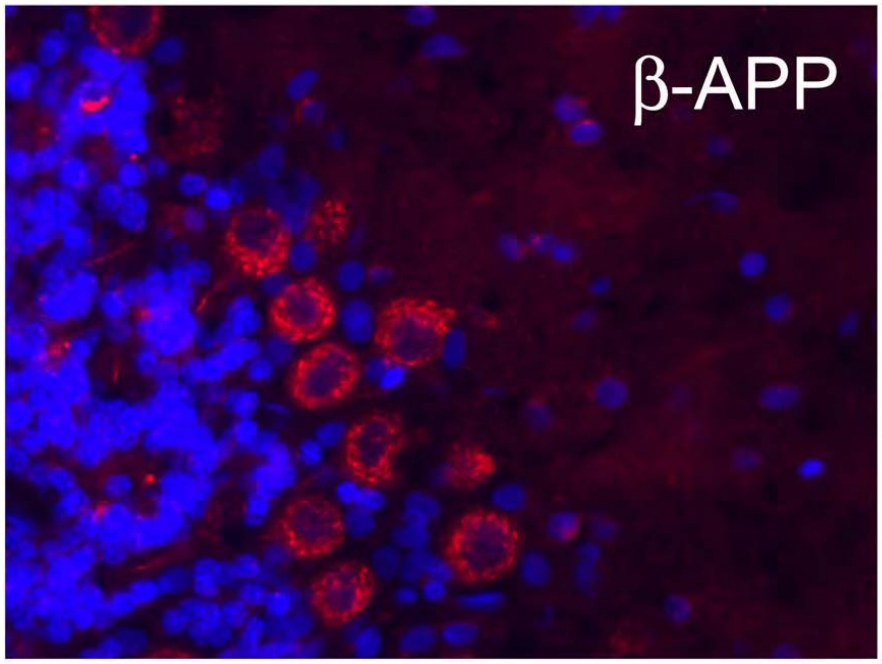

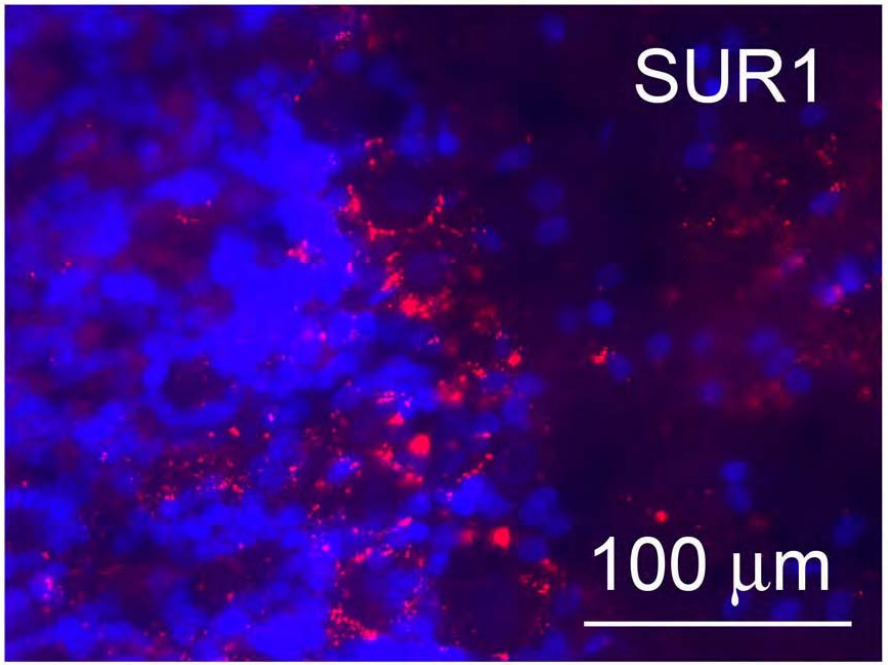

SUR1 in cerebellar Purkinje cells and white matter

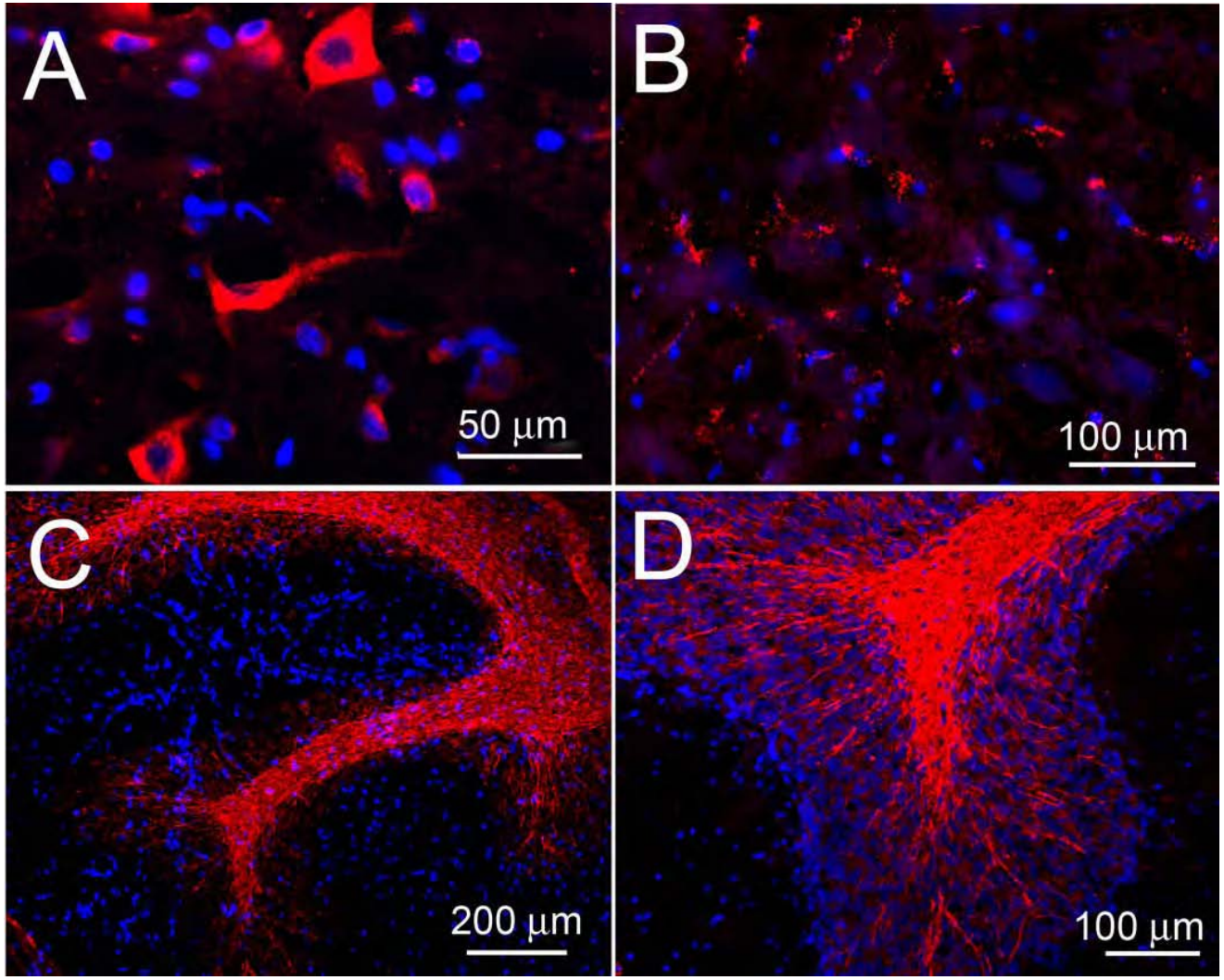

IgG, activated caspase-3 and β-APP in cerebellum at 4 8 hr

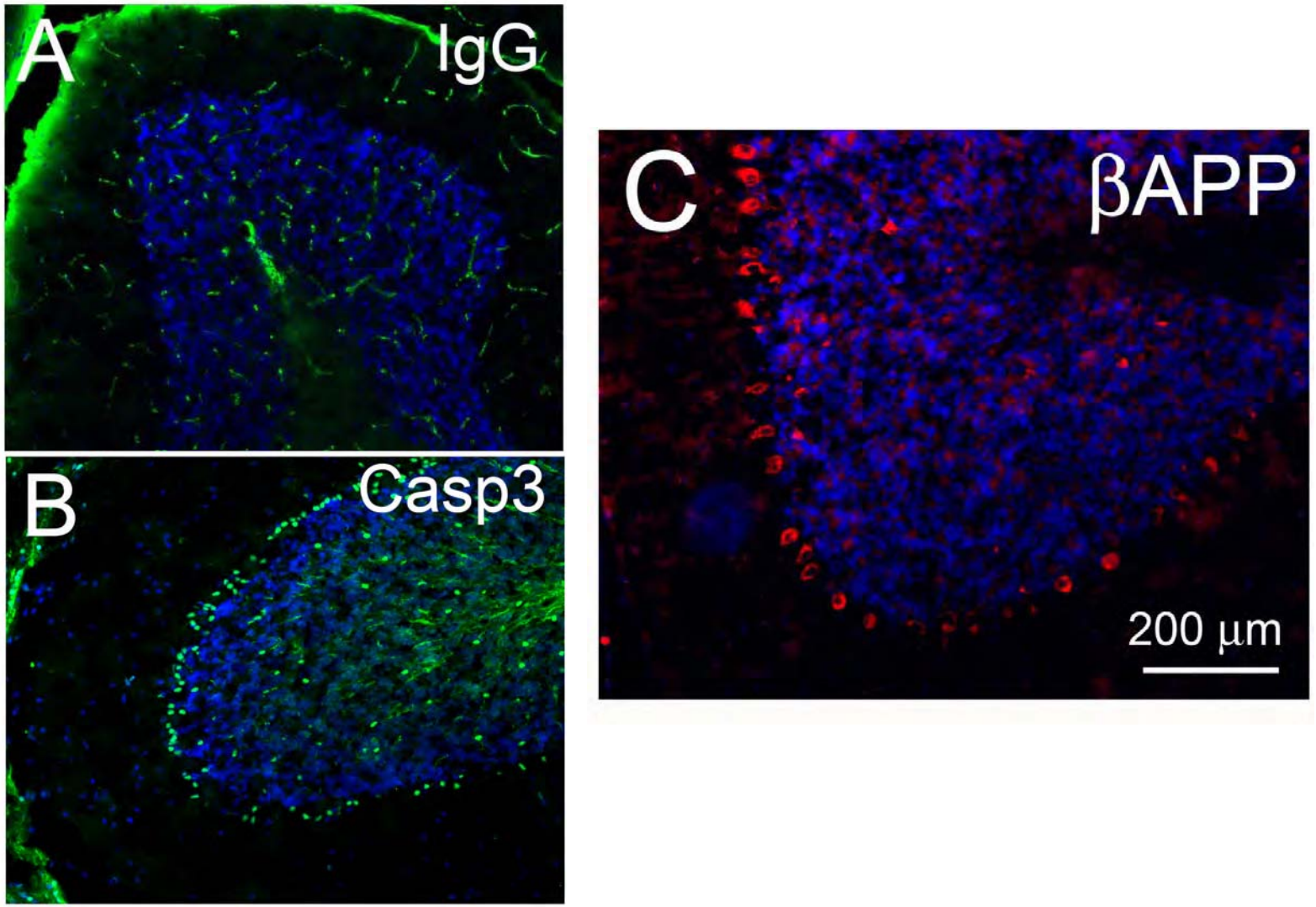

Fluoro-jade staining in hippocampus 4 weeks after blast-TBI

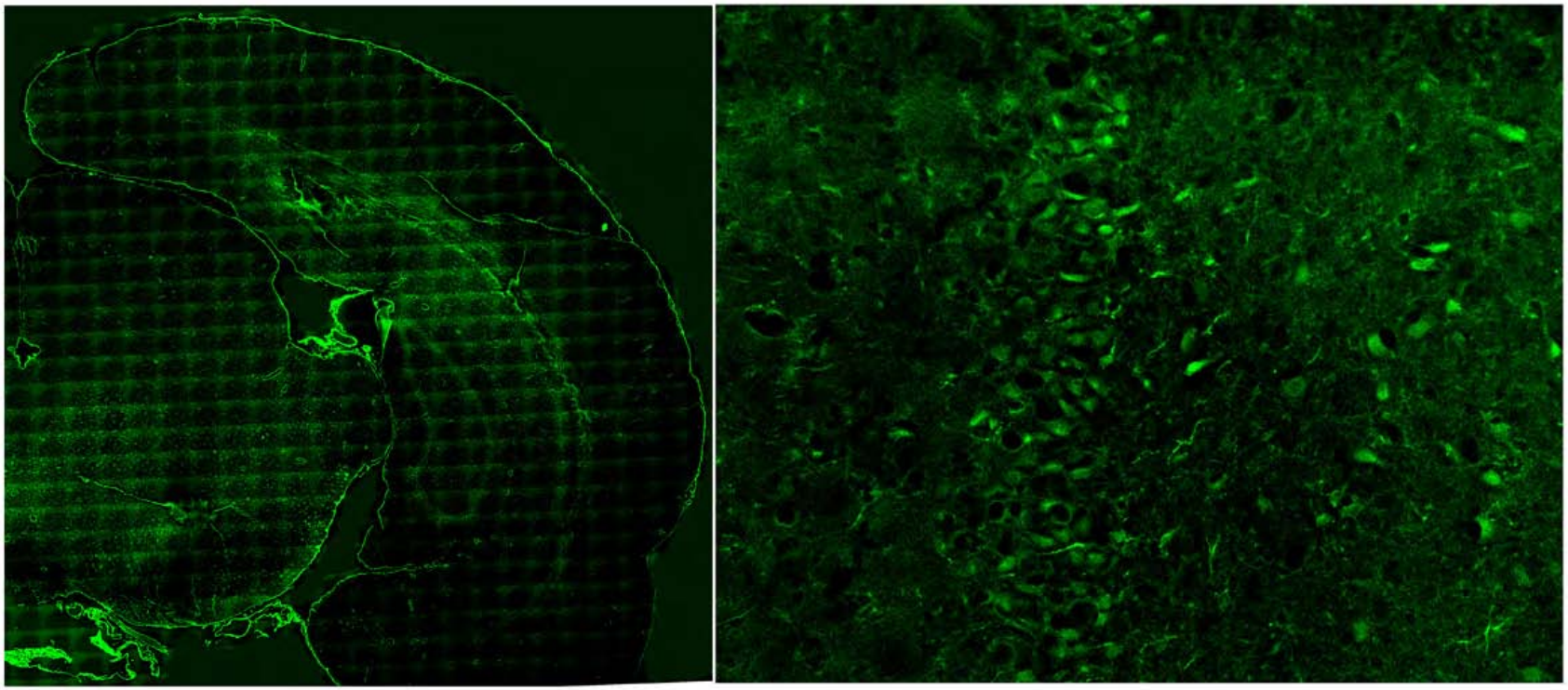

Fluoro-jade staining in cerebellum 4 weeks after blast-TBI

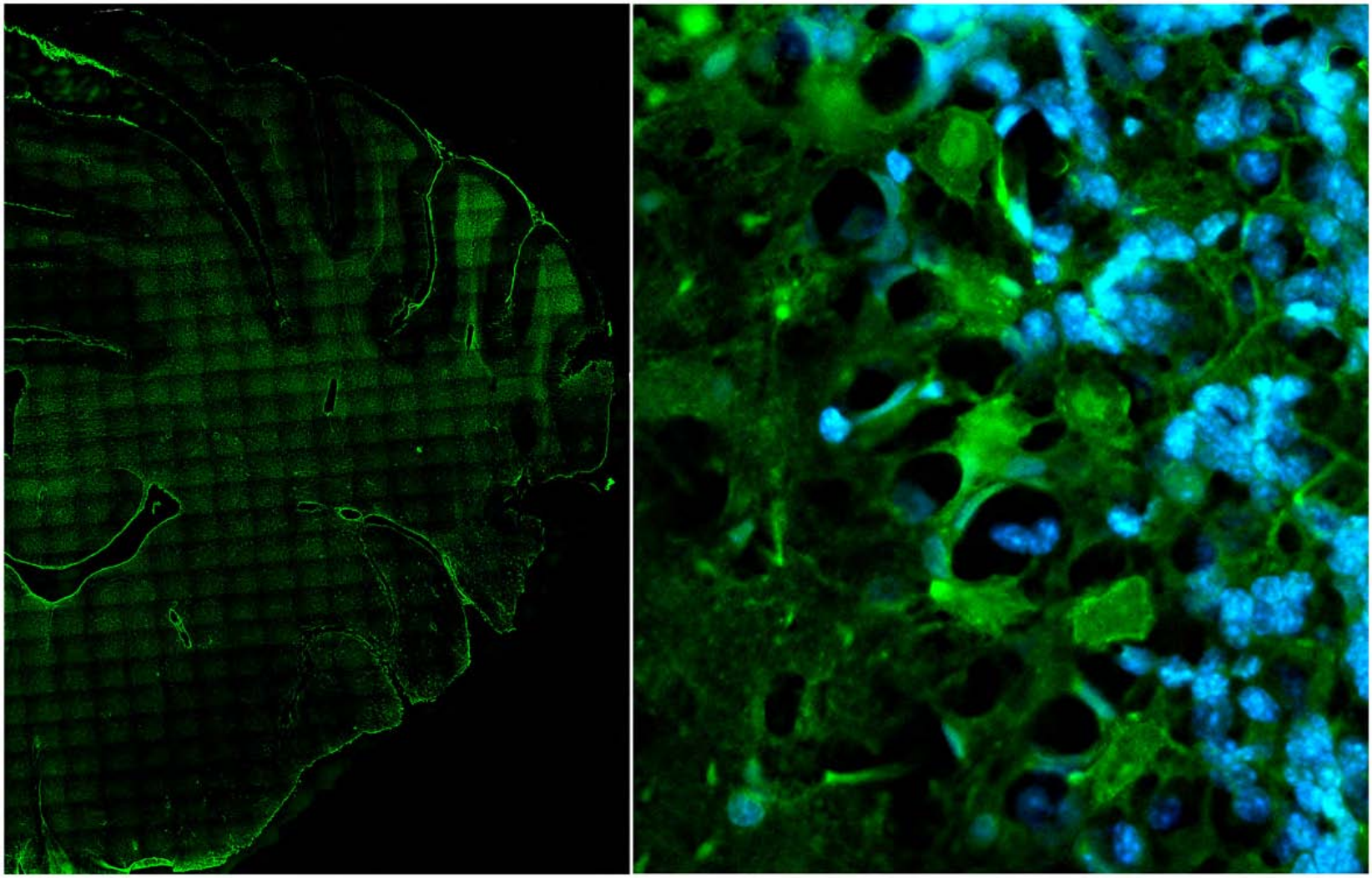

Beam Walk

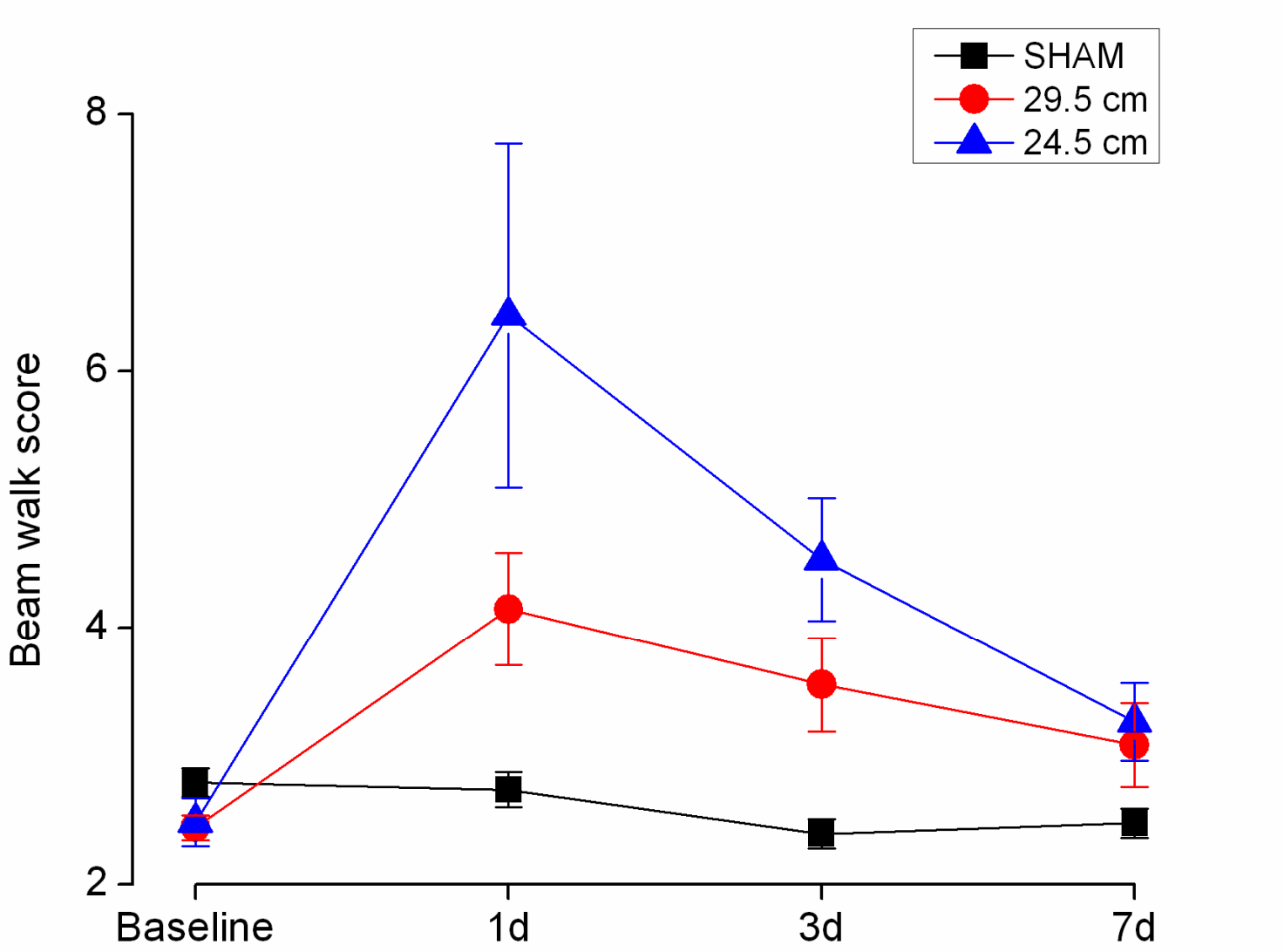

Beam Balance

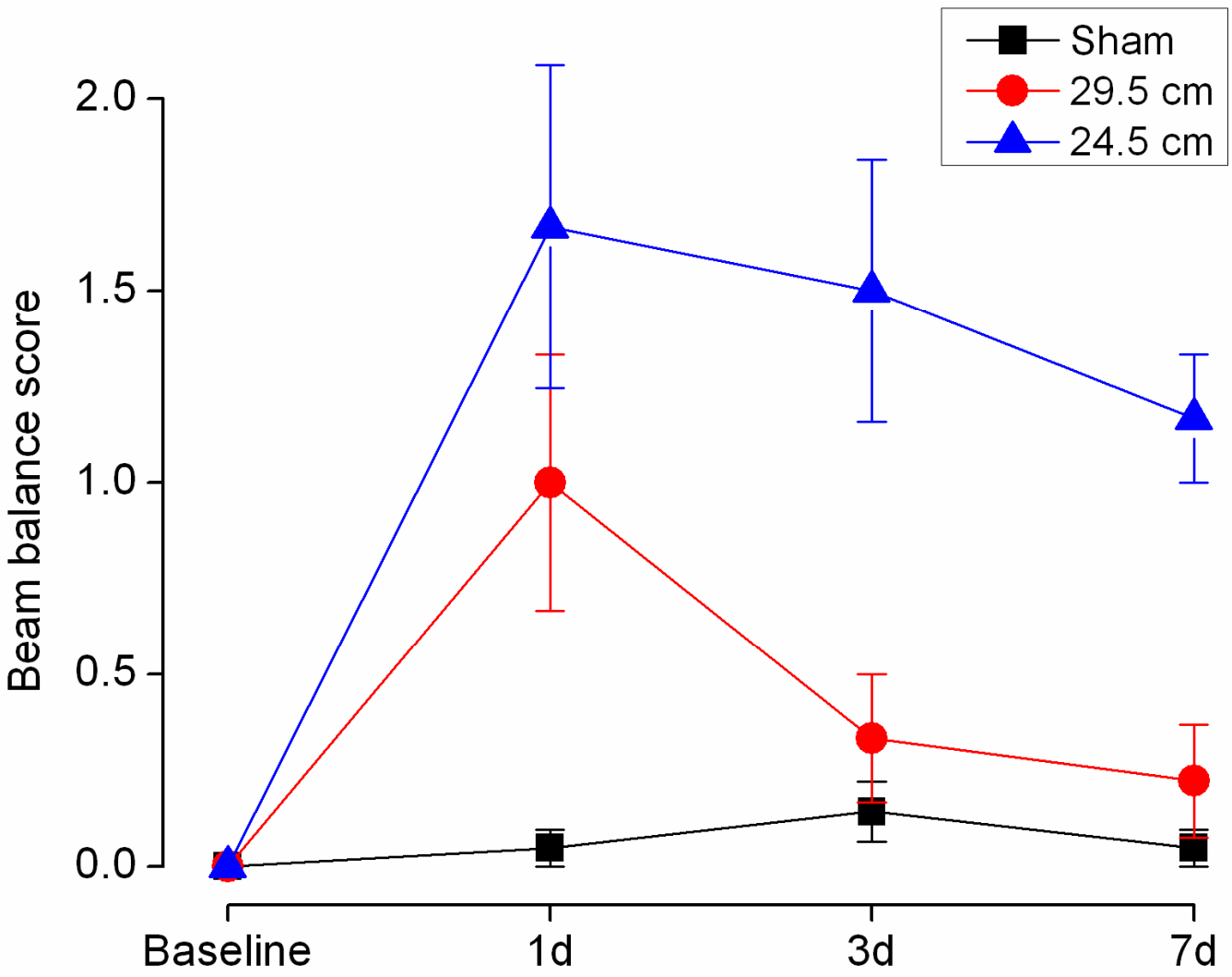

Rearing

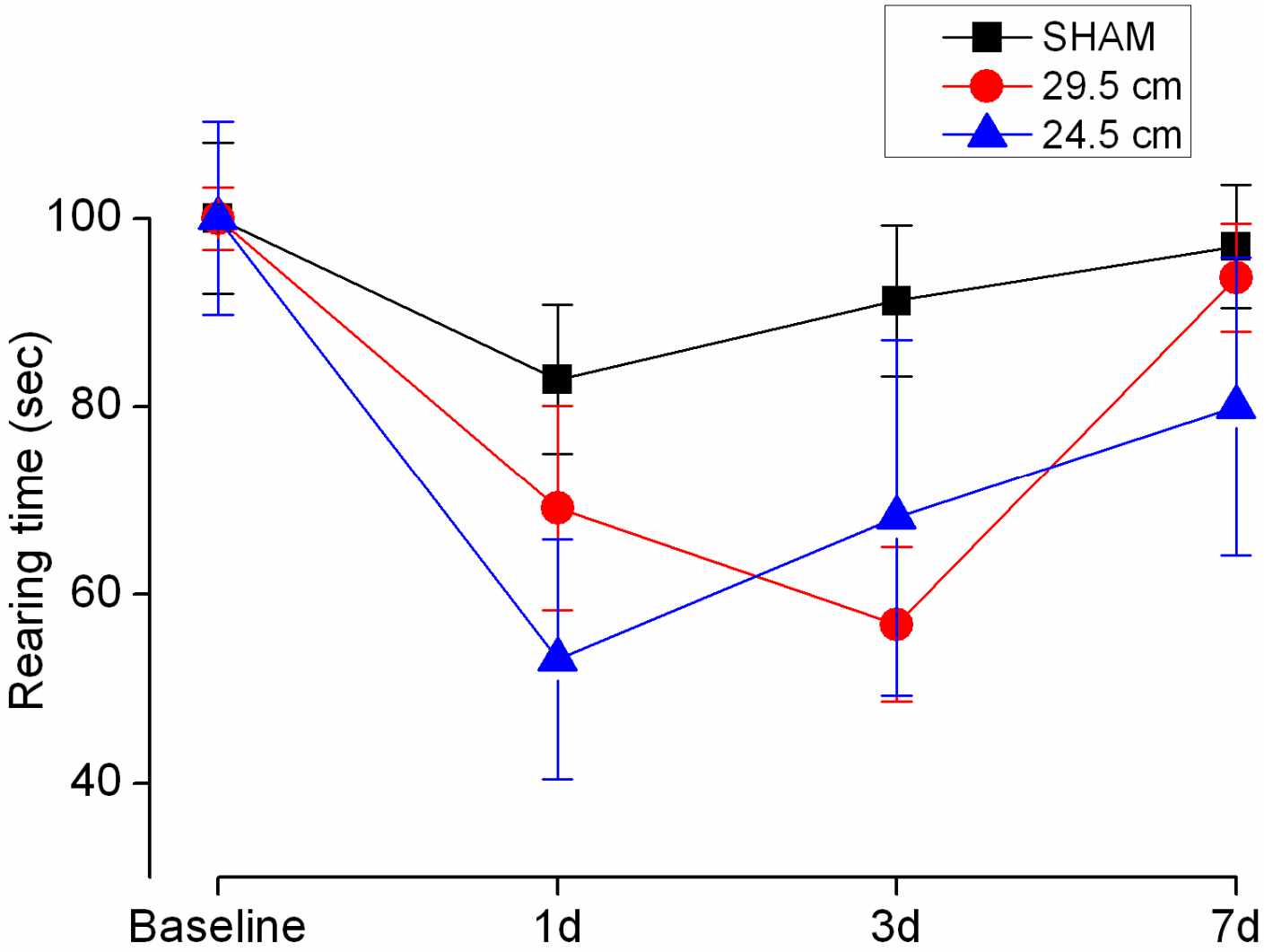
SHAM
29.5 cm
24.5 cm
Rearing time (sec)
100
80
60
40
Baseline
1d
3d
7d

Accelerating RotaRod

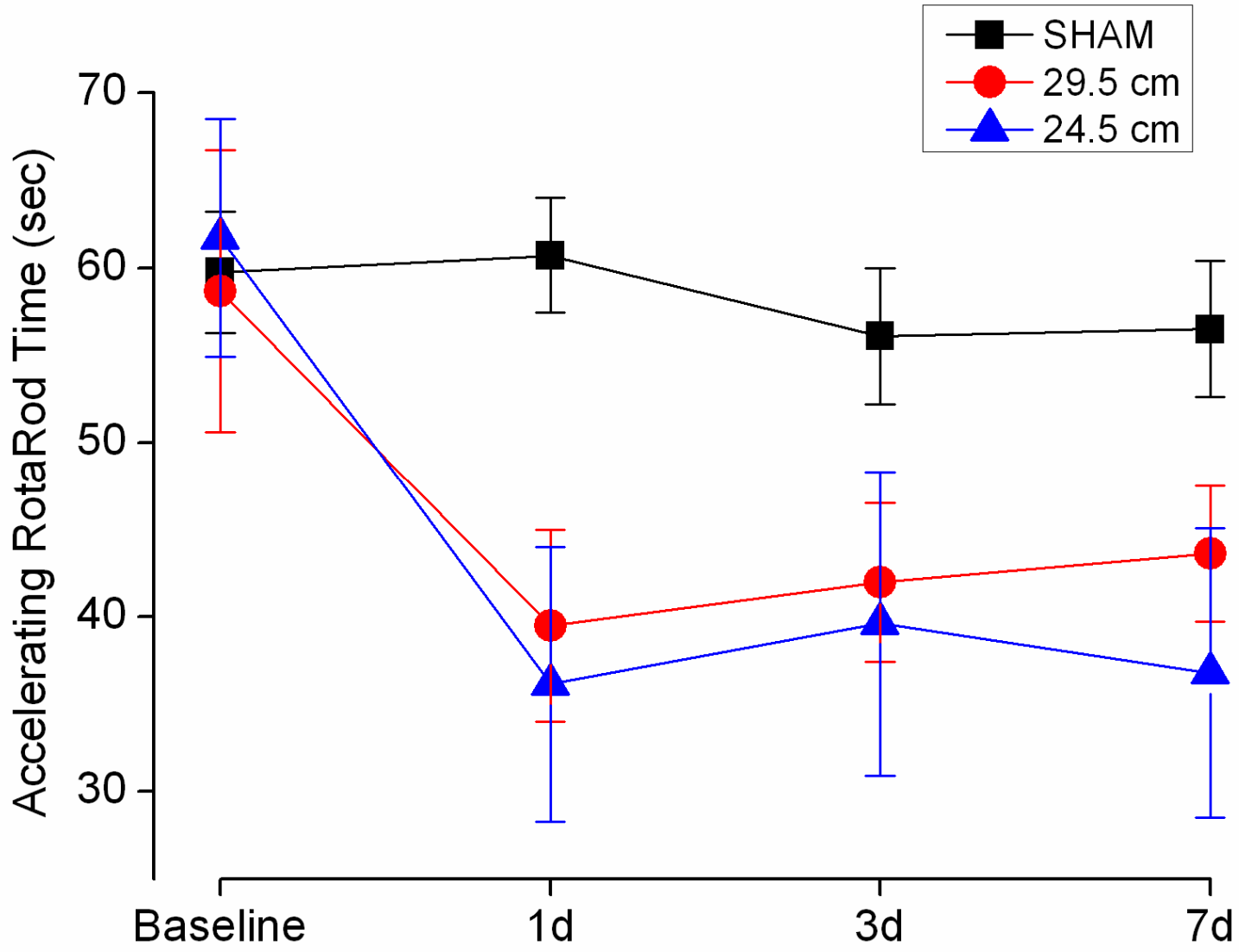

Morris Water Maze up to Day 21

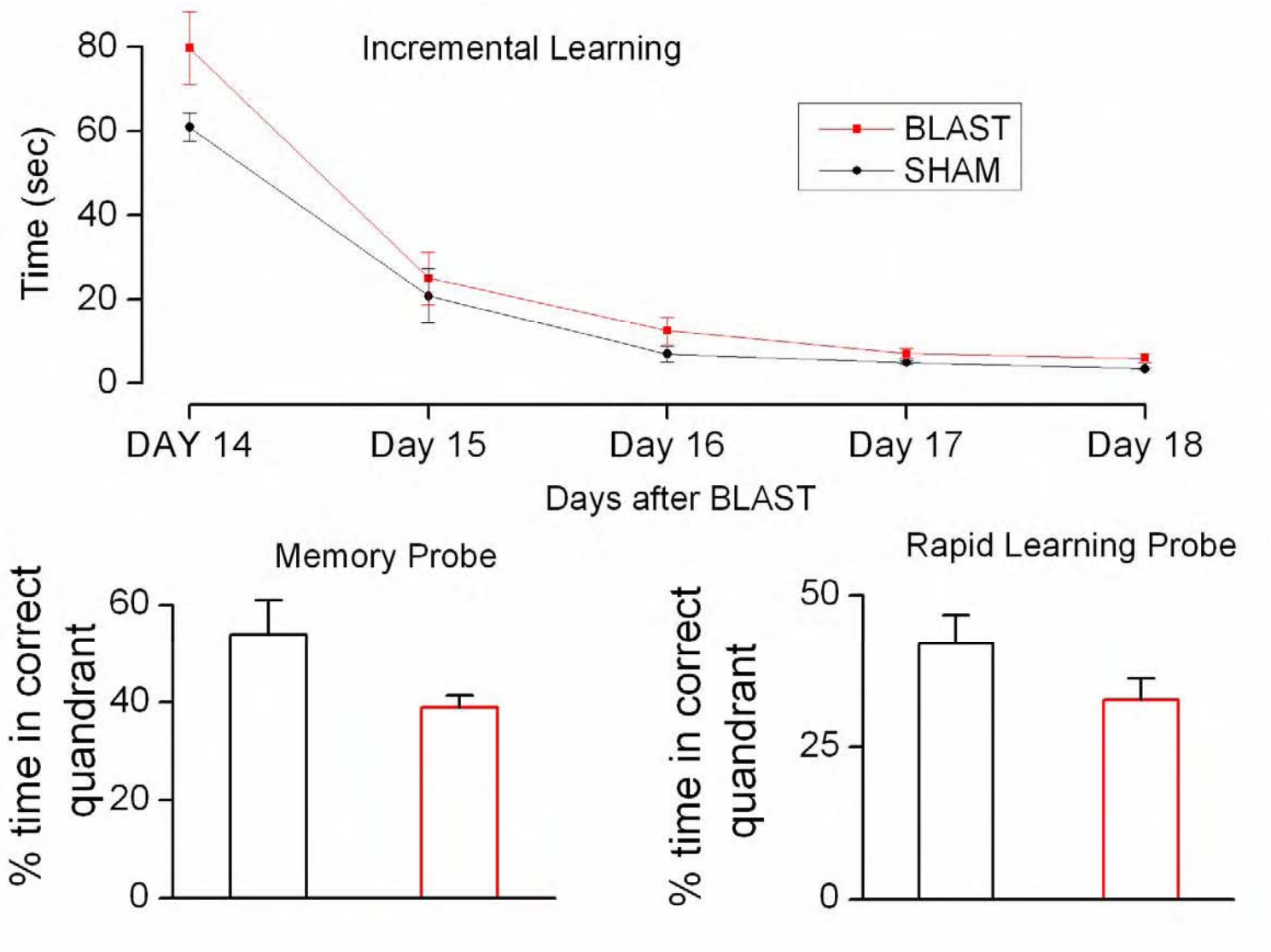

CONCLUSION

- Novel model that segregates direct vs. indirect effects of blast on the brain
- Reproduces *some but not all* of the acute effects of blast TBI observed in humans
  - SAH
  - *Not* vasogenic edema or delayed death
  - Acute and chronic neurological dysfunction
- Produces effects with long-term consequences
  - SUR1 $\rightarrow$ oncotic (necrotic) cell death
  - Activated caspase-3 $\rightarrow$ apoptotic cell death
  - Fluoro-jade staining for damaged neurons
  - β-APP up-regulation $\rightarrow$ Predisposes to Dementia?

THE FUTURE

- How does a shock wave physically interact with the head and brain (density boundaries?)
- What is the fundamental cause of death – what is the physiology associated with cessation of brainstem function?
- What is the mechanism of brain edema in blast-TBI? (not seen with “pure” shock wave)
- Is the unprotected face a portal of entry for blast waves in warfighters? (Should they wear face shields?)